MASTER´S THESIS IN CHEMICAL ENGINEERING

Investigation and Optimisation of Fusarubins Production in *Fusarium solani* via Targeted Deletion

Samba Evelyne Kabemba Kaniki
June 2020

AALBORG UNIVERSITET

Department of Chemistry and Bioscience

Section of Chemical Engineering

Aalborg University Esbjerg

Title Page

Title:	Investigation and Optimisation of Fusarubins Production in *Fusarium solani* via Targeted Deletion
Department:	Department of Chemistry and Bioscience
Location:	Aalborg University Esbjerg
Supervisors:	Jens Laurids Sørensen, Mikkel Rank Nielsen
Submitted:	June 2020

Abstract

Fusarubins are naphthoquinones produced by species of the *Fusarium* genus. This group of metabolites has been studied for antimicrobial and anti-tuberculotic properties. The gene cluster responsible for their production, the *PKS3* cluster, comprises of 6 essential genes, *fsr1* to *fsr6*. Various studies have proven the importance and functions of these genes individually by the knock-out method, which consists of deleting the genes and observe the related phenotypic changes. Current literature has proposed the putative roles of *fsr1*, *fsr2*, *fsr3* and *fsr6* as nrPKS, O-methyltransferase, FAD-monooxygenase and transcription factor respectively. In *F. solani*, the organisation of the *PKS3* cluster differs from the rest of *Fusarium* species as it contains 17 extra genes located between *fsr3* and *fsr4*. This study aimed at investigating the roles of the genes within the *PKS3* cluster of *F. solani* and elucidating the functions of the 17 genes by knock-out method. At first, a synteny alignment for the *PKS3* cluster was executed with some of the members of the FSSC to observe the conservation of genes within the complex. This indicated that most genes including the 17 extra genes are conserved across the species of FSSC. The protein prediction of those genes also hints that they have a role in the secondary metabolism of *F. solani.* Experimentally, the deletion of the *PKS3* genes was performed in *F. solani* via *Agrobacterium* mediated transformation. This included the individual knock-out of the *fsr* genes and the extra genes predicted to be part of the cluster. The resulting deletion mutants did show clear phenotypic changes in pigmentation and growth. Due to the corona circumstances, the deletion of 8 genes was achieved and the chemical analysis of the metabolites issued from each mutant is pending. This report provides a deep investigation on the *PKS3* cluster in *F. solani* and comparison to similar *Fusarium*, a phenotypic analysis of *PKS3* deletion mutants in *F. solani* and a concise protocol for AMT in *F. solani*.

Preface

This project was made during the period of 1/9-2019 – 4/6-2020, and submitted as my thesis concluding my master's degree in the Chemical Engineering department at Aalborg University Esbjerg. The background for this study was defined as investigating the biosynthetic pathway of polyketides pigments in *F. solani* through knock-out of a gene cluster. The experimental aim was to generate knock-out mutants of the fusarubin gene cluster, and analyse the effect on the pigment production. The interruption of the experimental work, caused by the Covid-19 pandemic crisis, affected the yield of knock-out mutants within the cluster. However, the generated knock-outs were sent out for pigment production analysis. This report provides insight into the identification of the essential biosynthetic genes in the *PKS3* cluster, the construction of knock-out vectors, a design study and protocol on fungal transformation of *F. solani* and knock-out validation.

I sincerely express my gratitude to my supervisors Mikkel Rank Nielsen and Jens Laurids Sørensen, who have been greatly supportive, inspiring and guiding me with valuable expertise and advice throughout the period of this project work. I would also like to thank the PhD students Tobias Bruun Pedersen, Sebastian Birkedal Kristensen and Charlotte Overgaard Wilhelmsen for their support inside and outside the laboratory, as well as the heads of the laboratory technicians Linda Birkebæk Madsen and Dorte Spangsmark for their technical advice.

Sincere thanks go to my family and friends in Denmark, Belgium and in DR Congo for their constant encouragement and all the people that contributed small or big to the realization of this thesis.

I could not have achieved this without your help and assistance,
Thank you all for your invaluable support.

Samba Evelyne Kabemba Kaniki

Abbreviations

ACP	Acyl carrier protein
AGE	Agarose Gel Electrophoresis
AMT	Agrobacterium Tumefaciens mediated Trans-formation
AS	Acetosyringone
bp	Base pairs
F. graminearum	*Fusarium graminearum*
F. fujikuroi	*Fusarium fujikuroi*
F. solani	*Fusarium solani*
FSSC	*Fusarium solani* species complex
HPLC	High performance liquid chromatography
HR	Homologous recombination
KO	Knock-out
KS	Ketosynthase
LB	Left border
MAT	Malonyl-CoA ACP transacylase
MQ	Milli-Q
NR-PKS	Non-ribosomal polyketides
NRPS	Non-ribosomal peptides
nt	Nucleotide
OE	Overexpression
PCR	Polymerase chain reaction
pKO	Knock-out plasmid
PKS	Polyketides
PT	Product template
RB	Right border
SAT	Starter unit ACP transacylase
SM	Selection marker
T-DNA	Transfer DNA
TE	Thioesterase
tf	Transcription factor
T_m	Melting temperature
Δ	Deletion mutant

Table of Contents

Investigation and Optimisation of Fusarubins Production in *Fusarium solani* via Targeted Deletion
4 June 2020
Samba Evelyne Kabemba Kaniki

1. Introduction

The *Fusarium* genus and species were first introduced in 1809 and has been increased since. It comprises of ubiquitous species present in highly varied ecological niches. *Fusaria* species are isolated from many kinds of substrates in most climatic conditions; tropical, subtropical, cool or warm weather. Commonly known as plant pathogens, *Fusaria* species also shows pathogenicity to humans and animals. The phylogenetic analysis has been supporting the taxonomic classification of the species, resulting in over 20 different species. (1,2) The *Fusarium solani* species complex (FSSC) has been classified through numbers of studies. Usually found in soil as decomposers, they are also famously known for causing important economical crop losses around the world, namely in South East Asia, Northern Africa and Middle East. The fungi are isolated from different plants like rice, tree bark, beans, peas, corn, peppers, fruits, on roots, stems and seeds. Figure 1 represents a phylogenetic tree executed with alignment of 20 housekeeping genes of 31 *Fusarium* species. The lineage of FSSC is located as a distant related species complex from the rest of the analysed species. In terms of taxonomy, the FSSC is divided in two groups: *Ventricosum* and *Martiella*. The latter includes seven mating populations annotated MPI to MPVII. The phylogenetic analysis by the strong evolutionary indicator gene sequences (28S rDNA, internal transcribed spacer and *tef1*) of at least 55 members revealed three clades within the *Martiella* group. Clade 1 includes only two species, clade 2 includes all of the species pathogenic to soy beans and lastly clade 3, the largest clade, includes all of the known pathogens to plants, animals and humans. (3,4)

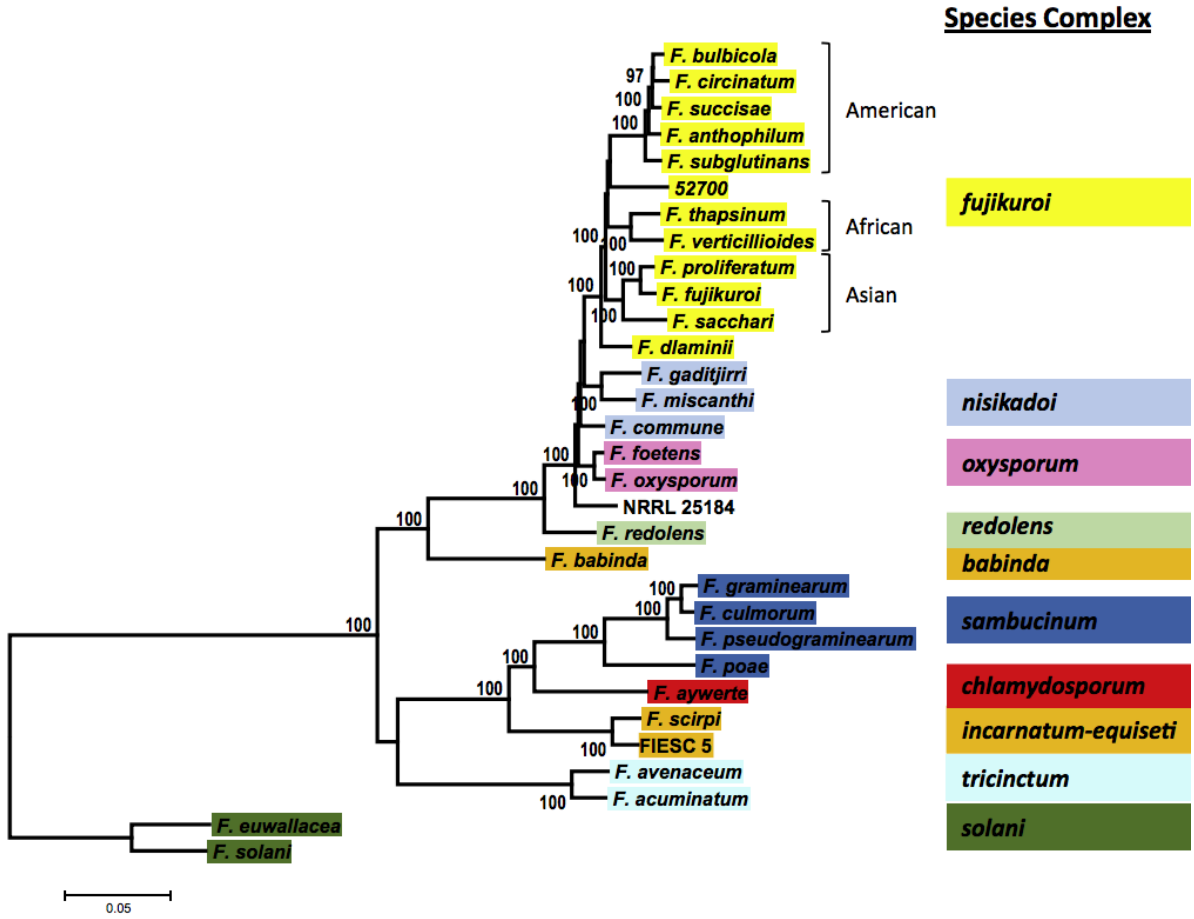

Figure 1: Phylogeny tree of 31 species within *Fusarium* genus by alignment of 20 housekeeping genes. The *F. solani* species complex in green is distantly related to most of the other *fusaria*. (5)

FSSC members are capable of producing aggressive and defensive agents such as enzymes part of their secondary metabolism, to ensure their pathogenicity onto their plant host. Pisatin demethylase, for example, is an enzyme that deactivates the antimicrobial pisatin produced by the hosts. (1) FSSC also produces a group of secondary metabolites, naphthoquinones, to protect themselves from the external environment (1,6). These represent a vast group of compounds responsible for the red-purple pigmentation of *F. solani* species but have no correlation with its toxicity on plants hosts. (1) These pigments, fusarubins and related compounds, have been studied for antibiotic, insectidal, phytotoxic and antitumoral properties. (7,8) Their wide range of therapeutic and pathogenic characteristics is caused by the ability of fusarubins to produce superoxide and semi-quinone radicals (8). These properties correlate with the hypothesis that secondary metabolites have a protective role for fungi. Moreover, fusarubins are excreted in the extracellular environment and/or in the perithecia. The pigments in the perithecia of *Fusarium* species have a protective role against UV radiation and inhibit the germination of spores located inside (6). Most current literature has covered the biosynthesis and production of fusarubin in species of *Fusarium fujikuroi* and *Fusarium graminearum*. This study will overview the potential differences between the biosynthesis of fusarubins in *F. fujikuroi, F. graminearum* and *F. solani*. This investigation will be the foundation to construct a compatible experimental work with the aim to elucidate the biosynthesis of fusarubins in *F. solani.*

2. Fusarubins Spectrum

Fusarubins are red-yellow polyketide pigments characterised by being issued from the *PKS3* cluster. The spectrum of fusarubins and derived compounds comprises of fusarubin, javanicin, bostrycoidin, novarubin, anhydrojavanicin, nor-javanicin, anhydrofusarubin, solaniol, fusarobinoic acid, martinicin, nectriafurone, and (de-)methyl products derived of fusarubin, javanicin, and bostrycoidin (1,9–11). The production of each fusarubin is species and conditions dependent. In *F. fujikuroi* for example, 8-O-methylfusarubin, 8-O-methylnectriafurone, 8-O-methyl-13-hydroxynorjavanicin and 8-O-methylanhydrofusarubinlactol are the major fusarubins issued from the *PKS3* gene cluster. (8) In *F. solani*, bostrycoidin, fusarubin and javanicin were observed in the mycelial tissue as some of the main pigments (12). Figure 2 showcases a few of the many discovered fusarubins, bostrycoidins and javanicins produced within the *Fusarium* genus.

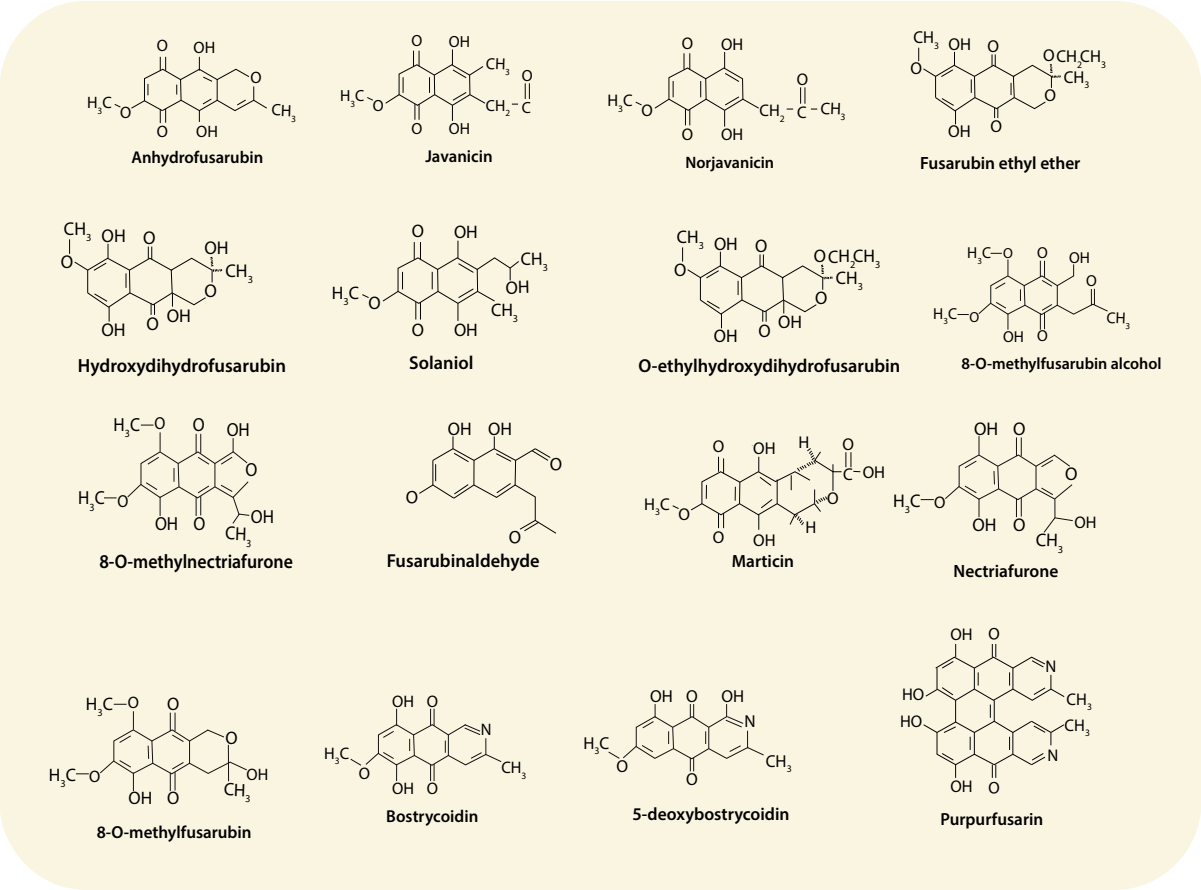

Figure 2: Chemical structures of described fusarubins compounds. Fusarubins are naphthoquinones with two aromatic rings with oxo groups at C1 and C4. (1,8–12) **Fusarubins are all compounds produced by the *PKS3* cluster, this group also includes variants of bostrycoidins and javanicins.**

As observed, fusarubins have similar structures of methylated rings, sometimes synthesised with an amine group. Some compounds can be unstable and equilibrate with another intermediate. Namely, 8-O-methylfusarubin equilibrates with 8-O-methylnectriafurone. Therefore, the conditions of the external environment have a strong influence on the fusarubins production. The fusarubins production is directed by the *PKS3* cluster, on which next section covers the organisation and biosynthesis within *F. fujikuroi* and *F. graminearum*.

3. Gene Cluster and Biosynthetic Pathway

3.1 *PKS3* Cluster

The fungal secondary metabolism gene clusters have been kept from species to species despite the evolutionary steps, supporting their importance for the well-being and development of the microorganisms. (6) The organisation of the fusarubin gene cluster, the *PKS3* cluster, shows rather strong similarities in its organisation across all concerned species. (8) Current literature shows that the *PKS3* gene cluster comprises of six essential genes; *fsr1, fsr2, fsr3, fsr4, fsr5 and fsr6*. In and out of the GFC (*Gibberella fujikuroi* species complex), all strains containing the six core genes of the *PKS3* cluster synthesize fusarubins, at the exception of *F. graminearum* which produces bostrycoidins (8). Figure 3 illustrates the presence of the PKS3 core genes in different *Fusarium* species.

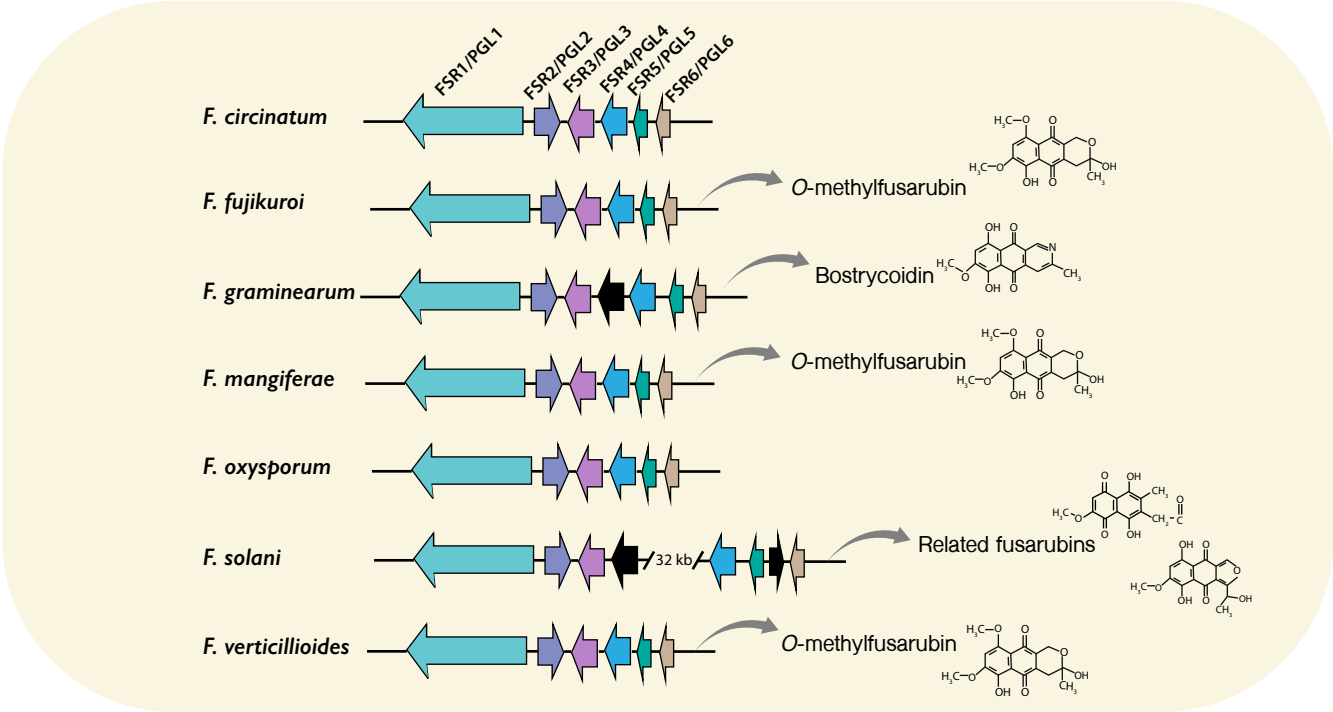

Figure 3: *Fusarium* species with the fusarubin gene cluster. The coloured arrow represents the present genes while the black arrow indicates genes unrelated to the fusarubin production. The grey arrow represents the production of bostrycoidin, O-methylfusarubin or related fusarubins. *F. graminearum* is the only species to comprise all core genes but to not produce fusarubins but bostrycoidins (8)

The nomenclature of the genes and respective enzymes within the *PKS3* cluster varies from study to study depending on which research group analysed it. Table 1 provides a translation of the nomenclature to facilitate the understanding. In this study, the genes of the cluster are annotated as *fsr1, fsr2, fsr3*, etc and their respective enzymes FSR1, FSR2, FSR3, etc.

Table 1: Translation of nomenclature of enzymes encoded by the *PKS3* cluster. In this study, the annotations of FSR1, FSR2, FSR3, etc will be utilised.

***F. graminearum* (Frandsen)**	***F. fujikuroi* (Studt)**	***F. solani* (In this study)**
PGL1	PGL1	FSR1 or PKS3
PGLJ	PGL2	FSR2
PGLM	PGL3	FSR3
PGLX	PGL4	FSR4
PGLV	PGL5	FSR5
PGLX	PGL6	FSR6

While six core genes have been identified within the *PKS3* gene cluster, *fsr7* the neighbouring gene of *fsr6* has not yet been recognised as essential for the production of fusarubins but has however been preserved among species. Similarity in promoter motifs and gene sequences can be recognised in the concerned species. *Fsr1* is syntenic in all *Fusarium* sp. containing the cluster (6). The organisation of the seven genes is systematically in that order with only a few disparities caused by evolutionary changes in species outside of GFC like *F. solani* as shown in Figure 4 (6,8). *F. graminearum*, *F. proliferatum*, *F. solani* and *F. virguliforme* have an insert of gene(s) between *fsr3* and *fsr4* of up to 17 genes, which functions still have to be experimentally determined (6).

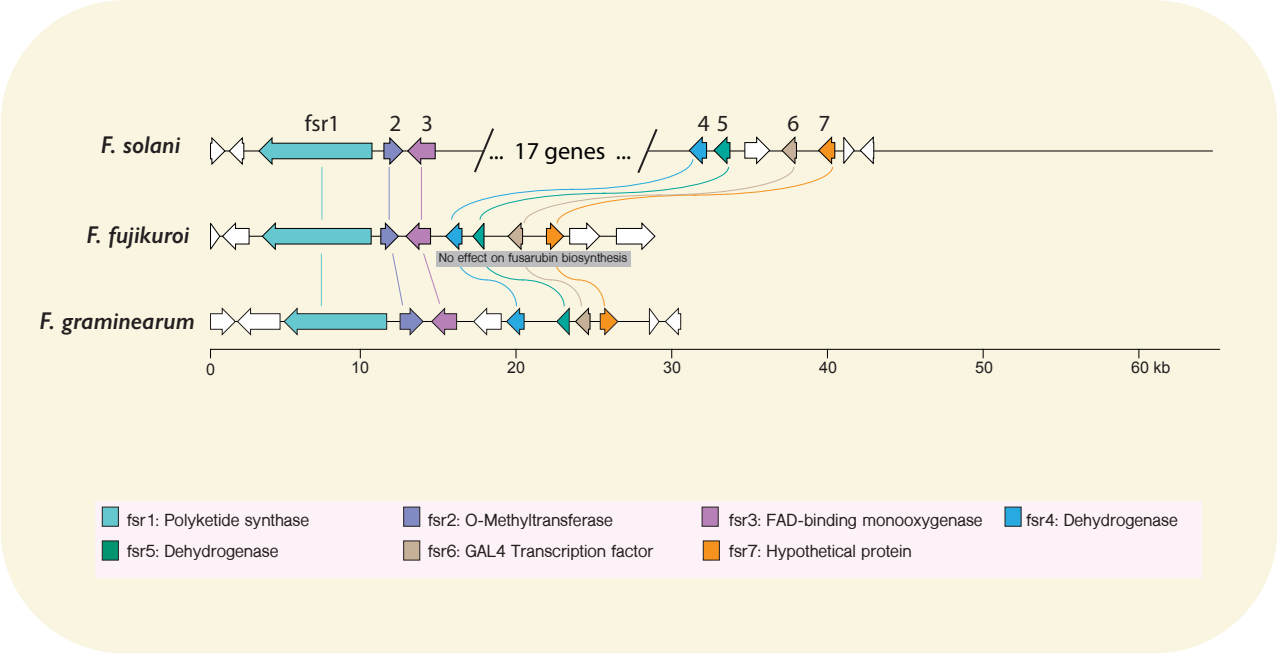

Figure 4: Homology analysis between *F. fujikuroi*, *F. solani* and *F. graminearum*. The *PKS3* gene cluster is intact in all 3 species. *fsr1* to *fsr7* is present but an insert of 17 genes lies between *fsr3* and *fsr4* in *F. solani*.

F. fujikuroi belongs to the GFC, *F. graminearum* belongs to the *Graminearum* complex and *F. solani* to the FSSC complex. However, consistently in all concerned species, the different core genes *fsr1* to *fsr7* have the same putative roles as illustrated in Figure 4. *fsr1* is encoding for a nrPKS, *fsr2* encodes an O-methyltransferase, *fsr3* encodes a FAD-dependent monooxygenase and *fsr6* is a $Zn_2(II)Cys_6$ family transcription factor (tf). *fsr4* and *fsr5* have unknown functions but appear to have regulatory roles like *fsr6* in *F. fujikuroi*. *fsr1* to *fsr3* are the only genes responsible for the actual biosynthesis of fusarubins in *F. fujikuroi* and *F. graminearum*. (8) Experimentally, the activation of the gene cluster

is done by variation of culture conditions, overexpression of transcription factors and other related gene clusters or with the help of epigenetic controls (13). The different functions of each gene in the different species were elucidated via those methods.

Fusarubins found in *Fusarium* comprise of a large group of naphthoquinones, all produced by the enzymes encoded by the *PKS3* cluster. As mentioned before, the main fusarubins produced by the *PKS3* cluster are species and conditions dependent. *F. solani*, shows a bigger gene cluster and therefore could explain the disparities in the biosynthetic pathway. As fusarubins pathway in *F. solani* has not been described yet, the biosynthetic pathway of fusarubins in *F. fujikuroi* and *F. graminearum* is used as reference.

3.2 Biosynthesis of Fusarubins in *F. graminearum* and *F. fujikuroi*

The following section covers the biosynthetic pathway of bostrycoidin and fusarubin as suggested in *F. graminearum* and *F. fujikuroi.* All intermediates and compounds mentioned are referring to the Figure 5.

8-O-methylfusarubin [4] is the major fusarubin produced by the *PKS3* gene cluster in *F. fujikuroi*. However, in the perithecia of *F. graminearum*, bostrycoidin [10] is the major pigment which is also issued from the same gene cluster. The biosynthesis of these two pigments initiate similarly as shown in the proposed pathway in Figure 5.

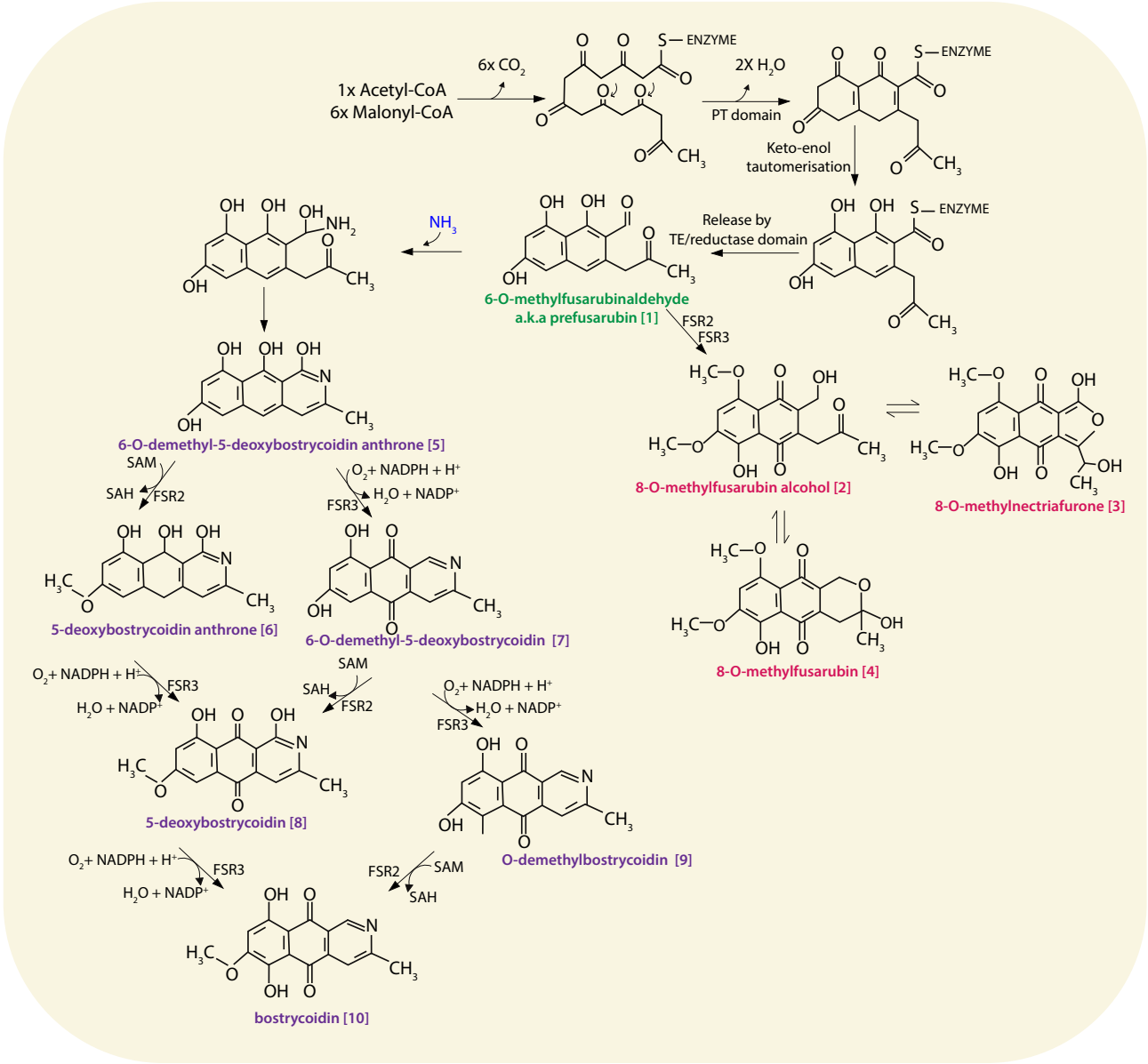

Figure 5: Proposed biosynthetic pathway for the formation of bostrycoidin and 8-O-methylfusarubin. The black arrows lead to the formation of pre-fusarubin, which is the shared precursor between both metabolites. The purple intermediates indicate the pathway leading to bostrycoidin in *F. graminearum* and the red intermediates correspond to pathway leading to 8-O-methylfusarubin in *F. fujikuroi* (6,13). Note that FSR2 is a methyltransferase mediated by the loss of the methyl group from SAM to form SAH and FSR3 is a monooxygenase that incorporates hydroxyl groups by the reduction of O_2 to H_2O.

All studies have consistently elucidated that FSR1, FSR2 and FSR3 are the only enzymes directly related to the biosynthesis of fusarubins. The biosynthesis of 8-O-methylfusarubin and bostrycoidin starts with one unit of acetyl-CoA and six malonyl-CoA units. PKS3 is a non-reducing polyketide synthetase (nrPKS) present in all *Fusarium* species. nrPKS are specifically synthesised with domains like SAT starter unit acyl transferase, KS ketoacyltransferase, MAT malonyl acyltransferase, ACP acyl carrier protein, and PT product template. They are characterised by the absence of reductive steps in the chain elongation of the polyketides. (13,14)

Just like most nrPKS, FRS1 (PKS3) has SAT, KS, MAT, ACP, PT domains and a release domain (15). At first, the MAT domain loads malonyl-CoA units and transfers units to ACP to form malonyl:ACP. The KS domain conducts a decarboxylation condensation of the malonyl units to form a linear heptaketide:ACP. PT performs a C2/C11 and C4/C9 aldol cyclisation to form a naphthalene ring bound to ACP. TE reduces the thioester bonds which leads to the release of the precursor of fusarubins, a $C_{14}H_{12}O_5$ aldehyde heptaketide chain, 6-O-demethylfusarubinaldehyde also called pre-fusarubin [1] (8,15). Pre-fusarubin goes through further configuration with FSR2 which methylates the hydroxyl groups at C6/C8 (8). FSR2 is an O-methyltransferase enzyme with two catalytic subdomains; N-terminal to bind to the substrate, in this case pre-fusarubin, and C-terminal subdomain to bind to the required co-factor, in this case S-Adenosylmethionine (SAM) (14,16). A methyl group is transferred from SAM which becomes S-Adenosylhomocysteine (SAH) in an ATP-dependent reaction as illustrated in Figure 6. (17)

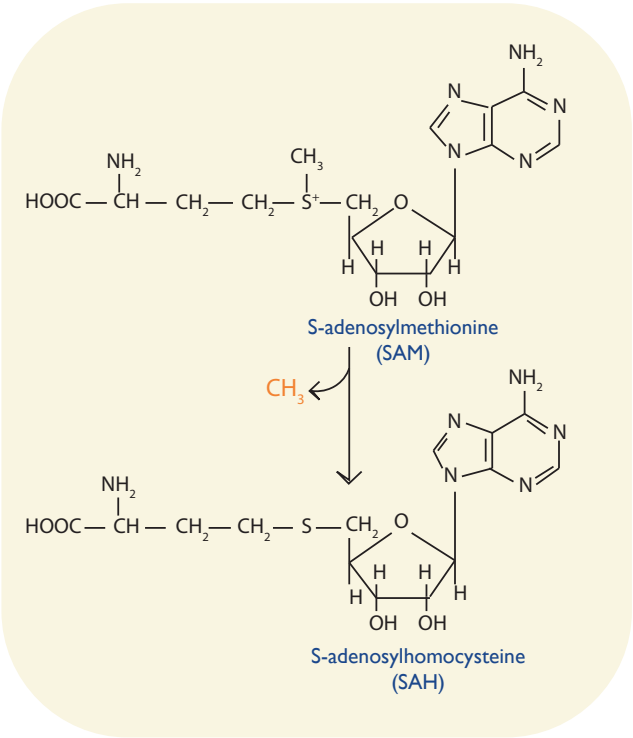

Figure 6: Methyl group transfer from the SAM cofactor catalysed by methyltransferase enzymes like FSR2. FSR2 requires SAM cofactors to methylate pre-fusarubin. (17)

Simultaneously, FSR3, a FAD-dependent monooxygenase, adds hydroxyl groups at C5/C10 (8). Monooxygenases are enzymes involved in redox biological reactions. They have an insertion site for flavin adenine dinucleotide (FAD), a respective cofactor, and add molecular oxygen to substrates with the help of NAD(P)H. Flavin monooxygenases like FSR3 are known to oxidise aldehydes and aromatic compounds. For oxidation reactions, the FAD cofactor catalyses the transfer of electron from the substrate to NAD(P)H. For reduction reactions, it catalyses the transfer of electron from NAD(P)H to the substrate, see Figure 7. (18,19)

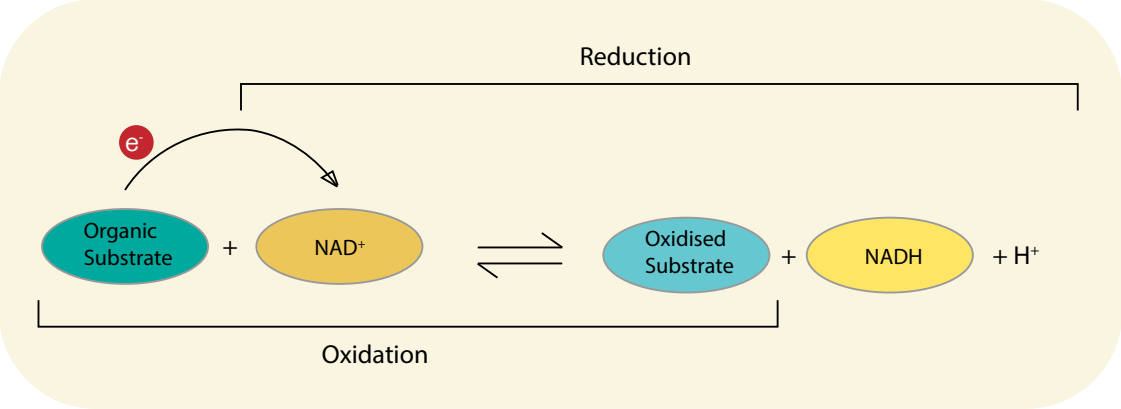

Figure 7: Biological redox reaction by monooxygenases mechanism. In oxidation, NAD^+ accepts the electron and proton from the substrate, resulting in oxidation of the substrate and reduction of NAD^+ to NADH. One remaining proton is released into the medium. The reverse reaction can also occur for reduction of the substrate. This reaction is catalysed by FAD-dependent monooxygenases like FSR3 for polyketides biosynthesis (19).

As shown in Figure 5, FSR3 is responsible for the reduction of the pre-fusarubin aldehyde to an alcohol, 8-O-methylfusarubin alcohol [2] which equilibrates with 8-O-methylfusarubin, also called fusarubin [4] and 8-O-methylnectriafurone [3]. Pre-fusarubin can also be oxidised to a carboxylic acid which equilibrates with a lactone. The latter can go through further configuration, catalysed by FSR3, and form 8-O-methylanhydrofusarubinlactol or 8-O-methyl-13-hydroxynorjavanicin. (8) Variation of the chronology of the different catalysed steps by FSR2 and FSR3 can occur, revealing to the complexity and wide array of compounds produced by the fusarubin gene cluster. To form bostrycoidin, an amine group is added to pre-fusarubin to create 6-O-demethyl-5-deoxybostrycoidin anthrone [5]. With FSR2 and FSR3 the latter compound can be configurated into 5-deoxybostrycoidin anthrone [6] and 6-O-demethyl-5-deoxybostrycoidin [7]. FSR3 forms bostrycoidin [10] from the anthrone while FSR2 is required to form bostrycoidin from 6-O-demethyl-5-deoxybostrycoidin. FSR4 and FSR5 are dehydrogenases and have no identified functions in the biosynthetic pathway yet (13). FSR6 is a $Zn_2(II)Cys_6$ transcription factor acting as an upregulating activator for the gene cluster. Similarities in promoter sequences of the genes lead to conclude that FSR6 activates the transcription of the genes within the *PKS3* cluster and possibly another gene cluster responsible for mycelial pigmentation in *F. graminearum*. *F. solani* produces bostrycoidin and fusarubin from the same precursor in the mycelium (15). The addition of an amine group to the precursor after its release from the TE domain differentiate the biosynthesis of the two pigments (6).

F. graminearum

In *F. graminearum*, the *PKS3* gene cluster is responsible for the perithecial pigmentation caused by the accumulation of 5-deoxybostrycoidin. Frandsen et al. (2016) (6) shows that the deletion of *fsr1* leads to complete loss of pigmentation in the perithecia of *F. graminearum* (6). Similar results have been observed in *F. verticillioides* and *F. fujikuroi*. As mentioned, FSR1 is responsible for the biosynthesis for 6-O-demethylfusarubinaldehyde, known as the precursor of bostrycoidins and fusarubins. However, bostrycoidin alone is the pigment present in the perithecia in *F. graminearum* (6). Overexpression of *fsr1* in *F. graminearum* did not result in overexpression of the other genes on the gene cluster but led to the higher production of bostrycoidin pigments and of five intermediates not found in the *F. graminearum* wild type; 6-O-demethyl-5-deoxybostrycoidin, 5-deoxybostrycoidin, 5-deoxybostrycoidin anthrol in equilibrium with 5-deoxybostrycoidin anthrone, 6-O-demethyl-5-deoxybostrycoidin anthrone in equilibrium with 6-O-demethyl-5-deoxybostrycoidin anthrol and the dimer

purpurfusarin (6). The overexpression of *fsr6* resulted in overexpression of *fsr1*,2,3,4,5 and led to production of fusarubins as well during mycelial growth. Along with the increased concentrations of fusarubins, two intermediates were observed in the EO:*pglR* (overexpression of *fsr6*) mutant; 5-deoxybostrycoidin and 5-deoxybostrycoidin anthrol in equilibrium with 5-deoxybostrycoidin anthrone. (6) Additionally, the mycelial pigmentation of EO:*pglR* turned to yellow, suggesting that *pglR* could also activate another gene cluster responsible for the mycelial pigmentation. The deletion of *fsr2* and *fsr3* led to light yellow perithecia respectively and *Δfsr5* (deletion of *fsr5*) resulted in a dark brown perithecia (6). The overview of all deletion mutants grown on three different media is shown in Figure 8.

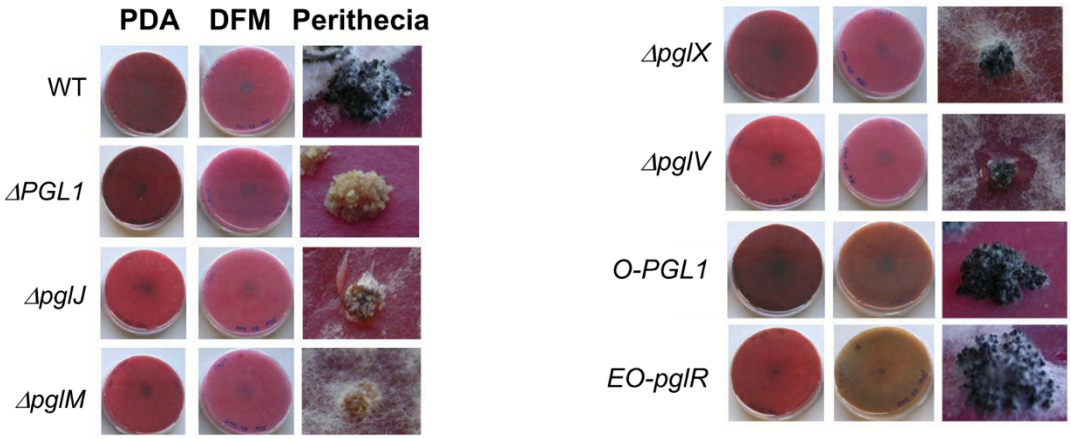

Figure 8: Deletion mutants of *F. graminearum* cultivated on PDA, DFM and carrot agar. The deletion of *fsr1* (*PGL1*) shows complete loss of the black pigmentation. All deletion resulted in a smaller perithecia. Deletion of *fsr2* (*pglJ*) , *fsr3* (*pglM*) and *fsr5* (*pglX*) resulted in a change of colour of pigment in the perithecia indicating their influence on the production of pigments. (6)

F. fujikuroi

In *F. fujikuroi*, 8-O-methylfusarubin is hypothesised to be responsible for the pigmentation of the perithecia. Similar to *F. graminearum*, when *fsr1* is deleted, the perithecia lost completely its pigmentation. In Studt et al. (2012) (13), Δ*fsr2* mutant led to production of 6-O-demethyl-10-deoxyfusarubin and 6-O-demethylfusarubinaldehyde. While Δ*fsr3* was not able to produce the pre-fusarubin, 6-O-demethylfusarubinaldehyde. (6,8) Deletion of *fsr4* and *fsr5* had no visual differences or production from the *F. fujikuroi* wild type. Moreover, individual deletions of *fsr2* to *fsr5* did not result in the downregulation of their neighbouring genes. (13) Similar results as for *F. graminearum* were obtained for *F. fujikuroi* from Studt et al. (2012, (13)) where the deletion of *fsr6* in *F. fujikuroi* resulted in the downregulation of all core genes in the *PKS3* cluster (13), proving the strong transcription regulation role of *fsr6*. It was concluded that *fsr4* to *fsr6* have regulatory roles which appear to only alter the quantity of fusarubin. The pictures of different knock-out mutants cultivated for the Studt et al. (2012, (13)) study illustrate the phenotypes of *F. fujikuroi*, as seen in Figure 9.

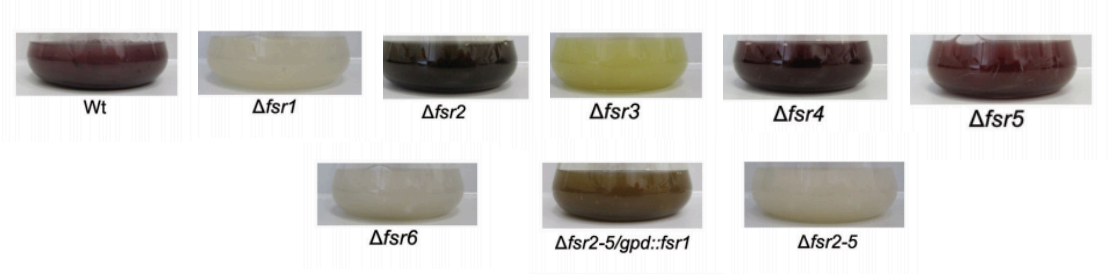

Figure 9: *F. fujikuroi* deletion mutants grown in synthetic ICI (Imperial Chemical Industries Ltd., UK) medium with 6mM sodium (13).

The regulatory system highly differs from species included within GFC. For example, an acidic environment is favourable for fusarubin production in *F. proliferatum* but is inhibitory for *F. fujikuroi*. (8) In *F. fujikuroi*, the optimal conditions for fusarubins are alkaline and a low nitrogen environment. The production of fusarubins highly depends on culture conditions (8). In the studies of *F. graminearum* and *F. fujikuroi* fusarubins pigmentation, different media were used for inoculation of the organisms, PDA and DFM for *F. graminearum* and ICI for *F. fujikuroi*, which is suspected to have influenced the biosynthetic pattern between fusarubins and bostrycoidins as well. In summary, the *PKS3* cluster reveals to have similar functions in *F. fujikuroi* and *F. graminearum*. It could be expected that the functions and pathway is similar to *F. solani*.

3.3 Fusarubins in *F. solani*

In *F. solani*, despite the differences in the organisation of the cluster, the binding sites motifs of the *fsr6* tf are still present in the promoter regions of the *fsr* genes except for *fsr3* and *fsr5*. (6) Moreover, fusarubins are produced in the mycelium for *F. solani* while they are present in the perithecia for *F. fujikuroi* and *F. graminearum* (6). Studies have revealed javanicin, bostrycoidin and fusarubin as main pigments produced in *F. solani* (12,15). This phenotypic difference could be a hypothesis for the disparities in the gene clusters. Note that the FSSC is a far-related complex to *F. fujikuroi* and *F. graminearum* supporting why the clusters look different.

Current literature provides a substantial overview of the biosynthesis of fusarubins in *F. graminearum* and *F. fujikuroi* despite some areas still needing clarification. *F. fujikuroi* and *F. graminearum* have the six core genes and produces 8-O-methylfusarubin and 5-deoxybostrycoidin respectively. *F. solani* also comprises of the same core with an insert of 17 unidentified genes. Their role could be linked to the diversity of the fusarubins produced in *F. solani,* and for the release of bostrycoidin, fusarubin and javanicin in the mycelium. Table 2 is a non-exclusive list of fusarubins compounds mentioned in the study. Note that some compounds were found in the perithecia and mycelium due to overexpression of transcription factor, namely in *F. fujikuroi*.

Table 2: Non-exclusive summary table of fusarubins produced in *F. solani (Fs)*, *F. fujikuroi (Ff)* , *F. graminearum (Fg)* and *F. demecellure (Fd).* Red compounds were described in the mycelium while purple compounds were found in the perithecia. (1,8–12)

Names	Tissue	Strain
8-O-methylfusarubin		*Fs, Ff, Fd*
Javanicin		*Fs, Fd*
Bostrycoidin		*Fs, Fg, Fd*
Anydrofusarubin		*Fs, Fd*
Solaniol	**Mycelium**	*Fs*
Martinicin		*Fs*
Nectriafurone		*Fs*
O-demethylfusarubin		*Fd*
O-demethyljavanicin		*Fd*
8-O-methylnectriafurone		*Ff*
8-O-methyl-13-hydroxynorjavanicin		*Ff*
8-O-methylanhydrofusarubinlactol		*Ff*
13-hydroxyjavanicin		*Ff*
6-O-demethyl-10-deoxyfusarubin		*Ff*
6-O-demthylfusarubinaldehyde		*Ff*
Fusarubinaldehyde	**Perithecia**	*Ff*
5-deoxybostrycoidin		*Fg*
6-O-demethyl-5-deoxybostrycoidin		*Fg*
5-deoxybostrycoidin anthrol		*Fg*
5-deoxybostrycoidin anthrone		*Fg*
6-O-demethyl-5-deoxybostrycoidin anthrone		*Fg*
6-O-demethyl-5-deoxybostrycoidin anthrol		*Fg*
Purpurfusarin		*Fg*

4. Research Objective

Fusarubins are fungal pigments characterised by being the secondary metabolites issued from the expression of the *PKS3* cluster. The latter is a nrPKS present in *F. solani* comprising the genes *fsr1* to *fsr6*. Current literature has developed the putative roles of *fsr1*, *fsr2*, *fsr3* and *fsr6* as nrPKS, O-methyltransferase, FAD-monooxygenase and transcription factor respectively. Together, *fsr2* and *fsr3* work on the main configuration of pre-fusarubin to fusarubin. However, *F. solani* has 17 extra non-annotated genes between *fsr3* and *fsr4* that have a hypothesised relation with the configuration of the many diverse fusarubins yielded by *F. solani.* The overexpression of the transcription factor, *fsr6*, fully activates the gene cluster transcription. This genetic modification makes it easier to observe the complete network of fusarubins in *F. solani.* If so, the OE::fsr6 mutant is better fitted host organism for studying the cluster rather than the wild type.

The questions this study would try to answer are at first: Do the 17 genes insert in Fs-*PKS3* participate in the cluster and fusarubins production? Is *fsr6* a transcription factor effective on the 17 extra genes as well? If so, would it be possible to link those additional genes to the biosynthesis?

In order to identify the genes active within *Fs-PKS3* cluster, a knock-out experiment, similar to the study for *F. fujikuroi* in Studt et al. (2012) (13) will be executed. After individual deletion of each gene in the cluster, including the 17 gene insert, a chemical investigation will follow to possibly link the resulted produced metabolites to the targeted genes. The chemical analysis of the resulting compounds, possibly equilibrating intermediates or uncomplete conformed fusarubins, will help understand the pathway reactions. Targeted deletion would be performed with integration of a drug cassette that replaces the targeted *PKS3* genes and ensure selection of the transformants at the same time. Through individual knock-out of each gene within the gene cluster and chemical analysis of the metabolites, it will be possible to know which genes participate in the production of fusarubins and which enzymatic reactions they are responsible for.

The main objective of this research project is to determine the roles of the *PKS3* genes in the fusarubins production of *F. solani*. The *PKS3* genes are responsible for the mycelial pigmentation of the species and the different functions and interactions between the genes are yet to be recognised. Moreover, the additional genes located in the cluster have no linked action to the biosynthetic pathway. In order to clarify their hypothetical roles in the fusarubin production, a knock-out approach was designed combined with a metabolite chemical analysis. The investigation of the biosynthesis of fusarubins would provide great support for potential optimisation of the strain in pigment production but would also add to the clarification of the secondary metabolism in *Fusarium* species.

5. Theoretical Background for Experimental Methods

The targeted deletion of the *PKS3* genes is conducted via *Agrobacterium* mediated transformation of *F. solani*. The following sections cover the concepts of the knock-out method and *Agrobacterium* mediated transformation as support to facilitate the understanding of the experimental work.

5.1 Knock-Out of Genes for Biosynthesis Investigation

The production of fungal secondary metabolites often requires genetic manipulation. Naturally, polyketide genes can remain silent in optimal cultivating conditions or the natural concentration yields can be low or sometimes the pigments toxicity inhibits the healthy growth of the microorganisms. These aspects make it difficult to naturally observe and understand the production for some metabolites. Therefore, biotechnology engineering techniques have been developed to elucidate and optimise the biosynthetic pathways of fungal pigments. Methods such as overexpression of silent genes or entire gene clusters via integration of constitutive promoters have been done. Heterologous expression of the genes of interest in a well-studied host or even deconstruction or swapping of PKS domains have been successfully achieved on various fungi to shed light on the complexities of secondary metabolism. At last, the investigation of a specific pathway can be achieved by selected inactivation of the genes. (14) Through knock-out, it will be possible to define the roles of the composing genes of the *PKS3* cluster. The replacement of the target gene by a compatible drug cassette would inherently delete the activity of the gene. When succeeded, the emerging mutants can show phenotypic and metabolic changes caused by the absence of the gene's enzymatic reactions. The different engineering method for characterisation of gene functions, including knock-out, are represented in Figure 10.

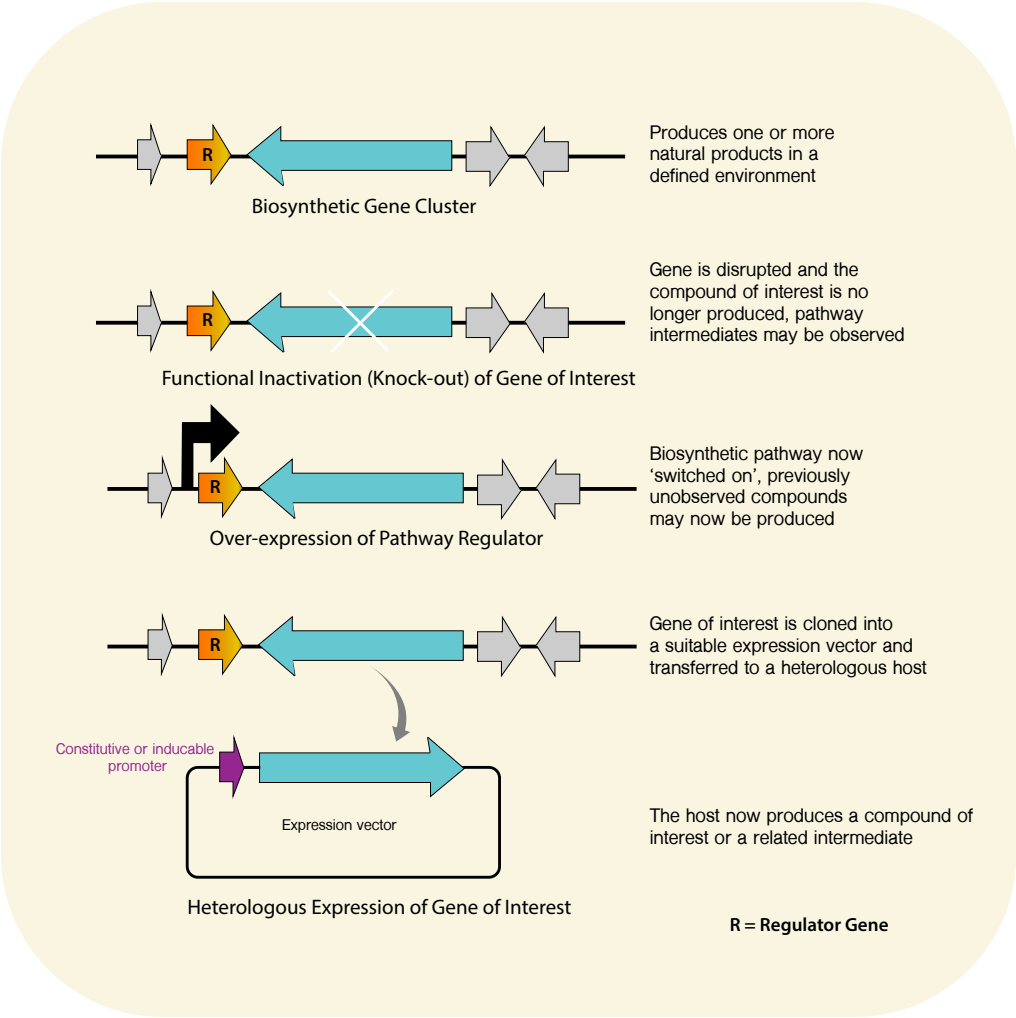

Figure 10: Biotechnology engineering methods for characterisation of gene functions in fungal polyketides biosynthesis: Knock-out or heterologous expression of the target gene, overexpression of a regulator can help elucidate a gene cluster and the compounds associated. (14)

As illustrated in Figure 10, the knock-out of a gene leads to lack of production of the specific compound and/or yielding of intermediates as the corresponding enzyme is now missing. In this manner, the missing enzymatic function or compound can be associated to the deleted gene. By overexpressing the pathway, the cluster is activated constitutively. Observation of new compounds and difference in growth pattern of the fungus could be noticed. Lastly, the heterologous expression is a great way to isolate a target gene and associate its function to the observed production in the new host.

The inactivation of a gene is mediated by a drug cassette, which will replace the targeted gene and ensure selection for recombined mutants. The transformation relies on the homologous recombination ability of the fungus. Therefore, in current protocols, the minimal genetical materials required for knock-out are a linear dsDNA comprising targeted homologous regions and a drug-resistance gene (20).

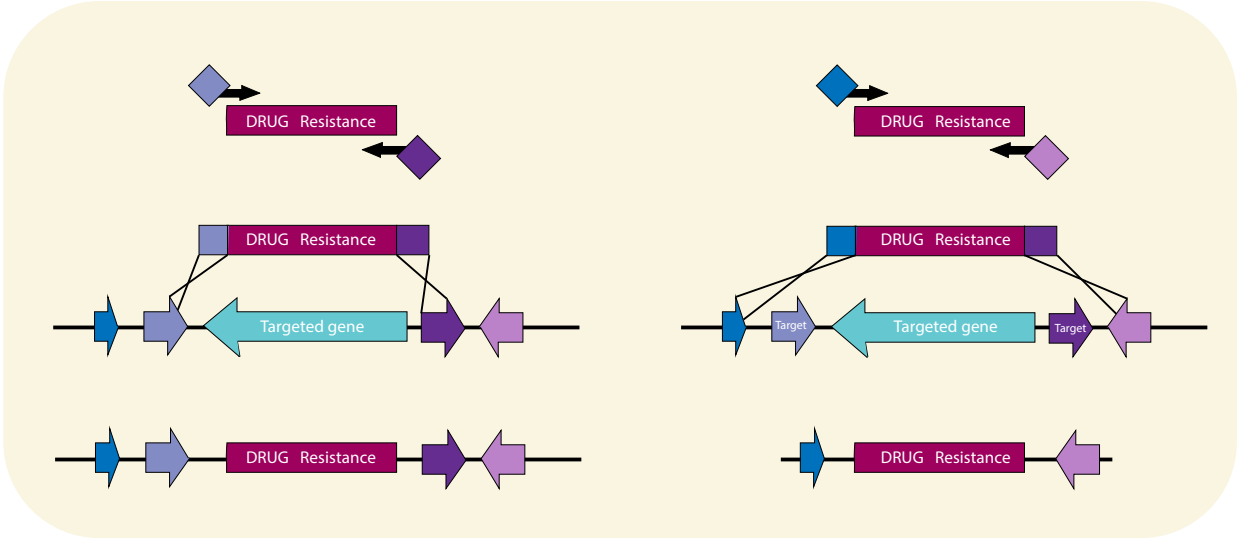

Figure 11: Target replacement for knock-out of genes. The dsDNA of selection marker and homologous extremities regions are amplified by PCR. The resulting drug cassette can recombine and replace the targeted gene. This method can only delete one gene (left side) or many adjacent genes (right side). (20)

Antibiotic-relying selections have the advantages of selecting the correct strain early in the transformation process. These work well for single gene deletion or adjacent genes deletion as shown in Figure 11. On the left side of the figure, a drug resistance cassette is amplified with homologous up and downstream regions. Thanks to the homology to the target gene locus, the drug cassette can replace the gene. The similar process is illustrated on the right side, with several adjacent genes. Aminoglycoside antibiotics such as geneticin or hygromycin B are familiar drugs used for their toxicity to prokaryotes and eukaryotes (21). Their mechanism of action depends on the strain exposed but mainly inhibits protein synthesis and misreads polypeptides synthesis (22,23). Integration of the bacterial *neoR* gene allows protection from the lethal inhibition caused by geneticin (21). The resistance against hygromycin is generated by integrating the *hph* gene (22). The cells containing the resistance genes encode proteins which can defect the antibiotic four ways: changes in cell wall permeability, chemical inactivation of the antibiotic, modification of the target molecule or efflux of the antibiotic outside of the cell (24,25).

The *neoR* and *hph* genes are therefore common selection markers in fungal transformation systems. As there are only a few number of selection markers genes for filamentous fungi, recycling of the same selection marker is a possibility in cases of multiple gene deletion within the same strain. (26) The selection marker is integrated with flanking region recognisable by recombinases for latter excision or insertion. (27) When working with a genetically modified organism, which has already been previously transformed with a selection marker, it is important to use a different SM for the ulterior transformations. This ensures a clear selection associated with the ulterior transformation.

It has been established that the different biotechnology engineering methods could be applied to fungi in order to activate or inactivate genes and investigate the biosynthetic pathways. Overexpression of a regulator gene, such as a transcription factor, ‘switches on’ the cluster leading to the production of all related compounds. Inactivation/knock-out of genes can be effectuated with the means of a drug cassette, replacing the targeted gene and ensuring selection of the transformants at the same time. The knock-out does indicate the function of a gene by associating the produced intermediates to the enzymatic reactions missing. In this study, the combination of these two methods; overexpression of a regulator and knock-out of a gene are combined. As mentioned before, the targeted deletion of the

PKS3 cluster is performed on the *fsr6* overexpression mutant. The reasoning being that effect of the missing genes would be more visible than in the wild type. There is a multitude of fungal transformation protocols used to mediate the integration of the cassette in genomic DNA and they are strain-dependent. *Agrobacterium* mediated transformation is applicable for *F. solani*; the next section covers the elementary technicalities of the procedure.

5.2 *Agrobacterium* Tumefaciens-Mediated Transformation

The methods for genetic transformation in filamentous fungi are numerous and protocols keep on being updated. Each have their advantages and inconvenience and/or are favoured by some fungal strains. When it comes to *F. solani*, *Agrobacterium tumefaciens* mediated transformation (AMT) has proven to be applicable. AMT principle is based on the naturally occurring infection of a plant by gram-negative *A. tumefaciens*. The bacterium contains a tumour-inducing plasmid (Ti plasmid) which becomes active when in contact with a specific plant hormone, acetosyringone (AS). The Ti plasmid comprises of different genes to turn on the virulence of the bacterium, including a fragment of transfer DNA (T-DNA) located between a 'left' and 'right' border (LB and RB) to be inserted into the nucleus of the plant. The T-DNA encodes growth-altering Vir proteins to weaken the plant (28). VirD2 is a protein issued from Ti which binds to the DNA and is recognised by the secretion channels of the bacterium, enabling its transfer to the plant host (28). The exact same principle is applied to fungi by co-cultivating the two microorganisms. A similar designed plasmid with the targeted T-DNA, LB and RB can be inserted in *Agrobacterium* to be transferred to the fungus. To avoid random inserts into the fungal genomic DNA, the T-DNA also comprises of homologous regions identical to the fungal genomic locus to facilitate homologous recombination.

AMT offers different advantages like replacing protoplasting, which happen to be difficult on some fungi. Moreover, the T-DNA is inserted in a single copy into the fungal genome allowing a clear visualisation of the phenotype changes (28). The efficiency of AMT depends on a few factors; the ratio of fungi and bacteria concentrations, the concentration of AS which triggers the transcription of the Vir proteins, the temperature and period of incubation. These should be empirically tested as they are highly dependent the strains.

In this study, the bacterium T-DNA is designed to target the deletion *PKS3* gene cluster and replacement by a drug cassette. The designed knock-out plasmid is inserted in *Agrobacterium* prior to *F. solani* transformation. This procedure is developed with an optimised AMT protocol for the *F. solani*-*Agrobacterium* system.

6. Materials and Methods

6.1 Experimental Workflow

The development of the experiment was designed as follows, which steps are also presented in Figure 12. The first step of the experimental work included the creation of the deletion targeted plasmids, specific to each *PKS3* genes. A total of 16 targeted knock-out plasmids (pKO-xxx) were constructed, each corresponding to a specific gene or group of genes of the *PKS3* cluster. The required fragments of the plasmids were amplified by PCR with homologous tails and then assembled inside *S. cerevisiae*.

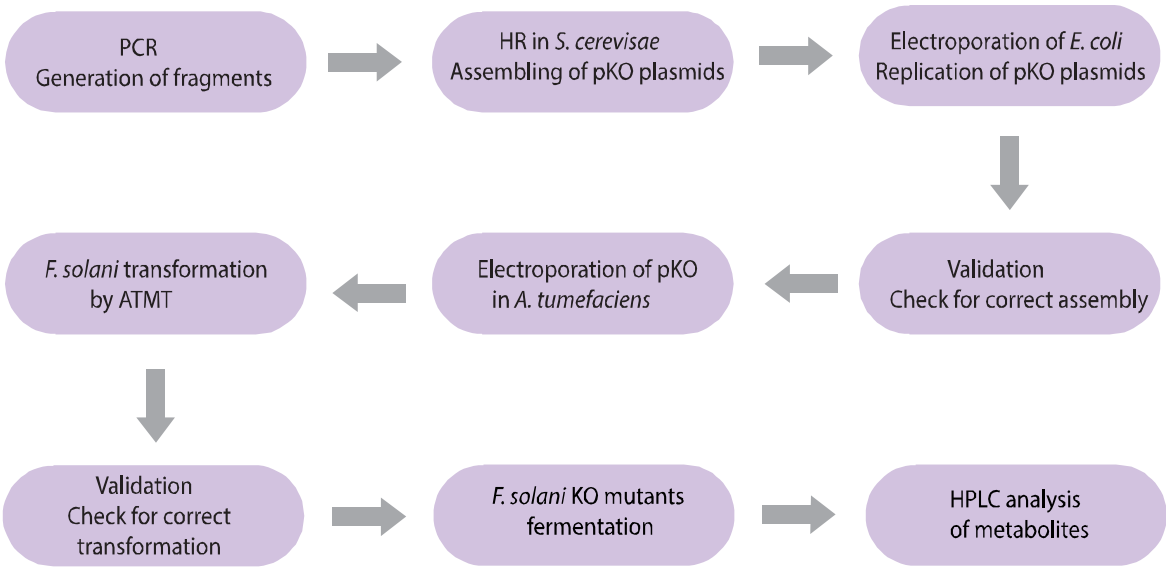

Figure 12: Simplified overview of the chronological steps followed in the experimental procedure with objective to create targeted deletion *F. solani* mutants and analyse their pigments.

The plasmids consisted of an upstream and downstream region homologous to the genomic upstream and downstream sequences of targeted gene. In between the up and down regions lied the drug cassette for hygromycin resistance which would replace the targeted gene and thereby delete it while allowing selection of the successful mutants. Finally, the plasmid is composed of a backbone cassette including all the required genes for the integration of the plasmid into *S. cerevisiae* and *E. coli*. Most importantly, the backbone contains the LB and RB necessary for the transfer of the T-DNA from *Agrobacterium* to the fungus. An example of a pKO-xxx plasmid is shown in Figure 13.

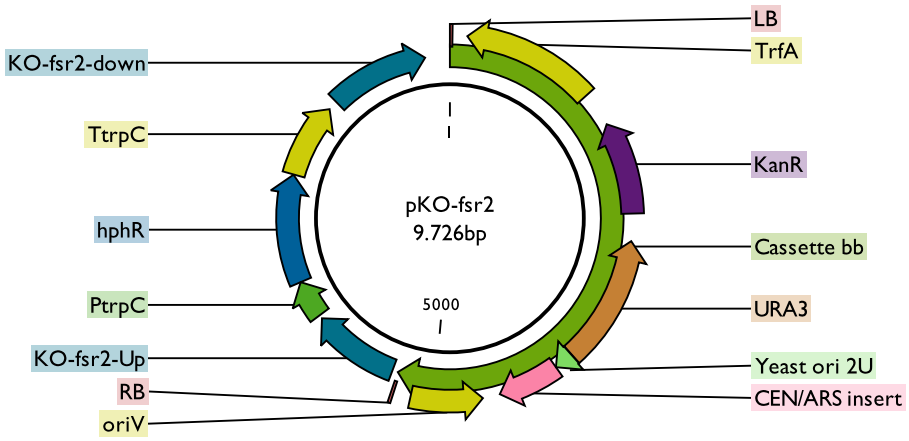

Figure 13: Assembled plasmid for pKO-fsr2. The plasmid was assembled inside *S. cerevisiae* with four fragments and homologous tails which were generated by PCR. The four amplified fragments are the up and down regions from *F. solani* (KO-FSR2-UP and KO-FSR2-DOWN), the drug cassette (*PtrpC* as promoter, *hphR* as resistance gene, *TtrpC* as terminator) from plasmid prf-H2U and lastly the backbone from pSHUT3-32 including the LB, RB, origins of replications for yeast and *E. coli*, *URA3* and *KanR* selection markers and *TrfA* for bacterial DNA replication. The figure is made using CLC Main Workbench 8.

The yeast colonies were selected by phototrophic selection without uracil. After the assembly of the plasmids in yeasts, they were electroporated into *E. coli* which is used as cell factories to create copies of the plasmids. Autotrophic selection with kanamycin was used on the bacteria. Validation of the assembly was executed in three manners on the purified plasmids from *E. coli*: restriction digestion of the known restriction sites, PCR amplification of the up and down regions and DNA sequencing. Following the verification of plasmids, they were inserted into *Agrobacterium* by electroporation. The last part of the procedure revolved around the transformation of the *F. solani* strains by AMT. Once the mutants were successfully generated, their fermentation and identification of their metabolites could be done to conclude the experimental work.

The objective of this research would be met by categorising the different pigments issued from the *PKS3* cluster by their corresponding genes. The findings would also provide an understanding of the internal regulation of the *PKS3* cluster in *F. solani*. The coming sections contain a detailed flow chart, and materials and methods of this study.

6.2 Flowchart

A flowchart was made to facilitate the understanding of the experimental procedure. This figure presents an overview of the various steps involved.

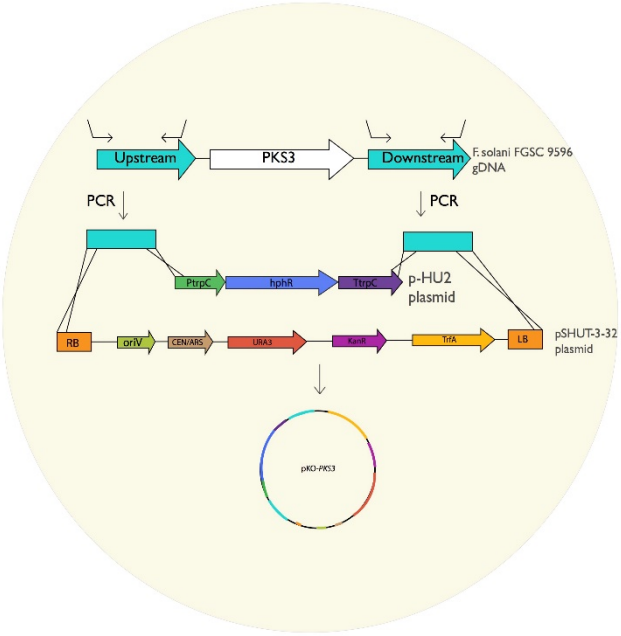

The upstream and downstream regions corresponding to each of the genes in the cluster were amplified by PCR with flanking tails homologous to the drug cassette and the backbone. The fragments were assembled in *S. cerevisiae* by HR and the cells were selected by auxotrophy towards uracil. The final pKO plasmid was extracted from yeast, electroporated into *E. coli* for replication and electroporated into *A. tumefaciens*.

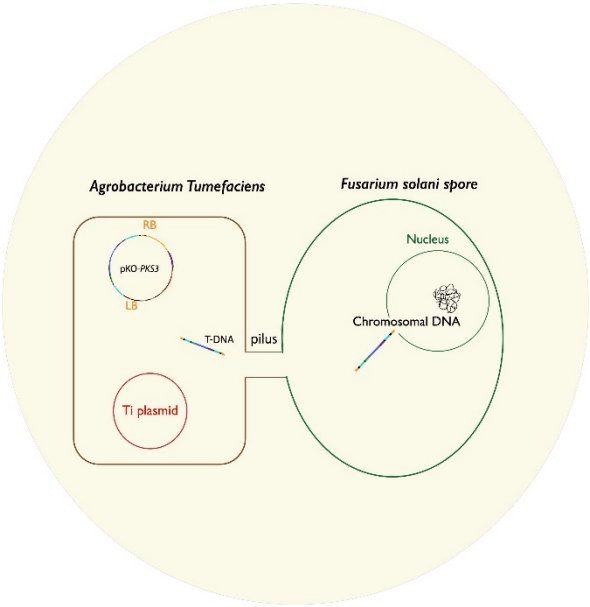

The plasmid containing the T-DNA of homologous regions and drug cassette lying in between the LB and RB will be transferred to the fungi spores through the bacterium pilus. This process, AMT, is enabled by the activation of the Ti plasmid and virulence of the bacteria when in contact with AS.

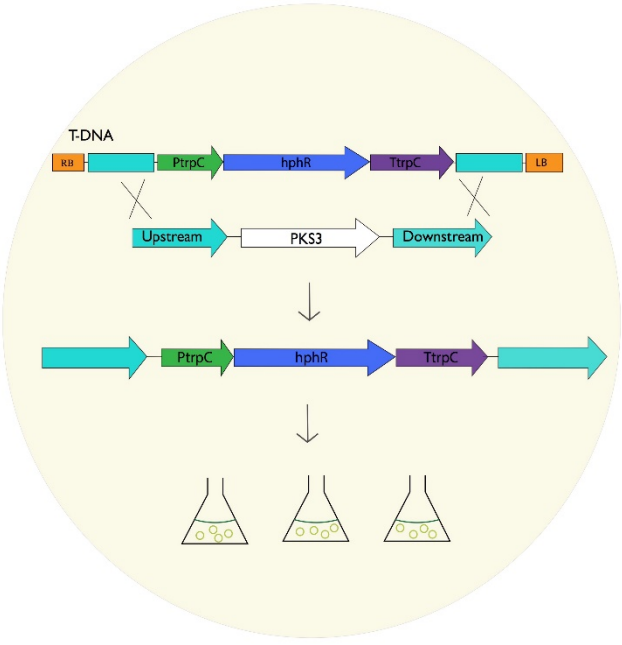

In the spores' nucleus, the T-DNA containing the homologous up and down region and selection marker will be recombined in the *PKS3* locus. The targeted gene will be replaced by the selection marker for hygromycin B resistance. The selected mutants will be fermented and their mycelial pigments analysed by HPLC.

6.3 Materials and Methods

Primer and pKO Plasmids Design

To perform the 16 deletions of targeted genes, 32 pairs of forward and reverse primers were designed and then ordered from Eurofins Genomics, Germany corresponding to the respective upstream and downstream regions. The complete *PKS3* gene cluster, referred to as NECHADRAFT_101778 from *Nectria haematococca* mpVI 77-13-4 in chromosome 10, was visualised with CLC Main Workbench 8, supporting the primer design which was done with the help of the online tool Primer3Plus. Additionally, two pairs of primers were designed from the template plasmids pRF-HUE and pSHUT3-32 to amplify the selection marker cassette and backbone respectively. All primers were designed with homologous tails to the upstream and downstream fragments to ensure homologous recombination in *S. cerevisiae*. The amplified up and down regions of each gene, drug cassette and backbone were amplified to be recombined in a knock-out plasmid. All pKO plasmids are to be found in Appendix I. The tail of forward primers of all up regions had homology to the backbone and the tail of reverse primer were homologous to the border of the selection marker. The tail of forward primer of all down region were homologous to the border of the selection marker and the reverse primer was homologous to the border of the backbone. The primers' sequences can be found in Appendix II.The 16 pKO plasmids are all identical except for the up and down regions which are respective to each gene. The selection marker *hphR* (hygromycin ß-phosphotransferase) which encodes for resistance against hygromycin B antibiotic is collated to its respective promoter and terminator, *PtrpC* and *TtrpC*. The backbone consists of thLB and RB which are signals for DNA exchange for the *A. tumefaciens*. *TrfA* is the bacterial DNA replication initiator. *KanR* encodes for kanamycin resistance, required for *E. coli* transformation. *URA3* encodes for uracil auxotrophy necessary for *S. cerevisae* transformation. *Yeast ori 2u* and *CEN/ARS* are the origins of replication and centromere sequence for DNA replication. The primers were designed to have a total size of 20 nt (an extra 20 nt was added as flanking tails), a melting temperature, T_m, of 60 °C and a GC content of 50-60 %. All subsequent primers designed for colony PCR and validation of the transformations had similar characteristics. Before use, all primers (100 pmol/µL) were diluted to 20x with Milli-Q (MQ) water.

PCR

50 µL of PCR reaction volume was carried out inside the PCR incubator (T100 Thermal Cycler Bio-Rad). Each reaction mix comprised 28.3 µL of MQ water, 10 µL HF buffer 5 µL dNTP (10mM), 1.2 µL of DNA template, 0.3 µL Phusion polymerase (2 U/µL), 2.5 µL of each primers (Thermo Fischer). The products were validated by size via agarose gel electrophoresis (AGE) (PowerPac Basic BioRad). Colony PCR was performed on the mutants for validation of the transformations. For that procedure, some mycelial material was taken from the PDA plates with an inoculation loop and transferred to 300 µL of lysate solution. After vortexing for 1 min, the solution was centrifuged to spin the mycelial particles to the bottom. 0.5 µL of the lysate was included in the PCR reaction mix as described earlier with addition of 5 µL BSA solution. A 1 % agarose gel was casted by solubilising 0.4 g agarose powder (Medium EEO by Fisher BioReagents) in 40 mL 1X TAE buffer (50 X TAE Electrophoresis Buffer, Thermo Scientific) and a drop of ethidium bromide solution (Thermo Scientific). The products were loaded in the wells of the gel and migrated through it for 40 min at 90 V. The size ladder (1 kb (0.5 µg/µL) gene ruler by Thermo Fischer) was loaded alongside of the products for verifying the sizes with the gel imaging apparatus (Gel Doc™ EZ Imager, Bio Rad). The PCR products were purified following the protocol of QIAquick® PCR Purification Kit (250) (QIAGEN GmbH) and eluted in 30 µL of EB buffer.

Gel Purification
When necessary, PCR products were purified from a 2 % agarose gel following the protocol of QIAquick® Gel Purification Kit (50) (QIAGEN GmbH). For example, the backbone fragment was purified from a gel to omit the original circular template which cannot be removed through the conventional QIAquick® PCR Purification Kit (250) (QIAGEN GmbH).

Yeast *S. cerevisiae* Transformation
The yeast transformations were performed following the protocol from 'High-efficiency yeast transformation using the LiAc/SS carrier DNA/PEG method' by Gietz et al (2007) (29) and 'Competent yeast cells that can be transformed with high efficiency using the LiAc/SS carrier DNA/PEG method' by Gietz et al. (2007)(30). The master mix and the DNA samples were prepared and refrigerated a day prior to the transformation. One plate of 200 µL yeast solution was used for each transformation. The concentration in fmol of each fragment utilised for the yeast transformations are listed in Appendix III.

Plasmid Extraction from S. cerevisiae, E. coli and A. Tumefaciens
The protocol included in 'Rapid generation of long tandem DNA repeat arrays by homologous recombination in yeast to study their function in mammalian genomes' by Vladimir Noskov et al. (2011)(31) was followed for isolation of the assembled pKO plasmids from *S. cerevisae*. The final precipitated DNA was dissolved in 1 mL of water. The isolation of the plasmids in *E. coli* and *A. tumefaciens* was executed with the QIAquick® Miniprep Kit (250) (QIAGEN GmbH) and precipitated in 25 to 50 µL of EB buffer. The final concentrations of extracted DNA from *E. coli* are listed in Appendix III – Nucleic Acid Concentrations III.

Electroporation of *E. coli* and *A. tumefaciens*
The pKO plasmids were inserted into *E. coli* and *A. tumefaciens* cells via electroporation according to the protocol described in BioRad protocol (32) with 0.2 cm cuvettes. Individual colonies were streaked on LB (35 g/L LB broth (Sigma-Aldrich), 20 g/L bacteriological agar (Sigma-Aldrich) plates until further proceedings. The following antibiotics were added to the plates' media to select the colonies: Kanamycin (50 µg/mL) for *E. coli* colonies and for *A. tumefaciens* kanamycin (50 µg/mL) with rifampicin (10 µg/mL).

Restriction Digestion
The purified pKO plasmids were digested with single or double restriction sites. The list of restriction enzymes used for each plasmid can be found in Appendix IV. The reagents, incubation temperatures and time were followed according to the user guide by Thermo Fischer Scientific (33).

Sequencing
Plasmid DNA samples were sent to Eurofins Genomics (Germany) in recommended concentrations according to their TubSeq service ordering guide (34). The Tubseq service was requested to sequence only the assembled up and down regions of the pKO plasmids.

Agrobacterium Mediated Transformation
The transformation of *F. solani* (*N. haematococca* mpVI 77-13-4) was executed according to optimised protocol described in Appendix V. The procedure is detailed and provides elementary technicalities and remarks on the transformation protocol. The resulting mutants were re-streaked twice on PDA plates.

Sequence Data and Phylogenetic Analyses

The genomic data of all analysed strains was recovered from the GenBank database. The protein prediction was conducted via CDD and the web-based tool Interpro (35). The prediction of proteins within the *PKS3* cluster inspired the naming for the knock-out plasmids. Phylogenetic analyses were performed by retrieving GenBank files, assembling them to the *PKS3* gene sequence reference in CLC Main Workbench 8 and lastly illustrated via the software Easyfig.

Fermentation and Liquid Extraction of Pigments

For the pigment qualification experiment, each mutant was inoculated in 30 mL CZ (1 g L^{-1} KH_2PO_4 (VWR Chemicals), 0.5 g L^{-1} $MgSO_4.7H_2O$ (VWR Chemicals), 0.5 g L^{-1} KCl (VWR Chemicals), 0.2 mL L^{-1} trace element solution consisting of 0.05 g mL^{-1} citric acid, 0.05 g mL^{-1} $ZnSO_4.6H_2O$, 0.01 g mL^{-1} $Fe(NH_4)_2(SO_4)_2.6H_2O$, 2.5 mg mL^{-1} $CuSO_4.5H_2O$, 0.5 mg mL^{-1} $MnSO_4$, 0.5 mg mL^{-1} H_3BO_3, 0.5 mg mL^{-1} $Na_2MoO_4.2H_2O$) and MAT liquid media (60 g L^{-1} D-(+)-Maltose monohydrate (6363-53-7), 9.2 g L^{-1} $C_4H_6O_6(NH_3)_2$, 1 g L^{-1} KH_2PO_4, 0.5 g L^{-1} $MgSO_4.7H_2O$, 0.01 g L^{-1} $FeSO_4.7H_2O$, 0.01 g L^{-1} NaCl, 0.01 g L^{-1} $CaCl_2$, 1 mL L^{-1} 1000X salt solution (1000X salt solution: 8.8 g L^{-1} $ZnSO_4.7H_2O$, 0.4 g L^{-1} $CuSO_4.5H_2O$, 0.06 g L^{-1} $MnSO_4.H_2O$, 0.06 g L^{-1} H_3BO_3, 0.04 g L^{-1} $(NH_4)_6Mo_7O_{24}.4H_2O$), pH adjusted to 5.9) in a 50 mL shaking flask and incubated at 28 °C and 100 rpm for 7 days. 10 mL of the culture media was recovered by filtration through Miracloth and liquid-liquid extraction, similar to the method described in Westphal et al. (2018) (36), was conducted. The medium was first acidified with 660 µL 5 M HCl (VWR Chemicals). Afterwards, the initial volume was doubled with chloroform (VWR Chemicals) and shaken. 6.6 mL 10 % NaCl solution and 6.6 mL methanol (VWR Chemicals) were subsequently added and the mixture was shaken again. After set-tling, the top phase was decanted. 6.6 mL of methanol were re-added and the mixture was poured into a separating funnel and allowed to settle into two distinct phases. The chloroform phase in the bottom was collected, the top phase discarded. 3.33 mL of methanol and 3.33 mL of 10 % NaCl solution were added to the chloroform phase and separated into the funnel again. The pigments were collected by decanting the chloroform phase into a test tube, which was dried in a heating block (MIKROLAB AARHUS, Supertherm) at 40 °C with a nitrogen gas flow. The resulting dried pig-ments were resuspended in 500 µL methanol (VWR Chemicals) and filtered through a 0.22 µm filter before going into the HPLC vials. The samples were sent to the analytical lab of Aalborg University in Aalborg for fusarubins initial qualification by HPLC-HRMS.

7. Results and Discussion

Despite the interruption of the experimental work due to the Covid-19 pandemic crisis, the creation of all 16 pKO plasmids was executed. In total, 8 out of the 16 deletion cassettes were successfully transformed into *F. solani*. The following section discusses the results obtained from the construction of pKO plasmids until the executed fungal transformations.

7.1 Bioinformatics

Before starting the experimental targeted deletion in *F. solani*, a few bioinformatics tools were applied for investigation of protein roles and synteny conservation of genes in the *PKS3* gene cluster.

Protein Prediction

As mentioned before, the *PKS3* gene cluster in *F. solani* contains 17 unidentified genes which functions would be clarified through targeted deletion and chemical analysis of the corresponding metabolites. In order to clarify the roles before deletion, a protein prediction analysis was applied to each of the genes within the cluster. This analysis helped making a first screening of which genes are likely to be related to the fusarubins biosynthesis. Two proteins prediction databases were used to identify and classify the genes: Conserved Domains Database (CDD) (37) and Interpro (35). Table 3 lists the results of protein putative functions predictions from the two databases for each gene. The core essential *fsr* genes are marked in grey, they have experimentally defined functions as described in previous sections.

Table 3: List of the targeted genes for knock-out in *F. solani PKS3* cluster and their predicted functions by CDD and Interpro.

Gene Target	Locus tag	Size (bp)	Function (CDD)	Function (Interpro)
fsr1/PKS3	NECHADRAFT_101778	7300	Non-reducing PKS	Non-reducing PKS
fsr2	NECHADRAFT_63896	1300	O-methyltransferase	O-methyltransferase
fsr3	NECHADRAFT_101780	1800	FAD-dependent monooxygenase	FAD-dependent monooxygenase
ER	NECHADRAFT_105423	1400	Enyol reductase	/
TF2	"NECHADRAFT_85473"	2100	Transcription factor	Zinc Transcription factor
DH1	NECHADRAFT_85474	1000	Dehydrogenase	Short-chain dehydrogenase/reductase
DH2	NECHADRAFT_96600	1300	Dehydrogenase	Zinc-containing alcohol dehydrogenase
OR	NECHADRAFT_49913	800	Oxidoreductase	/
T	NECHADRAFT_85476	2100	Transporter	Major facilitator, sugar transporter-like

MT	NECHADRAFT_96602	1500	Methyltransferase	/
EP	NECHADRAFT_96603	1100	Epimerase	/
9G_1	NECHADRAFT_49961	680	Nucleotide kinase	/
9G_2	NECHADRAFT_85480	850	/	/
9G_3	NECHADRAFT_85481	1650	X-Pro dipeptidyl-peptidase	Xaa-Pro dipeptidyl-peptidase
9G_4	NECHADRAFT_50458	1800	Transcription factor	Fungal transcription factor
9G_5	NECHADRAFT_85483	1000	Proline racemase	/
9G_6	NECHADRAFT_85484	1700	Major facilitator superfamily	/
9G_7	NECHADRAFT_85485	1100	VirB10, secretory pathway	/
9G_8	NECHADRAFT_85486"	1000	/	/
9G_9	NECHADRAFT_50449"	1100	Dehydrogenase	/
fsr4	NECHADRAFT_50006	1200	Alcohol dehydrogenase	Alcohol dehydrogenase
fsr5	NECHADRAFT_72175	1100	Short-chain dehydrogenase-reductase	Short-chain dehydrogenase-reductase
MFS	NECHADRAFT_72176	1300	Major facilitator superfamily	/
fsr7	NECHADRAFT_96610	1400	Esterase	/

Not all sequences could be predicted due to removed entries or simply no correlated data in the databases. The analysis with Interpro however, did add information about *DH2* as being a zinc-containing dehydrogenase and about *T* being a sugar-like transporter. Despite the lack of protein identification in Interpro, the functions predicted by both databases are similar. As no conflicts in functions were noticed in both prediction tools, it can be hypothesised that the predicted roles of the genes are compatible to what should be expected in practice. Based on the protein functions, the genes were classified by enzymes classes. Their naming is inspired from the predicted functions to simplify the annotations of this study. Figure 14 illustrates the resulting enzymatic classification of the *PKS3* cluster. In the cluster, some genes encode for transferases (*fsr2* and *MT*), oxidoreductases (*fsr3, ER, DH1, DH2, OR, fsr4 and fsr5, 9G_9*), isomerase (*EP*), transcription factors (*TF2, fsr6, 9G-4*) and transporters (*MFS, 9G_6*) enzymes and may have a linked function to the synthesis and regulation of fusarubins in *F. solani.*

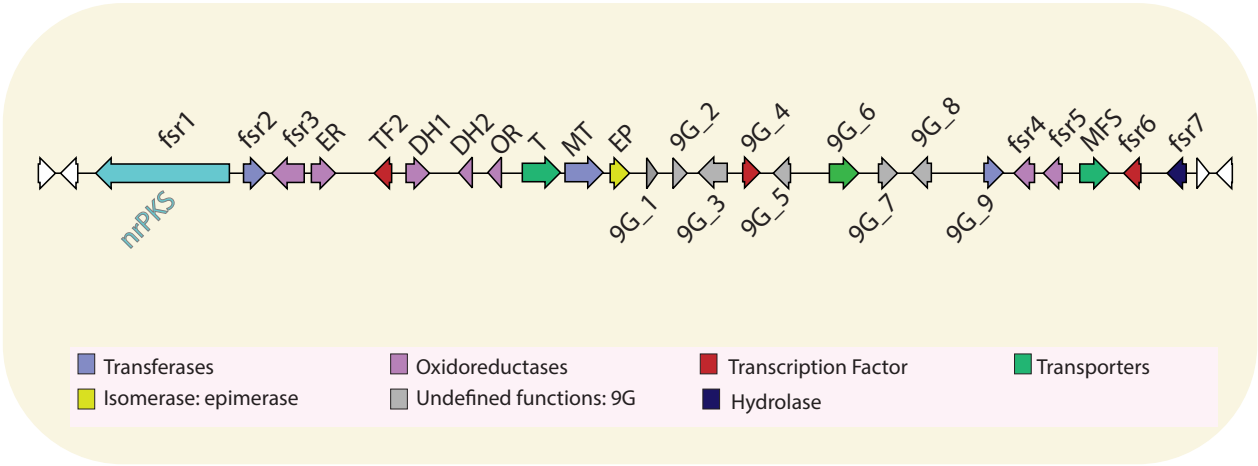

Figure 14: Enzyme classification of the *PKS3* cluster based on CDD and Interpro protein domains prediction. Those predictions inspired the annotations of the name of the genes throughout this study.

The *9G* group of 9 genes (in grey) including a kinase, racemase and peptidase and undefined proteins. It is unclear if those have a role in the biosynthetic pathway of fusarubins or in the regulation. *9G_9* is predicted to be a dehydrogenase and could be the only gene in the group to be influencing the biosynthesis. It is also a possibility that these are not related to the cluster at all. Each of the annotated genes were planned to be deleted individually. However, to simplify the experimental work, the group of 9 genes in *9G* will be deleted simultaneously. Another interesting observation is the presence of two transporters (*MFS* and *9G_6*) within the *F. solani* cluster. These transporters proteins could have a relation with the mycelial pigmentation of *F. solani* instead of perithecial like observed in *F. fujikuroi* and *F. graminearum*. Excretion of the fusarubins could be orchestred by those enzymes which are absent in the other *fusaria*.

Synteny alignment

A synteny alignment with members of the FSSC was executed in order to visualise the organisation of the *PKS3* cluster. The comparison of the PKS3 cluster with other members of the FSSC would help observing the more conserved genes in the cluster. At first, the *PKS3* gene was computed into GenBank to isolate the identified species in FSSC that contain the *PKS3* gene. Table 4 lists all the orthologues found in the database with at least 70 % of coverage of the DNA sequence of *PKS3*. The cut-off was made at 70 % to ensure a high similarity and so a comparison with only closely related orthologues.

Table 4: List of strains in FSSC described with *PKS3* gene in GenBank. In this report, all work revolves on *F. solani mpVI* 77-13-4, in bold. (37)

Strains in FSSC described with the *PKS3* gene and % coverage			
***F. solani* mpVI 77-13-4**	**100 %**	*Fusarium euwallaceae* strain HFEW-16-IV-019	98 %
Fusarium solani strain JS-169	99 %	*Fusarium sp.* AF-6 strain NRRL62590	98 %
Nectria haematococca isolate S2_018_000R2	99 %	*Fusarium virguliforme* Mont-1	98 %
Fusarium sp. AF-8 strain NRRL62584	99 %	*Fusarium virguliforme* strain NRRL 34551	97 %
Fusarium ambrosium strain NRRL 20438	99 %	*Fusarium brasiliense* strain NRRL 31757	97 %
Fusarium euwallaceae strain UCR1854	99 %	*Fusarium cuneirostrum* strain NRRL 31157	97 %
Fusarium floridanum strain NRRL62606	99 %	*Fusarium phaseoli* strain NRRL 31156	97 %
Fusarium metavorans FSSC 6	99 %	*Fusarium sp.* NRRL 22101	74 %
Nectria haematococca strain LQ1	99 %	*Fusarium tucumaniae* strain NRRL 31781	73 %
Fusarium kuroshium isolate UCR3666	98 %	*Fusarium tucumaniae* strain NRRL 31096	73 %

20 *PKS3* orthologues within the FSSC have high similarity to *F. solani*. To compare these orthologues even further, a phylogenetic tree was created, with *F. fujikuroi* and *F. graminearum* as outgroups. The tree served as a comparison tool of *PKS3* to organise the species based on similarity. Only one species of each kind was used in the designing of the tree in Figure 15.

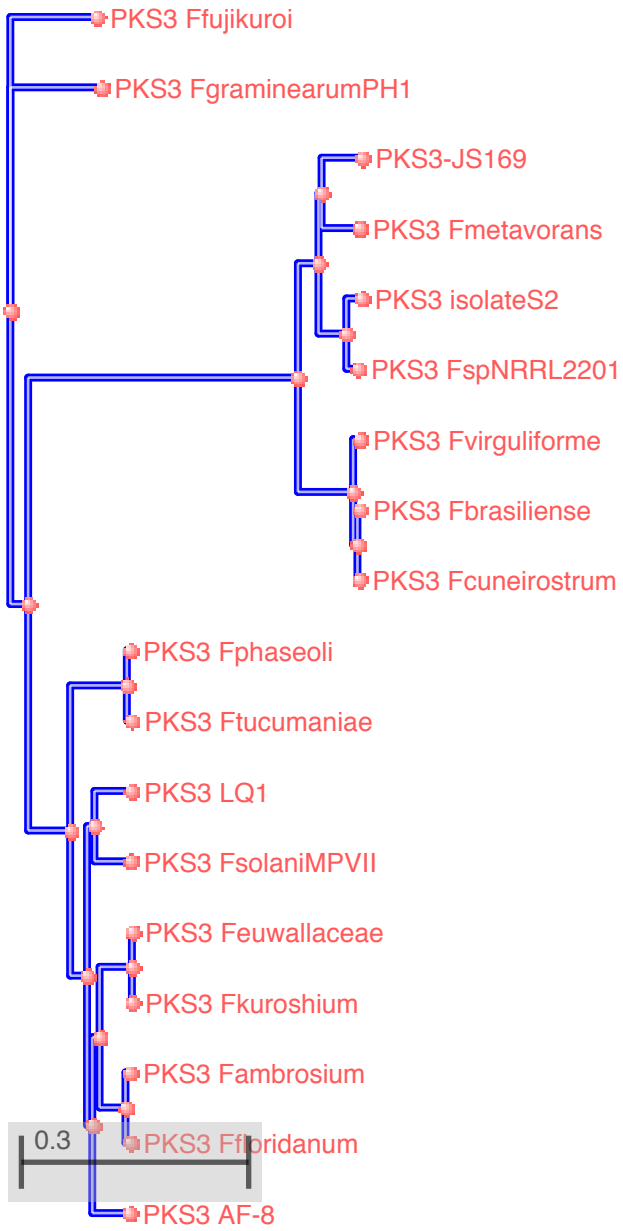

Figure 15: Phylogenetic tree of FSSC members based on *PKS3*, *F. fujikuroi* and *F. graminearum* are used as the outgroup.

Two groups are observed in the FSSC branch, a recent lineage where *F. solani* lies and a more ancestry lineage. The strain LQ1 had a 99 % coverage of the PKS3 gene and appears to be most closely related to *F. solani*. It is important to note that there is a large diversity within the FSSC, even only from the *PKS3* gene.

The next step consisted of looking further in the members of FSSC with aim to locate the *PKS3* cluster in their genomes and comparing them. None of the sequences found were annotated and some sequences of *PKS3* were located in small incomplete contigs. Since the whole *PKS3* cluster spans over approximately 70,000 bp, only the contigs containing more than 100,000 bp were selected for the alignment. This ensured that the alignment would include most of the cluster. The aim of the alignment analysis was to clarify and confirm the delimitation of the cluster and the conservation of

the genes within the complex. The synteny alignment in Figure 16 includes from top to bottom; *F. sp. AF-8, F. floridanum, F. solani, F. solani JS-169, F. kuroshium, F. metavorans, F. euwallaceae*.

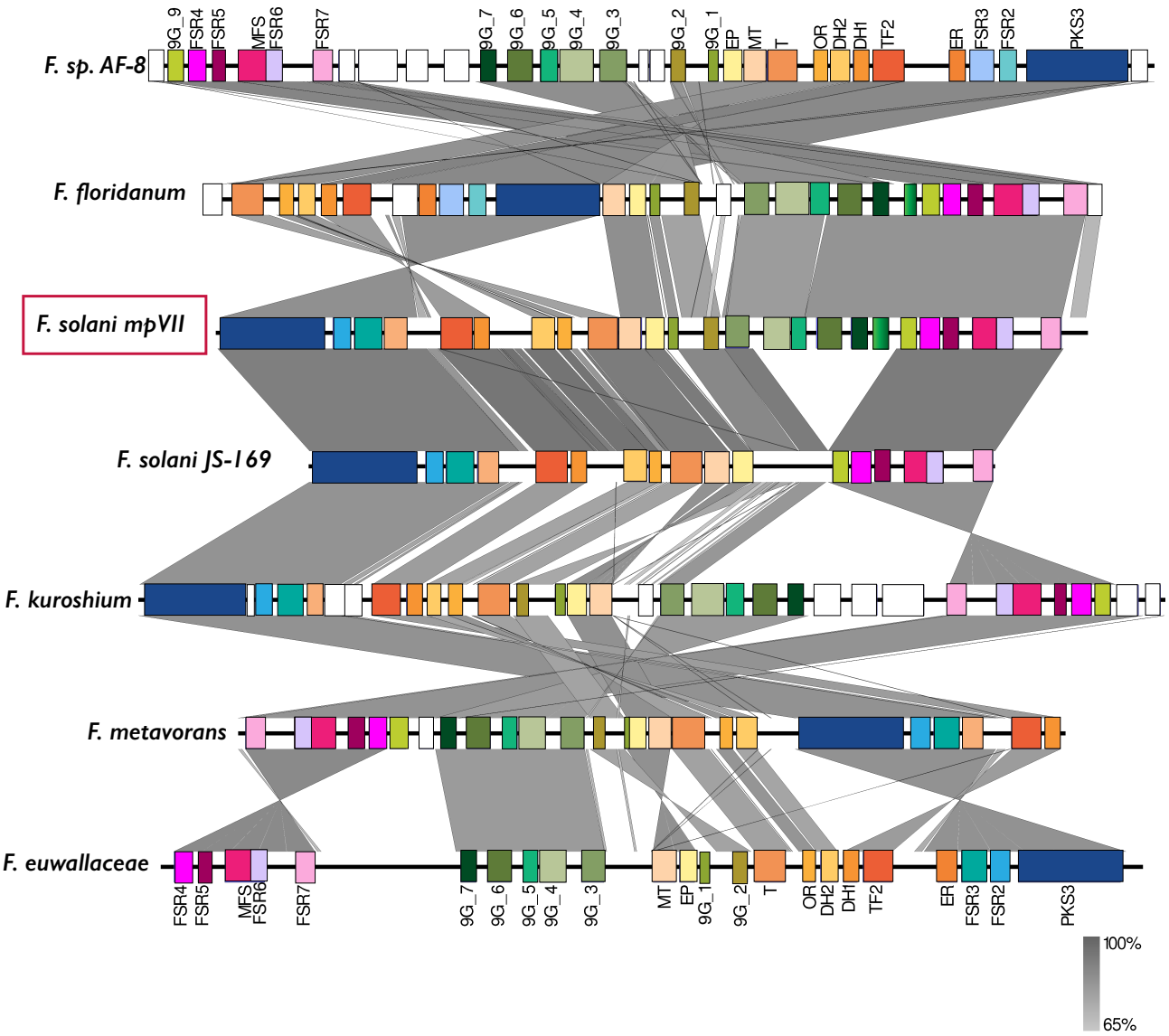

Figure 16: Synteny alignment of PKS3 cluster with members of the FSSC. *F. solani* is the third from the top. The vast majority of the genes are highly conserved throughout the complex.

As an initial observation, the majority of the *PKS3* genes are conserved across the FSSC. Moreover, the conservation of the genes is grouped supporting the hypothesis of horizontal gene transfer of important genes within the same genus. Four major groups of genes are observed across all clusters:

- The core essential biosynthetic *fsr* genes in blue scale, grouped as *fsr1-fsr3*.
- The pink colored scale group of *fsr4-fsr5-MFS-fsr6-fsr7*, described as encoding for dehydrogenases and regulator enzymes.
- The extra genes in orange scale represent *ER* to *MT,* translated into the potential additional polyketide tailoring genes.
- The genes of *9G*, in green, suspected to not be a part of the biosynthetic pathway nor cluster.

An interesting observation is that the locations of these grouped genes are systematic. *fsr1* to *fsr3* and *fsr4* to *fsr7* are always on the extremities, except in *F. floridanum*. Just as in *F. solani*, *ER* to *MT* and

9G follow each other with in most cases. However, some gaps of homology are observed in the ortholog genes of *9G*. This group of gene is the least conserved compared to the others. Some extra non-annotated genes (in white) are also present in *F. kuroshium* and *F. sp. AF-8* with no orthologs in other species. This indicates that the visible cluster could include non-related genes. Moreover, the genes upstream to *fsr1* and downstream to *fsr7* also showed strong similarity. It could be interesting to investigate the relationship of those genes to the polyketide synthesis. Another finding from this alignment concerns the non-annotated sequence between ER and TF2 in in *F. solani*. That 'space' is strongly conserved in all species and is annotated as un-identified genes (white) in *F. sp AF-8* and *F. kuroshium*. This suggests towards possible omitted conserved genes or highly conserved introns. Although the latter, seems less likely.

The synteny alignment has provided useful information about the *PKS3* cluster in *F. solani*. The most preserved genes include most of the cluster at the exception of the *9G* group. The organisation is systematic with *fsr1* at the beginning of the cluster and *fsr7* at the end. With these observations it was decided to delete individually, *fsr1*, *fsr2, fsr3, ER, TF2, DH1, DH2, OR, T, MT, EP, fsr4, fsr5, MFS, fsr7*. The *9G* group has shown to contain only one dehydrogenase protein with possible relation to the biosynthesis and is the least conserved group of genes across the FSSC. Therefore, it was decided to delete the whole group simultaneously as part of one targeted deletion. Accordingly, a total of 16 knock-out experiments were designed.

7.2 Targeted Deletion

Amplification of pKO Plasmid Fragments

Thanks to the protein prediction and synteny alignment, it was clearer to decide which genes to delete. *fsr1*, *fsr2, fsr3, ER, TF2, DH1, DH2, OR, T, MT, EP, fsr4, fsr5, MFS, fsr7* and the group *9G* were assigned as deletion targets for the rest of the experimental work. To start the targeted deletion, flanking homologous regions of each target had to be amplified and inserted into knock-out plasmids which would be in turn transformed inside *F. solani*. The amplification of all up and down regions for each 16 knock-outs was executed with temperature optimised PCR reactions. All PCR products had expected sizes of 600 to 1500 bp as seen in Figure 17, Figure 18 and Figure 19. (A table listing all the PCR settings for amplification of each fragments is listed in Appendix II – Primer Sequences and PCR Settings After the PCR reactions, the products were loaded on an agarose gel to validate the correct amplifications.

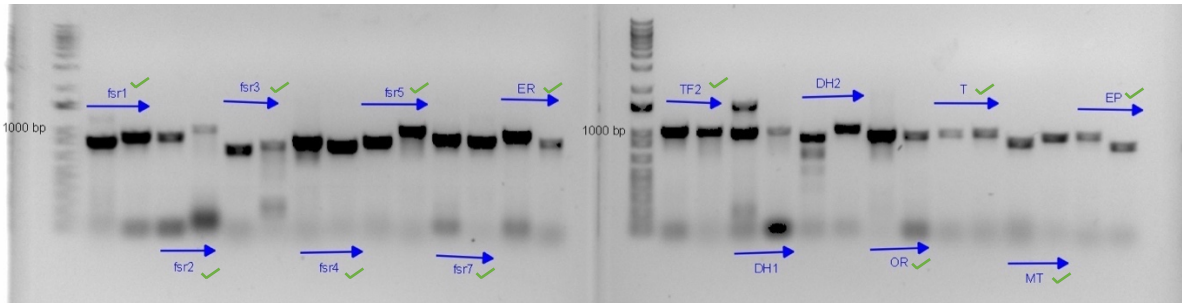

Figure 17: PCR products of up and down regions amplification. These regions are the homologous parts required for target deletion. All expected sizes were of 600 to 1500 bp. Each arrow designates a pair of PCR products analysed on the gel. The left band is the up region and the right band is the down region. These fragments are to be assembled in yeasts along with the backbone and drug cassette hyg B. The check mark represents successful reactions followed by PCR purification. DH1 and DH2 up regions required a gel purification.

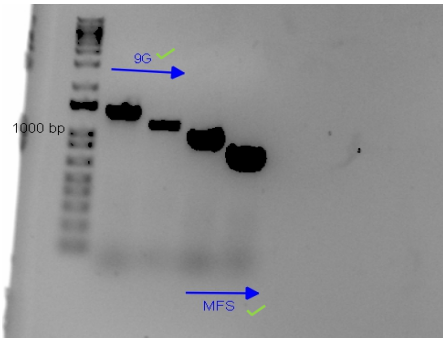

Figure 18: PCR products of up and down regions amplification. These regions are the homologous parts required for target deletion. All expected sizes were of 600 to 1500 bp. Each pair of products are to be recombined in yeast along with the backbone and drug cassette hyg B.

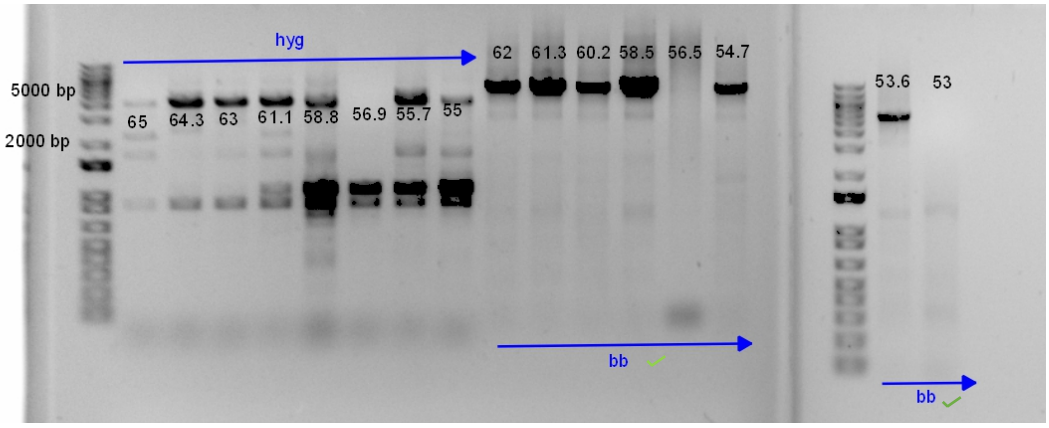

Figure 19: PCR products of the drug cassette hyg B and the backbone with expected sizes of 2000 and 5000 bp respectively. These fragments are required for the recombination of pKO plasmids inside yeasts cells.

The PCR reactions of up and down regions were conducted in four batches of eight, totalling to 32 reactions. Most reactions succeeded at a t_a of 55 to 58 °C. However, some products required optimisation such as gradient of 55 to 65 °C or touchdown (-1 °C) set from 63 or 65 °C. In general, a successful reaction was concluded when the band was the most intense at the expected size, regardless of fainter bands of other sizes. Sometimes the product needed to be gel purified if another unwanted product band appeared to be close in size to the desired product or if another unwanted product band with just as intense concentration was amplified. This occurred for DH1 and DH2 up regions which were purified from the gel, see Figure 17. An unsuccessful reaction was concluded when no product was amplified at all or when unspecific primer binding occurred leading to unwanted product bands. In the first case, the t_a was decreased and/or extension time extended to ensure a stronger annealing of the primers. In the second case, the t_a was increased to improve the specificity of the primers annealing. For the backbone and drug cassette presented in Figure 19, the same method of troubleshooting was applied. A gradient proved to be more suited to obtain more volume of the amplified products. All PCR fragments were purified via the PCR purification kit or gel purification kit when necessary, which worked satisfyingly for most. For the backbone and the drug cassette however, it would have been beneficial to always perform gel purification only to remove the leftover of circular DNA template.

Recombination of fragments into *S. cerevisiae*

All 16 pKO plasmids were recombined inside competent yeasts cells. The recombination experiments comprised the purified PCR products of the backbone, drug cassette and up and down regions respective to the deletion target. Two different protocol methods were tested for yeast transformation. The first one implied cultivating fresh yeast cells directly prior to the transformation, which required an extensive day of lab work. This protocol involves hours of yeast cultivation, yeast collection once the correct OD_{600} is reached and lastly heat-shock incubation with the purified fragments. To optimise the time spent in the lab, a second protocol method from Gietz et al. (2007) (38) was used which implied freezing a vast amount of competent yeast cells days prior to the transformation. This second method allowed an increase in number of simultaneous transformations as the transformation protocol was shortened to only the heat-shock incubation step. However, a decrease in emerging colonies has been noticed when using the frozen competent yeast cells. This could be due to the yeast samples surpassing the optimal OD_{600} and optimal growth stage while waiting to be frozen. The average of colonies emerging on a transformants plates' using the fresh yeast cells was 45.1 (total of eight transformations). While the average of transformants colonies using the frozen yeast cells which was of 28.3 (total of 24 transformations). However, the comparison of the number of colonies should not be assumed as complete reliable information. The iterations of transformations with each protocol were not equal and most importantly the samples were not statistically normally distributed. Even though those results are not reproducible, the average suggests that the competent frozen cells contribute to minor loss of colonies.

Three types of control transformations were designed to validate the yeast transformation: transformation with only the backbone, transformation with the backbone and drug cassette and lastly transformants with the backbone, up and down regions. In the first couple of transformations, it was noticed that some colonies emerged on the control plates. When the ratio of transformants to false positives was at least 10:1, the transformation was assessed as successful and the yeast colonies were stored. If the control colonies made up for more than a tenth of the transformants colonies, the transformation experiment was considered as foul and repeated. The false positives only occurred to be a problem when the transformation protocol was changed to the frozen yeast cells. As the colonies from the transformants decreased, the ratio of transformants to false positive was unsatisfactory. The source of false positives needed to be elucidated to eliminate it. The control design all included a fragment of the backbone which was previously purified with the PCR purification kit which does not separate the circular plasmid DNA template. Moving forward, the PCR backbone product was purified from a gel to ensure no leftover template. This improved the efficiency of the yeast transformation and decreased the number of false positives substantially from an average of 6 % of control colonies emerging to 1 % of control colonies as listed in Table 5.

Table 5: Average of colonies count from transformed colonies and control colonies with and without the purification of backbone

	Average transformed colonies	Average control colonies
Without prior purification	28.6	1.8
With prior purification	35.2	0.47
% False positives	6 %	1 %

Most transformations worked at the first try while others took up to five trials. The yeast transformation efficiency was assessed as 78 % of success per trial. It is important to remember that the purification of the backbone was implemented only in the later transformations. The assembly of pKO - DH2, ER and EP had to be executed several times as their later validation resulted to be unsuccessful.

pKO Plasmid Assembly Validation

After being extracted from yeasts, the plasmids were electroporated into *E. coli* for extensive copying. The assembling of pKO was validated with three different methods: restriction digest with specific restriction enzymes, PCR by amplifying the up and down regions of the plasmids and lastly by sequencing of the up and down regions by an external lab. All pKO plasmids were correctly validated at the exception of pKO-ER, pKO-DH2 and pKO-EP.

Restriction Digestion

Each plasmid digestion was designed individually with available compatible restriction enzymes. This method is a useful tool to get an overview of the integrity of the plasmid. After digestion, the circular plasmids were loaded on a gel next to their corresponding digestion reactions as shown in Figure 20, Figure 21 and Figure 22. Each plasmid was digested with two different enzymes and loaded on gel to check if the sizes of DNA fragments complied with the expected ones.

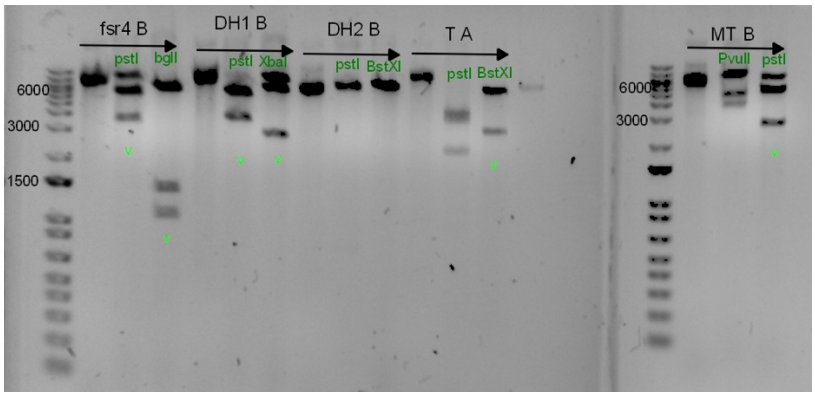

Figure 20: Restriction digestion of fsr4, DH1, DH2, T and MT from *E. coli* colonies. The circular pKO is loaded as a control next to the corresponding digestions. The successful digestions with correct sizes of digested fragments are marked with the green checkmark.

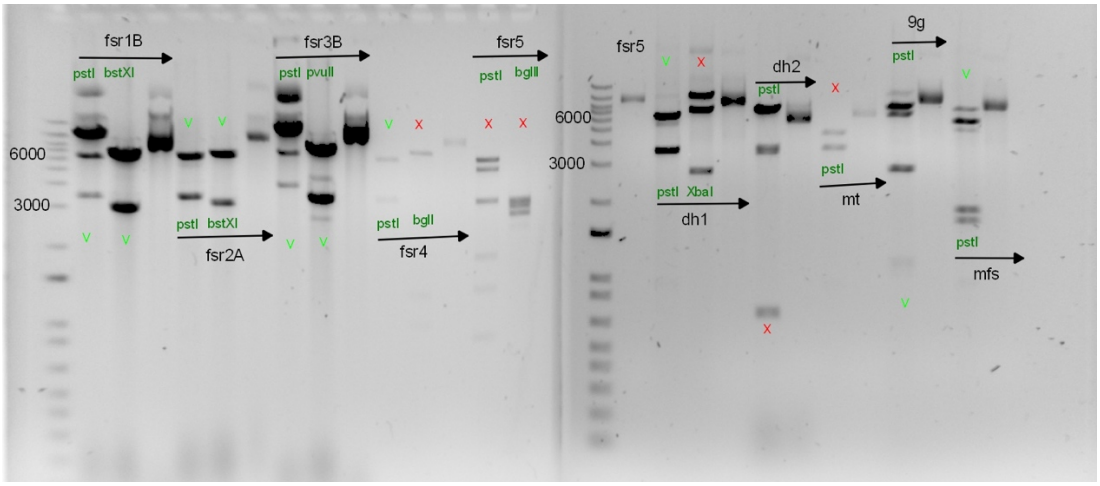

Figure 21: Restriction digestion of pKO - fsr1, fsr2, fsr3, fsr4, fsr5, DH1, DH2, MT, 9G and MFS from *E. coli* colonies. The circular pKO is loaded as a control next to the corresponding digestions. The successful digestions with correct sizes of digested fragments are marked with the green checkmark.

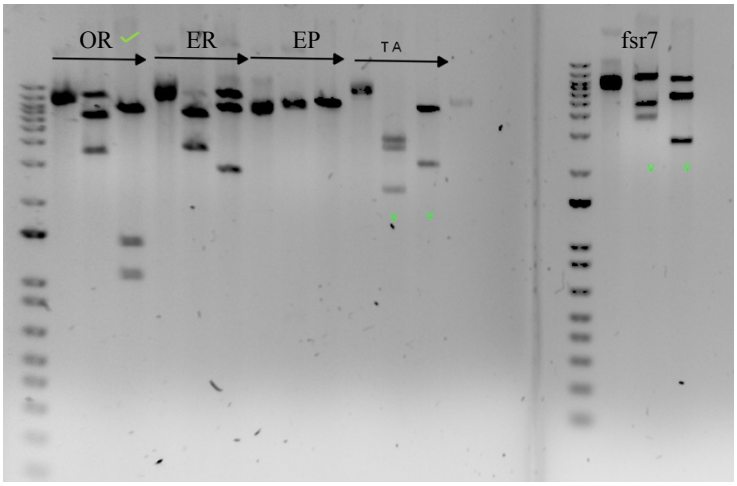

Figure 22: Restriction digestion of pKO - fsr7, ER, EP, T, OR from *E. coli* colonies A or B. The circular pKO is loaded as a control next to the corresponding digestions. The successful digestions with correct sizes of digested fragments are marked with the green checkmark.

As the pKO plasmids in *E. coli* cells was assumed to not be identical in all colonies, single colonies with each pKO were streaked and separated. A total of five colonies (A, B, C, D, E) were taken for each pKO transformation. The restriction digest helped sorting out which *E. coli* colonies were correct or not and narrowing down to only one or two colonies for each plasmid. It occurred that some colonies were 'false positives' as the digestion was not correct. Those colonies were discarded and only the successful ones were saved for further proceedings. All pKO plasmids were successfully digested as expected except for *fsr5, MT, DH2, ER* and *EP*. Those plasmids did not yield any correct digest in any of the copies. In some cases, such as *MT* and *fsr5*, the same colony would be digested correctly one time and incorrectly the other time. Despite the unsatisfactory digest, these copies were kept for the next validation method in order to clarify the uncertainties especially for *fsr5* and *MT*. All restriction digest results and the list of the restriction enzymes used can be found in Appendix VI.

PCR

The amplification of the regions including the joining of the drug cassette to backbone was used as validation of its integration. Two new sets of universal primers were designed to bind at the extremities of the backbone as shown in Figure 23. The orange regions represent the validation PCR products aimed to be amplified in each pKO plasmid.

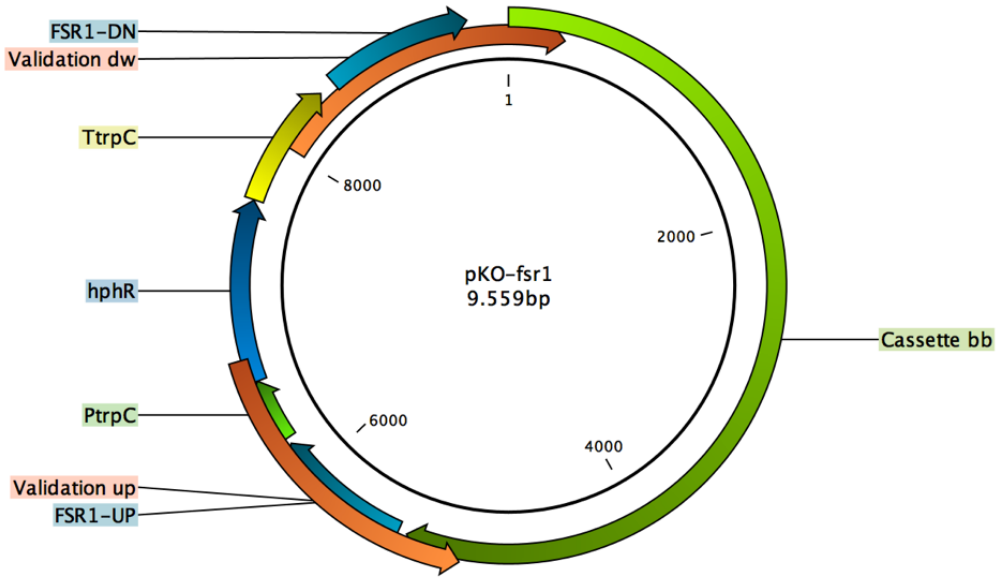

Figure 23: pKO-fsr1. The orange regions represent the PCR products amplified in all pKO to validate the recombination of the drug cassette, up/down region and backbone. Universal primers were designed to bind within the drug cassette and the backbone, the expected sizes depend on the size of the up and down regions respective to each pKO plasmid.

Again, the expected sizes of the regions are known and could be checked when loading the products on a gel as shown in Figure 24.

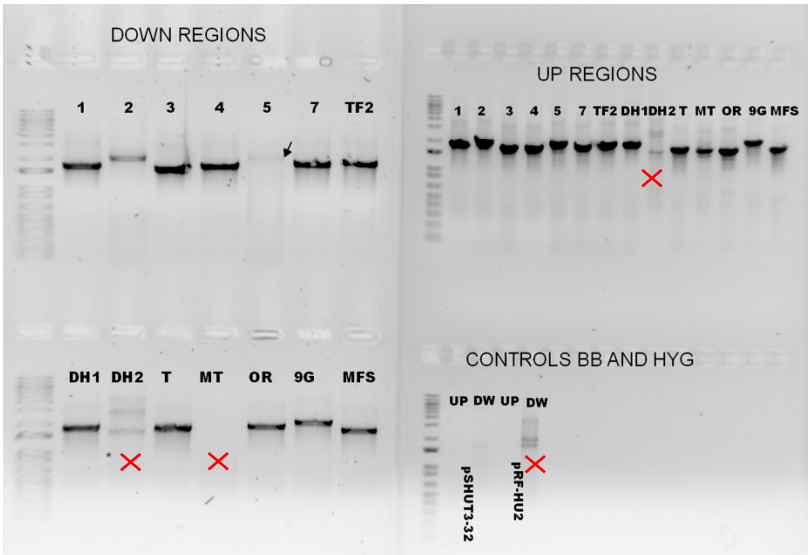

Figure 24: PCR amplification of the validation regions upstream and downstream to the drug cassette from the recombined pKO plasmids extracted from *E. coli*. All tested PCR validations were correct except for DH2 and MT. All reactions are correct except for the ones marked with a red cross.

All validations were amplified successfully except for *DH2, MT, ER* and *EP*. Since *DH2, ER* and *EP* did not give any satisfying validation from PCR and the restriction digestion, it was concluded that their recombination was uncomplete and needed to be re-assembled in yeast. *DH2* had expected size of up (1500 bp) and down (1600 bp) which was not accurately amplified here. *MT* and *fsr5* had unclear restriction digest results and a faint amplification band of the down regions with expected sizes of 1800 bp and 1500 bp respectively. As controls, the template plasmids from *hph* and the backbone were also tested with the same primers to ensure that the bands observed are from the recombined pKO plasmids and not from some leftover circular plasmid template. The controls PCR reactions were made on the plasmid templates pSHUT3-32 and pRF-HU2 with the same primers in order to confirm the validity of the results. Ideally, no bands should show as no up nor down regions belong in each of the template plasmids of the drug cassette and backbone. It appears however that the down region could be amplified in the template plasmid of the drug cassette hyg. This observation was disregarded as when repeated, little to no amplification was done The PCR validation was used to further validate the restriction digest results. In this case, it clarified the uncertainties which outcomes was unclear. It was concluded that *DH2, ER* and *EP* had to be retransformed into yeast. Since *MT* and *fsr5* did yield the expected products of upstream validation, these were kept for the last validation method.

Sequencing

The last and final validation method was assessing the sequencing results sent from Eurofins Genomics Germany. All sequenced samples returned desirable results. The main aspects of the results were the areas of consensus and the numbers of conflicts. The up and downstream regions that were previously amplified by PCR, were sequenced. Example of sequencing results are shown in Figure 25, the rest of sequence results can be found in Appendix VII.

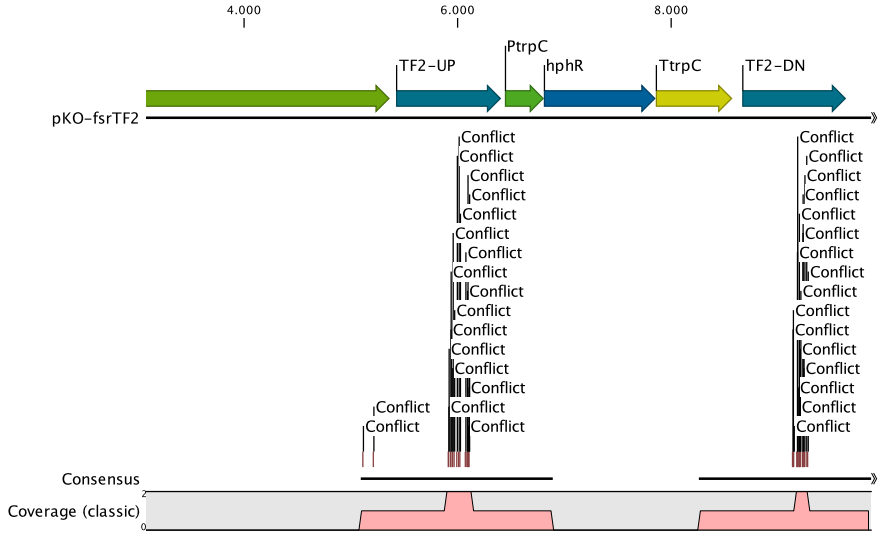

Figure 25: Results from sequence assembly of up and down regions of TF2 and sequenced results from Eurofins Genomics

Four sequencing reactions were executed for each pKO plasmid; at the 3' and 5' end of up and down regions. One reaction reads for approximately 1000 nt, and as most up and down regions are smaller than that, the reactions overlapped in the middle of the sequence. As shown in Figure 25, the coverage (in pink) is flat but increases in the middle. That middle point is where the reading reactions meet. It is important to note that the genomic sequence reading apparatus is less reliable at the beginning and end of fragments. Therefore, it is normal to see an increased amount of conflicts at the extremities of

the reads. Many conflicts in nucleotides occurred when assembling the reference sequences issued from online databases and the sequenced samples. However, the majority lied in the extremities of the reads, just as shown in Figure 25. All sequenced pKO plasmids resulted in satisfactory readings and could be stored for further proceedings.

pKO integration in *A. Tumefaciens*

The integration of all pKO plasmids except DH2, ER and EP was executed by electroporation. The transformed bacteria were plated on LB plates with rifampicin and kanamycin selection. Hundreds of colonies emerged from the transformations, underlining the ease of the bacteria to integrate the plasmids. Normally, *A. tumefaciens* requires 2 days before noticeable colonies. In this experimental work, they were given 4 days to grow bigger and ease the individual isolation of the colonies. A few plasmids required several trials for successful integration.

***Agrobacterium* Mediated Transformation**

Once the plasmids were integrated inside *A. tumefaciens*, the start of the fungal transformation was planned. As mentioned before, the bacteria could be slow to cultivate, therefore they needed 2 or 3 days of pre-cultivation in LB medium. After transferring of the LB pre-culture into IMAS medium, the bacteria needed an average of 17 hours before reaching the recommended OD_{600} of 0.5 with 500 µL of pre-culture. Three extra experiments were added to the original 16, consisting of the deletion of *fsr1*, *fsr2* and *fsr3* in the wild type as well. The fungal mutants were transformed in batches of four to eight and in periods of 2 weeks. Most transformations were completed after multiple trials. Only 35 % of the transformations succeeded at the first trial, another 35 % succeeded at the second trial, 17.5 % needed three trials and the remaining 12.5 % of transformation did not succeed after three trials. In practical terms, the transformation of Δ*fsr1*, Δ*fsr2* in the wild type, OE6Δ*fsr1*, OE6Δ*fsr3*, OE6Δ*fsr4*, OE6Δ*fsr5*, OE6Δ*fsr7*, OE6Δ*TF2* and OE6Δ*DH1* in OE::*fsr6* were completed. However, Δ*fsr3* was not achieved despite the three transformation trials. The reasons affecting the transformation efficiency was assessed as the concentration of the bacteria in the pre-culture before transformation, the quality of incubation chamber and the importance of the gene. It was observed that cloudy and dense cultures of bacteria that incubated for less than 3 days performed better in transformation. This could be ensured by streaking the bacteria colonies on LB plates a few days before the pre-culture, as they would be more viable than older colonies stored in the fridge for an extensive period of time. In the second round of transformations, the incubation chamber was changed from an acclimated room at 21 ºC to a ventilated incubator with fluctuating temperatures from 21 ºC to 23 ºC. In the latter case, most of the transformants did not emerge and the solid media in the plates was drying out at a faster rate which was not in favour of the fungus' well-being. It was concluded that the acclimated room was the best condition for fungal transformants, as the temperature was steady and the nutrition did not deplete fast. Lastly, the transformation of pKO-*fsr2* and pKO-*fsr3* proved to be the most laborious in OE::fsr6 and in the wild type respectively. This is most likely connected to the strong roles of these in the gene cluster, making it challenging for the fungus to grow. One hypothesis is that without *fsr2* or *fsr3*, an increased amount of harmful or lethal intermediates are present which are causing to the growing fungus to die in the early stages of growth.

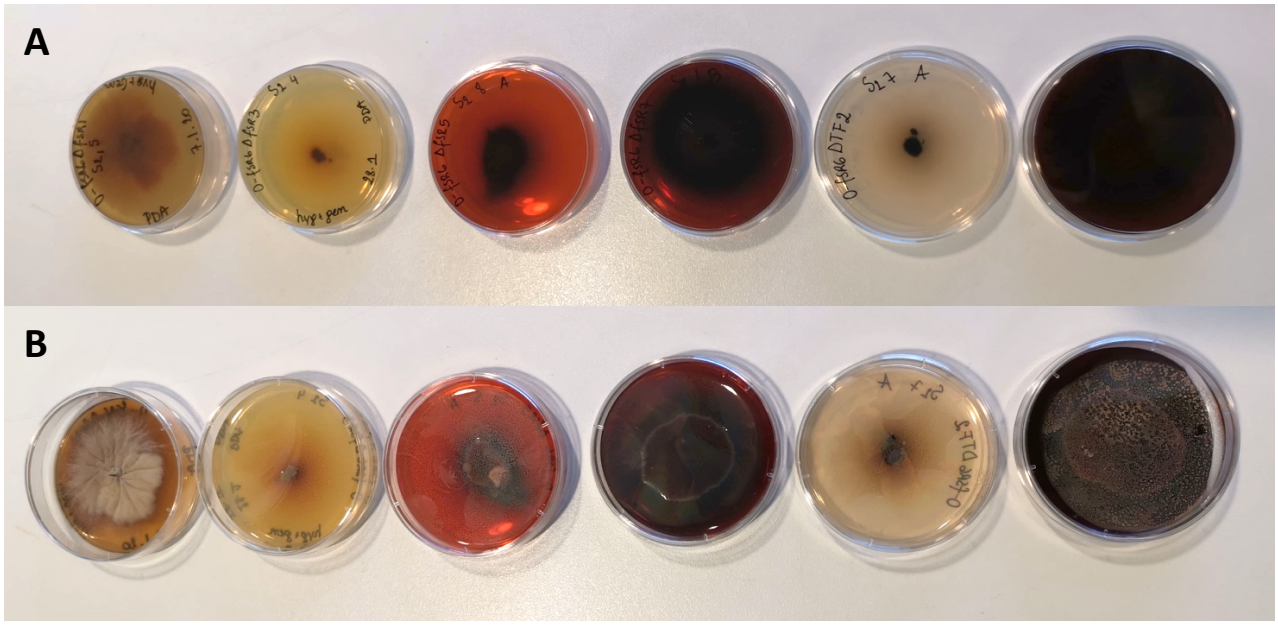

Figure 26: Mutants colonies emerged from initial three rounds of AMT A) Bottom face B) Top face. From left to right: OE6Δfsr1, OE6Δfsr3, OE6Δfsr5, OE6Δfsr7, OE6ΔTF2 and OE6ΔDH1

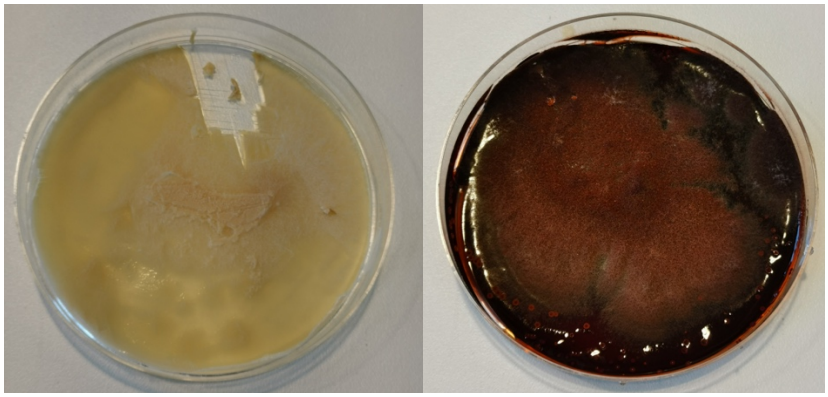

Figure 27: Mutants colonies emerged from fourth round of AMT. Left: Δfsr2, Right: OE6Δfsr4

Figure 26 and Figure 27 demonstrates a clear visual effects of the knock-outs on OE::fsr6. Δ*fsr1* shows a complete white mycelium in contrast to all other mutants, as expected from previous studies. This lack of pigmentation is linked to the ceasing of pre-fusarubin production, the precursor of all fusarubins. Δ*fsr2* is also completely white, which resembles a lot to the wild type. Unfortunately, all replications of Δ*fsr2* look the same. The complete lack of pigmentation hints towards a faulty transformation and the observable colonies to be a false positive. It could be possible that the drug cassette integrated the genome at an unknown location, causing the colony to sustain the antibiotic conditions. However, the *fsr2* gene does not appear to have been targeted. The PCR validation of the transformations will likely confirm these assumptions. The knock-out of *fsr3* shows an intense yellow/orange pigmentation. It is hard to assume which compounds are produced before any chemical analysis. Moreover, the configuration of FSR2 and FSR3 occur simultaneously, making it difficult to guess where the pathway has stopped. The similar statement applies to OE6Δ*fsr4*, OE6Δ*fsr5,* OE6Δ*fsr7,* OE6Δ*tf2* and OE6Δ*dh1*. However, it is assumed that OE6Δ*fsr4*, OE6Δ*fsr5* and OE6Δ*fsr7* would have a similar metabolite profile as the original OE::*fsr6* since these genes should not interfere with the biosynthesis. The pigmentation of these is also closer to the intense red from the original strain. OE6Δ*TF2* has the darkest pigmentation, near to black. It was also the mutant the slowest to grow,

suggesting that like *fsr2* and *fsr3* and *TF2* could be strongly relevant to the *PKS3* cluster. The liquid extraction and qualification analysis from these colonies would surely elucidate on the phenotypic characteristics observed.

Validation of Transformed Mutants

The validation of the mutants was executed with colony PCR. Colony PCR is a method inspired from the conventional PCR reaction, which uses alive colony cells as template instead of purified genomic DNA. It allows a fast-screening of the transformation by skipping the extraction of genomic material and replacing that step by quick lysis of the mycelium. It is important to note that this method is not always recommended when working with difficult samples. The lysis of the mycelium is not always complete as it depends on the strain. Moreover, the resulted lysate is not as clean as in an adequate DNA extraction. Therefore, the success of the colony PCR reaction is not always guaranteed. Part of the PCR validation work was interrupted due to the Covid-19 pandemic crisis. However, a few of the mutants have been positively validated. The homologous up and down regions that were aimed to be amplified from the mycelium material after fungal transformation as shown in Figure 28. New specific primers binding outside the drug cassette integration site were designed for each mutant. Three sets of PCR reactions were planned to be executed in order to validate the deletion of every target gene:

A) Upstream region of the drug cassette
B) Downstream region of the drug cassette
C) Within the drug cassette

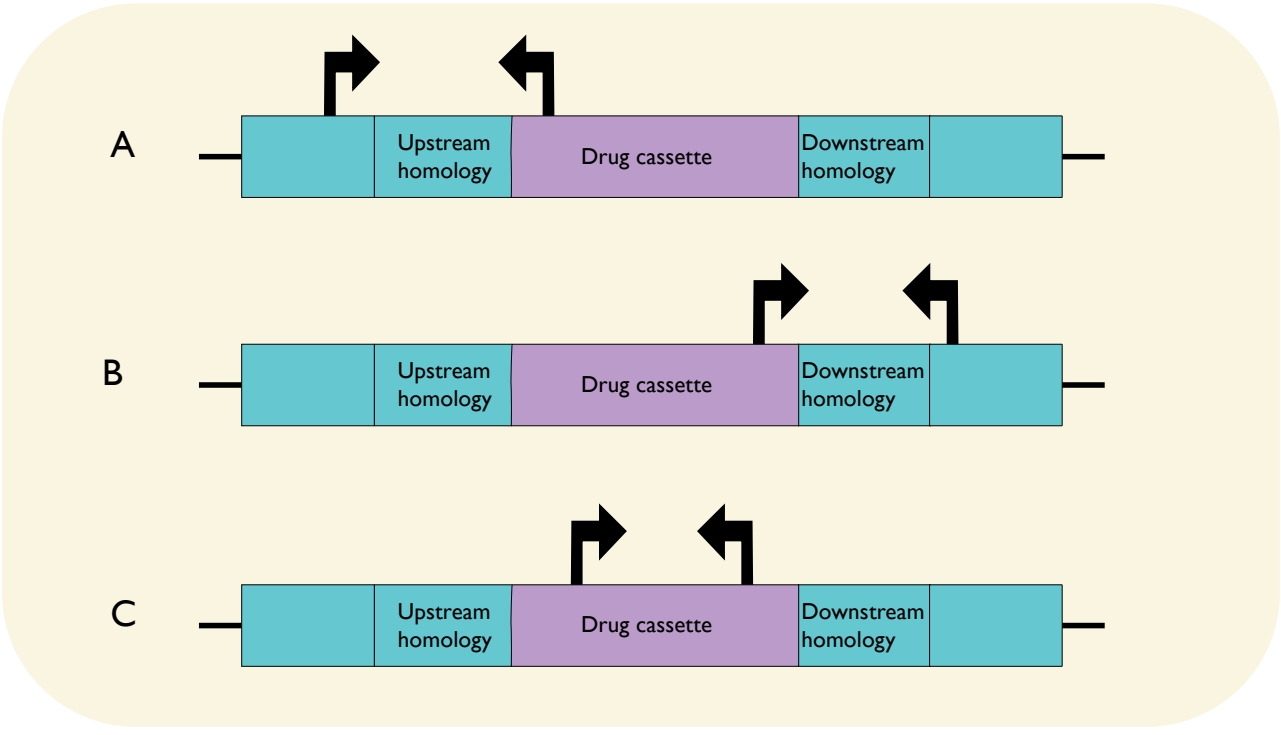

Figure 28: Illustration of the PCR reactions designed for validation of all transformed mutants. A) PCR reaction upstream of the drug cassette. B) PCR reaction downstream of the drug cassette. C) PCR reaction within the drug cassette.

Together, the results would show that the targeted gene was indeed deleted and replaced by the selection marker. Another type of reaction was considered to be implemented which would aim to amplify the targeted gene. The expected results would then be the absence of the amplified product to

prove that the gene in question was deleted. However, it was decided to not rely entirely on that reaction because, as mentioned earlier, colony PCR can be faulty and the absence of product could indicate an unsuccessful reaction rather than the expected result. Δ*fsr1* and OE6Δ*fsr1* were positively validated as shown in Figure 29.

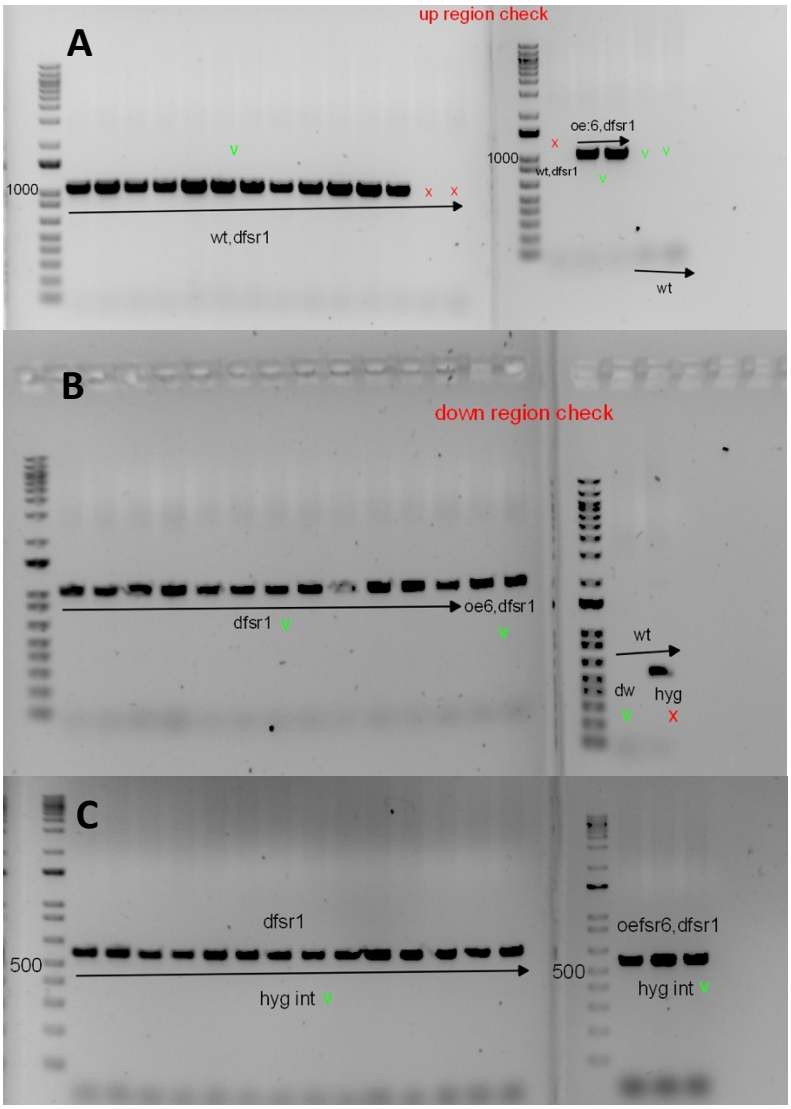

Figure 29: Colony PCR validation of wt,dfsr1 (Δfsr1) and OE6,dfsr1 (OE6Δfsr1) colony replicates, three sets of reactions were performed, A) the upstream region of the drug cassette, B) the downstream region of the drug cassette and C) the selection marker annotated as hyg int.

The many colonies collected from each transformation were positively validated. Most of the Δ*fsr1* in the wild type and OE6Δ*fsr1*colonies demonstrated a positive insertion of the up, down and selection marker regions. The up and down regions of the drug cassette were also tested on the wild type as a control and did not result in any product, proving that the result of the genetic modification is indeed noticeable only in the transformants. However, it appears that the internal reaction within *hph* does give a product in the wild type of the same expected size of 580 bp. It appears that the genomic DNA of *F. solani* has a sequence similar to *hph*, which is not favourable for the reliability of the results.

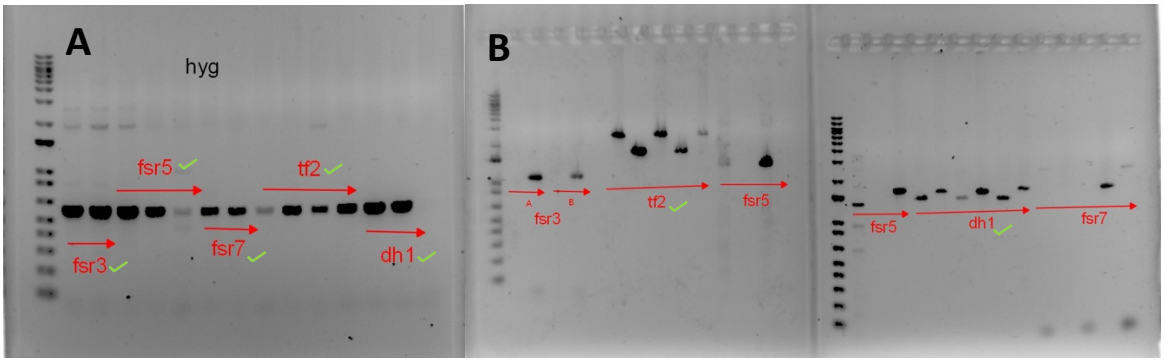

Figure 30 A) and B): Colony PCR validation of fsr3, fsr5, fsr7, TF2 and DH1, three sets of reactions were performed, the upstream region of the drug cassette, the downstream region of the drug cassette and the selection marker annotated as hyg.

Some of the colonies issued from OE6Δ*fsr3,* OE6Δ*fsr5*, OE6Δ*fsr7*, OE6Δ*TF2* and OE6Δ*DH1* were validated in time before the interruption of the experimental work. As observed in the first gel A) of Figure 30, all colonies demonstrated a positive insertion of the drug cassette. However, the validation of the up and down regions was not as satisfactory, shown in Figure 30 B). Some of the OE6Δ*TF2* and OE6Δ*H1* colonies replicates were positively validated. Note however, that not all the colonies have had the chance to be validated. It came to notice that the primer design for Δ*fsr3* and Δ*fsr7* was faulty, explaining why these colony validations show unsatisfactory results. It could be assumed that the presence of at least one of the regions (up or down) strongly indicates a successful transformation. In fact, the drug cassette should have integrated in the right locus to be able to amplify a region even if the validation of the other region is missing. The validation of the mutants is an important and required step to confirm any of the findings from this study. Strong indicators like antibiotic selection and colony PCR are great tools to assess a transformation success. As observed with Δ*fsr2,* the colony PCR validation is essential to confirm the success or failure of transformation. The antibiotic selection is not sufficient proof. However, sequencing of the loci of deletion would be the next step to reinforce the correct assembly of drug cassette in the right genomic location.

Table 6 summarises the status of the transformations accomplished and validated from the overall experimental work. The missing steps involve validation of the pKO-ER, pKO-EP and pKO-DH2 and the deletion of *DH2, ER, EP, T, MT, OR, 9G and MFS.*

Table 6: Summary table of achieved experimental work regarding the targeted deletion of the genes. All accomplished steps are marked with a green checkmark. The missing steps are marked with 0.

Target	Validated pKO plasmid	Transformed in *F. solani*	Validated transformation
fsr1	V	V (wt and OE6)	V
fsr2	V	V (wt)	
fsr3	V	V (OE6)	V
ER	0	0	0
TF2	V	V (OE6)	V
DH1	V	V (OE6)	V
DH2	0	0	0
T	V	0	0
MT	V	0	0
OR	V	0	0
EP	0	0	0
9G	V	0	0
fsr4	V	V (OE6)	0
fsr5	V	V (OE6)	V
MFS	V	0	0
fsr7	V	V (OE6)	V

8. Conclusion

Fusarubins represent a vast group of bioactive naphthoquinones. Part of the bioactivity of the fusarubins include antibiotic, insectidal, phytotoxic and antitumoral properties, which has been assigned to their ability to produce superoxide and semi-quinone radicals. Fusarubins are synthesised by the *PKS3* gene cluster consisting of *fsr1* to *fsr7* genes, present in most *Fusarium* species. However, *F. solani* and its sibling species in the *Fusarium solani* species complex (FSSC), contain an additional 17 genes located between *fsr3* and *fsr4*. Other than genetically, *F. solani* also presents metabolic and histological disparities in the fusarubins production. Compared to *F. fujikuroi* and *F. graminearum*, *F. solani* produces a larger spectrum of fusarubins and excretes the compounds in the mycelium. The complexity of the chemical structures of fusarubins was associated with the different additional encoded enzymes found in *F. solani*. The synteny alignment of the *PKS3* cluster with species of the FSSC showed that most of the additional 17 genes are conserved across the species complex. Conserved genes are usually a strong indicator that genes have a relatively important role in the concerned cluster. Additionally, the protein prediction of the non-identified genes confirmed the possibility of their relation to the cluster. The putative roles of the genes were defined as transcription factors, oxidoreductases, transferases and an isomerase which resemble the domains of polyketide enzymes.

Experimentally, the targeted deletion of the *PKS3* cluster was inspired by previous literatures with the aim to elucidate the functions of the genes. The phenotypic changes observed from the available mutants demonstrates the consequential enzymatic effects. It is clear that the deletion of the genes, including some of the additional ones between *fsr3* and *fsr4*, removes some configurational reactions of fusarubins. The chemical analysis is still pending but surely will elucidate more on the biosynthetic consequences of the knock-outs. Some of the knock-out mutants did show some hinderance in mycelial growth compared to others. The deletion of *fsr3* and *TF2* resulted in a slow and small mycelial expansion, suggesting that the intermediates produced could be harmful for the fungus itself.

The report here provides a deep investigation on the *PKS3* cluster in *F. solani*, justifying the importance of the 17 insert genes. An in-depth protocol for AMT transformation of *F. solani* is also provided in Appendix V as a publication contribution to ‘Engineering Natural Product Biosynthesis: Methods and Protocols’ in MIMB Springer Nature.

9. Perspectives

Given the circumstances of the Covid-19 pandemic crisis, parts of the experimental work could not be concluded. Those parts are essential to the completion of the research objectives and should therefore be a priority in future perspectives. Despite the interruption, the deletion of *PKS3* gene cluster in *F. solani* via AMT was proved to be possible and a useful protocol is included in the Appendix V – Protocol for Transformation of *F. solani* via AMTwhich is aimed for publication in 'Engineering Natural Product Biosynthesis: Methods and Protocols' in MIMB Springer Nature. Pursuing work should include the completion of the individual knock-outs in the *PKS3* cluster, the chemical analysis from all liquid extractions and an experimental suggestion for the functions of the genes. A comparison with other members of the FSSC could also add information to the investigation. Recreating the knock-outs in a closely related strain and analyse the metabolites could possibly confirm some of the assumptions concluded in this thesis. However, the knowledge provided in this report is highly valuable as it can be used as a base to draft out and facilitate the consequent experimental work.

10. Bibliography

1. Coleman JJ. The Fusarium solani species complex: Ubiquitous pathogens of agricultural importance. Mol Plant Pathol. 2016 Feb 1;17(2):146–58.
2. Chandra NS, Wulff EG, Udayashankar AC, Nandini BP, Niranjana SR, Mortensen CN, et al. Prospects of molecular markers in Fusarium species diversity. Vol. 90, Applied Microbiology and Biotechnology. 2011. p. 1625–39.
3. Chehri K. Molecular phylogeny of the Fusarium solani species complex (FSSC) isolated from soils in Iran. Botany. 2014 Aug 7;92(11):815–20.
4. Chehri K, Salleh B, Zakaria L. Morphological and Phylogenetic Analysis of Fusarium solani Species Complex in Malaysia. Microb Ecol. 2015;69(3):457–71.
5. Brown DW, Proctor RH. Insights into natural products biosynthesis from analysis of 490 polyketide synthases from Fusarium. Fungal Genet Biol. 2016;89:37–51.
6. Frandsen RJN, Rasmussen SA, Knudsen PB, Uhlig S, Petersen D, Lysøe E, et al. Black perithecial pigmentation in Fusarium species is due to the accumulation of 5-deoxybostrycoidin-based melanin. Sci Rep. 2016 May 19;6(1):26206.
7. Shah AM, Rather MA, Hassan QP, Aga MA, Mushtaq S, Shah AM, et al. Discovery of anti-microbial and anti-tubercular molecules from Fusarium solani: an endophyte of Glycyrrhiza glabra. J Appl Microbiol. 2017 May 1;122(5):1168–76.
8. Studt L, Tudzynski B. Gibberellins and the Red Pigments Bikaverin and Fusarubin. In Springer, New York, NY; 2014. p. 209–38.
9. Medentsev AG, Arinbasarova AY, Akimenko VK. Biosynthesis of Naphthoquinone Pigments by Fungi of the Genus Fusarium. Appl Biochem Microbiol. 2005 Sep;41(5):503–7.
10. Tatum JH, Baker RA. Naphthoquinones produced by Fusarium solani isolated from citrus. Phytochemistry. 1983 Jan 1;22(2):543–7.
11. Ammar M, Gerber N, McDaniel L. New antibiotic pigments related to fusarubin from fusarium solani (mart.) sacc. i. fermentation, isolation, and antimicrobial activities. J Antibiot (Tokyo). 1979 Jul;32(7):679–84.
12. Nielsen MR, Holzwarth AKR, Brew E, Chrapkova N, Kaniki SEK, Kastaniegaard K, et al. A new vector system for targeted integration and overexpression of genes in the crop pathogen Fusarium solani. Fungal Biol Biotechnol. 2019 Dec 11;6(1):25.
13. Studt L, Wiemann P, Kleigrewe K, Humpf H-U, Tudzynski B. Biosynthesis of Fusarubins Accounts for Pigmentation of Fusarium fujikuroi Perithecia. Appl Environ Microbiol. 2012 Jun 15;78(12):4468–80.
14. Cox RJ, Skellam E, Williams K. Biosynthesis of Fungal Polyketides. In: Physiology and Genetics. 2018. p. 385–412.
15. Awakawa T, Kaji T, Wakimoto T, Abe I. A heptaketide naphthaldehyde produced by a polyketide synthase from Nectria haematococca. Bioorg Med Chem Lett. 2012 Jul 1;22(13):4338–40.
16. Keatinge-Clay AT. The structures of type i polyketide synthases. Vol. 29, Natural Product Reports. Royal Society of Chemistry; 2012. p. 1050–73.
17. Talwar G. Textbook of Biochemistry, Biotechnology, Allied and Molecular Medicine. 2016. 1632 p.
18. Eswaramoorthy S, Bonanno JB, Burley SK, Swaminathan S. Mechanism of action of a flavin-containing monooxygenase. Proc Natl Acad Sci U S A. 2006 Jun 27;103(26):9832–7.
19. Kopacz M (Małgorzata M, Fraaije MW, Rijksuniversiteit Groningen. Exploring the cofactor-binding and biocatalytic properties of flavin-containing enzymes. 2014. 3–5 p.
20. Lorsch J, editor. Laboratory methods in enzymology : cell, lipid and carbohydrate / . Elektronis. Amsterdam: Academic Press; 2013. (Methods in enzymology, volume five

hundred and thirty three.).
21. Zhang XG, Mason PW, Dubovi EJ, Xu X, Bourne N, Renshaw RW, et al. Antiviral activity of geneticin against dengue virus. Antiviral Res. 2009 Jul 1;83(1):21–7.
22. Rao RN, Allen NE, Hobbs JN, Alborn WE, Kirst HA, Paschal JW. Genetic and enzymatic basis of hygromycin B resistance in Escherichia coli. Antimicrob Agents Chemother. 1983;24(5):689–95.
23. Eustice DC, Wilhelm JM. Mechanisms of action of aminoglycoside antibiotics in eucaryotic protein synthesis. Antimicrob Agents Chemother. 1984;26(1):53–60.
24. Doi Y, Wachino J ichi, Arakawa Y. Aminoglycoside Resistance: The Emergence of Acquired 16S Ribosomal RNA Methyltransferases. Vol. 30, Infectious Disease Clinics of North America. W.B. Saunders; 2016. p. 523–37.
25. Gerard J. Tortora, Berdell R. Funke CLC. Microbiology: An introduction. 12th ed. Pearson Education Limited; 2016.
26. Zhang DX, Lu HL, Liao X, St. Leger RJ, Nuss DL. Simple and efficient recycling of fungal selectable marker genes with the Cre-loxP recombination system via anastomosis. Fungal Genet Biol. 2013 Dec;61:1–8.
27. Kopke K, Hoff B, Kuck U. Application of the saccharomyces cerevisiae FLP/FRT recombination system in filamentous fungi for marker recycling and construction of knockout strains devoid of heterologous genes. Appl Environ Microbiol. 2010 Jul;76(14):4664–74.
28. Idnurm A, Bailey AM, Cairns TC, Elliott CE, Foster GD, Ianiri G, et al. A silver bullet in a golden age of functional genomics: the impact of Agrobacterium-mediated transformation of fungi. Fungal Biol Biotechnol. 2017;4(1):6.
29. Gietz RD, Schiestl RH. High-efficiency yeast transformation using the LiAc/SS carrier DNA/PEG method. Nat Protoc. 2007 Feb;2(1):31–4.
30. Gietz RD, Schiestl RH. Frozen competent yeast cells that can be transformed with high efficiency using the LiAc/SS carrier DNA/PEG method. Nat Protoc. 2007;2(1):1–4.
31. Noskov VN, Lee NC, Larionov V, Kouprina N. Rapid generation of long tandem DNA repeat arrays by homologous recombination in yeast to study their function in mammalian genomes. Biol Proced Online. 2011;13(1):8.
32. MicroPulser ™ Electroporation Apparatus Operating Instructions and Applications Guide Catalog Number 165-2100. :800–424.
33. ThermoFisher Scientific. User Guide: Fast Digestion of DNA [Internet]. Available from: https://www.thermofisher.com/document-connect/document-connect.html?url=https%3A%2F%2Fassets.thermofisher.com%2FTFS-Assets%2FLSG%2Fmanuals%2FMAN0012413_Fast_Digestion_DNA_UG.pdf&title=VXNlciBHdWlkZTogRmFzdCBEaWdlc3Rpb24gb2YgRE5B
34. Eurofins Genomics. Tube sequencing [Internet]. 2017. Available from: https://www.eurofinsgenomics.eu/en/custom-dna-sequencing.aspx
35. InterPro [Internet]. Available from: http://www.ebi.ac.uk/interpro/
36. Westphal KR, Wollenberg RD, Herbst FA, Sørensen JL, Sondergaard TE, Wimmer R. Enhancing the production of the fungal pigment aurofusarin in Fusarium graminearum. Toxins (Basel). 2018;10(11):1–11.
37. NCBI. NCBI Blast:Nucleotide Sequence [Internet]. NIH Public Access. 2020. Available from: https://blast.ncbi.nlm.nih.gov/Blast.cgi#alnShow_7
38. Gietz R, Schiestl R. Frozen competent yeast cells that can be transformed with high efficiency using the LiAc/SS carrier DNA/PEG method. Nat Protoc [Internet]. 2007;2(1):1–4. Available from: http://search.proquest.com/docview/19879570/

11. Appendices

11.1 Appendix I – Plasmid and Annotations from CLC

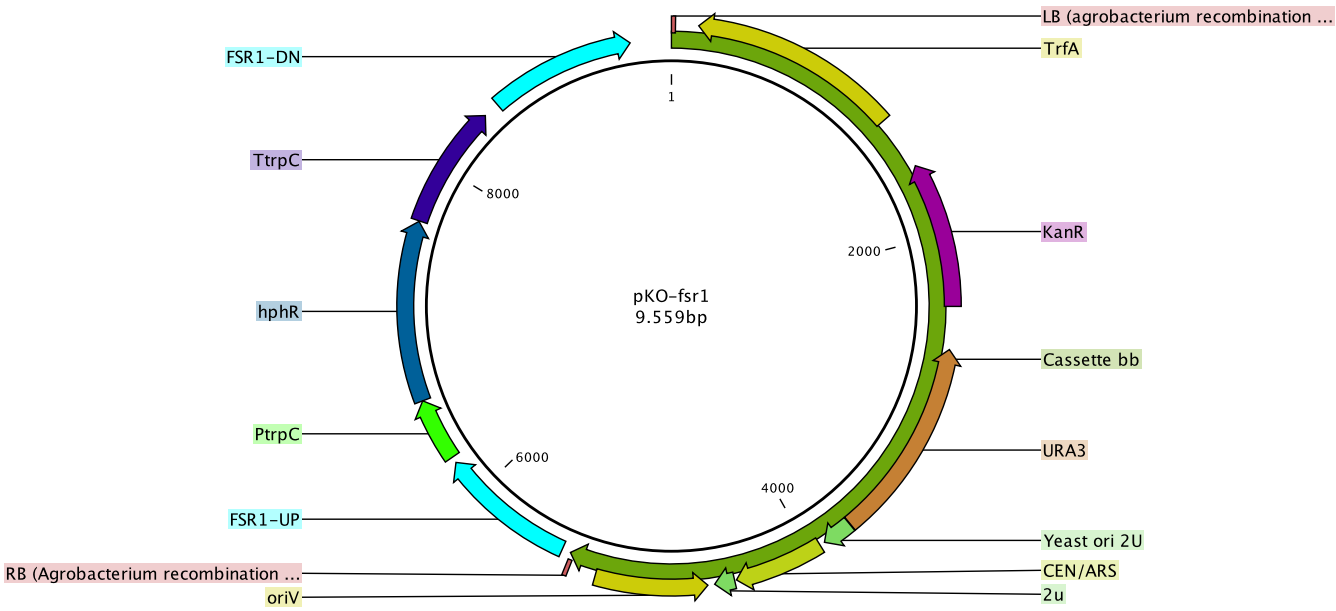

Figure 31: pKO plasmid for fsr1 gene deletion

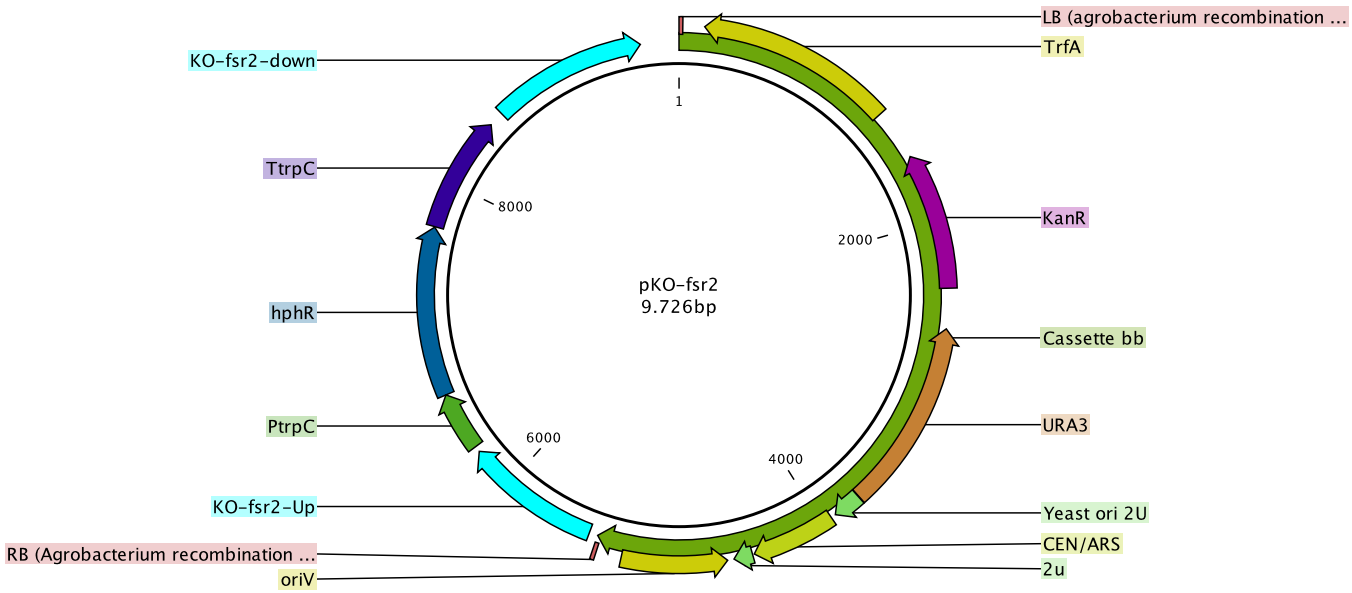

Figure 32: pKO plasmid for fsr2 gene deletion

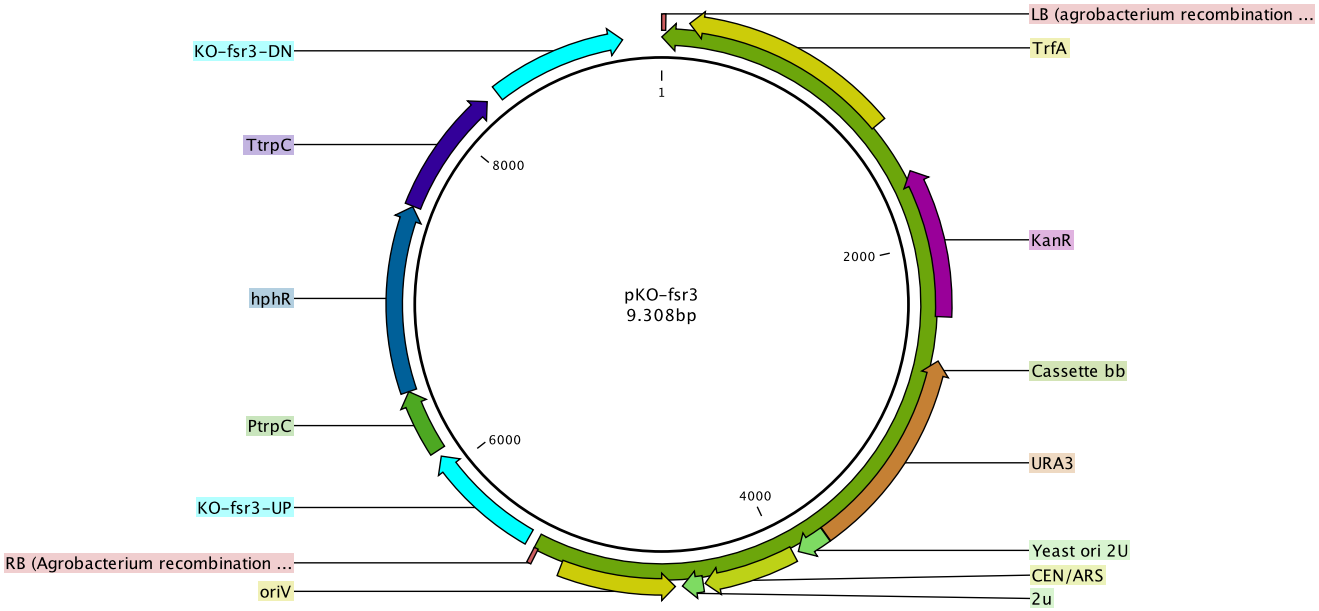

Figure 33: pKO plasmid for fsr3 gene deletion

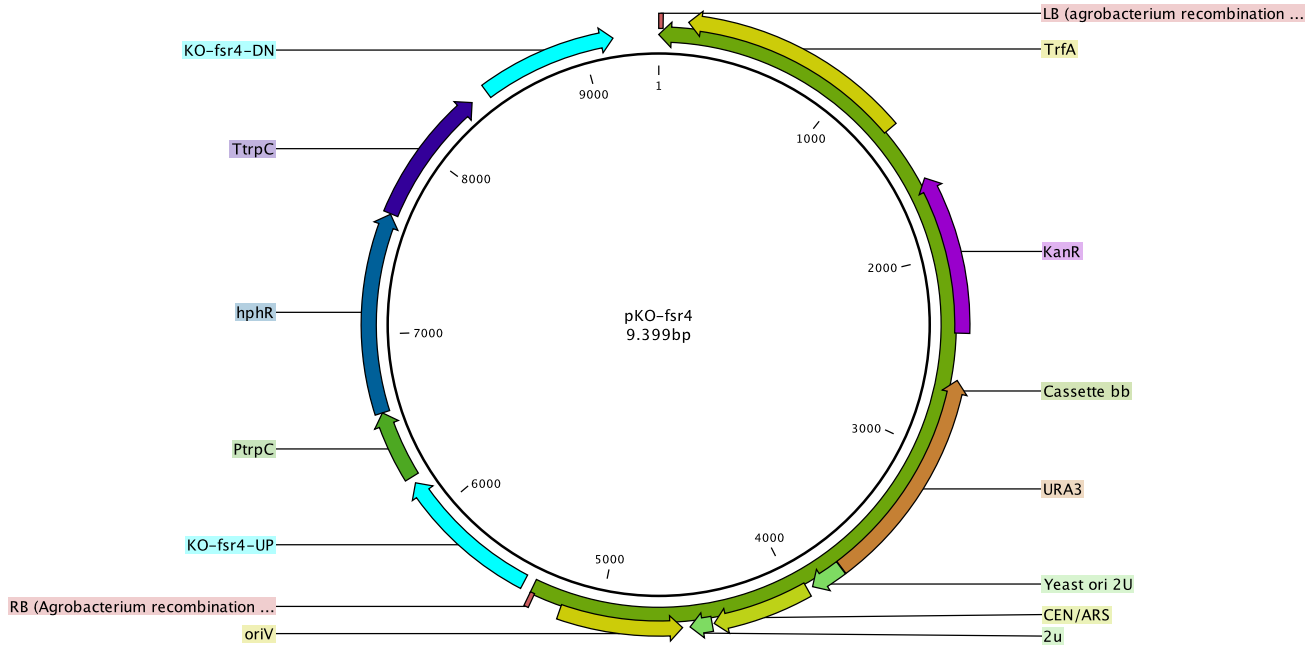

Figure 34: pKO plasmid for fsr4 gene deletion

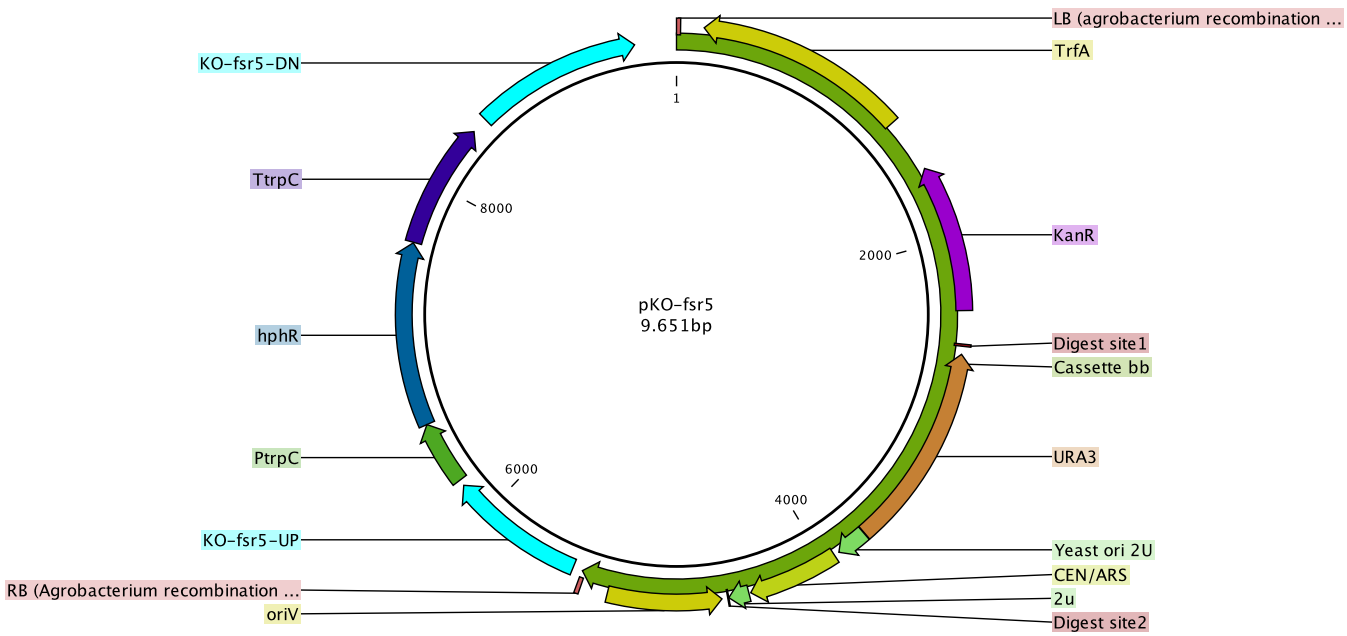

Figure 35: pKO plasmid for fsr5 gene deletion

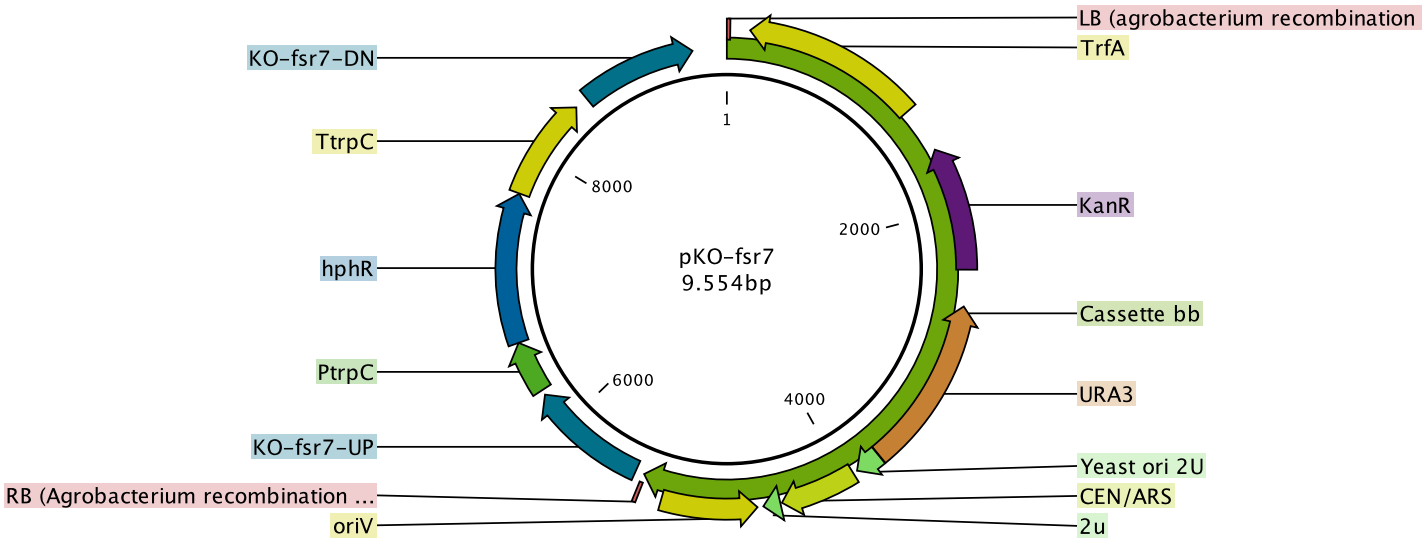

Figure 36: pKO plasmid for fsr7 gene deletion

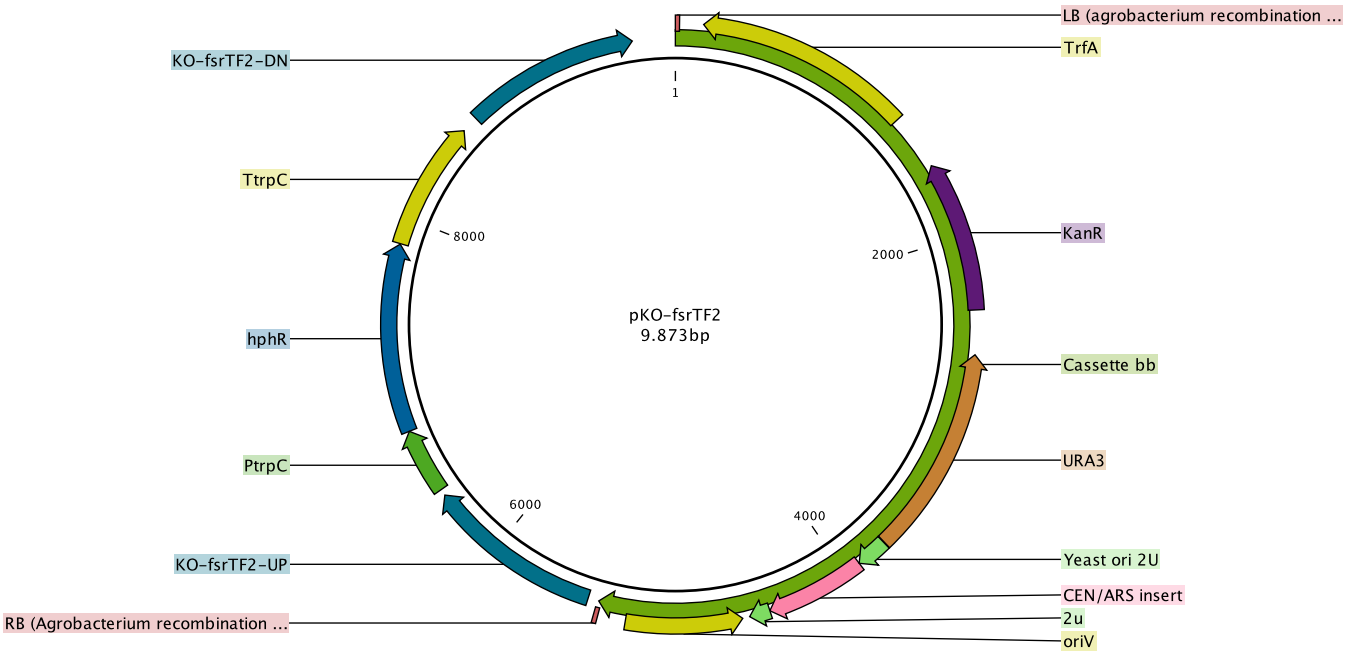

Figure 37: pKO plasmid for TF2 gene deletion

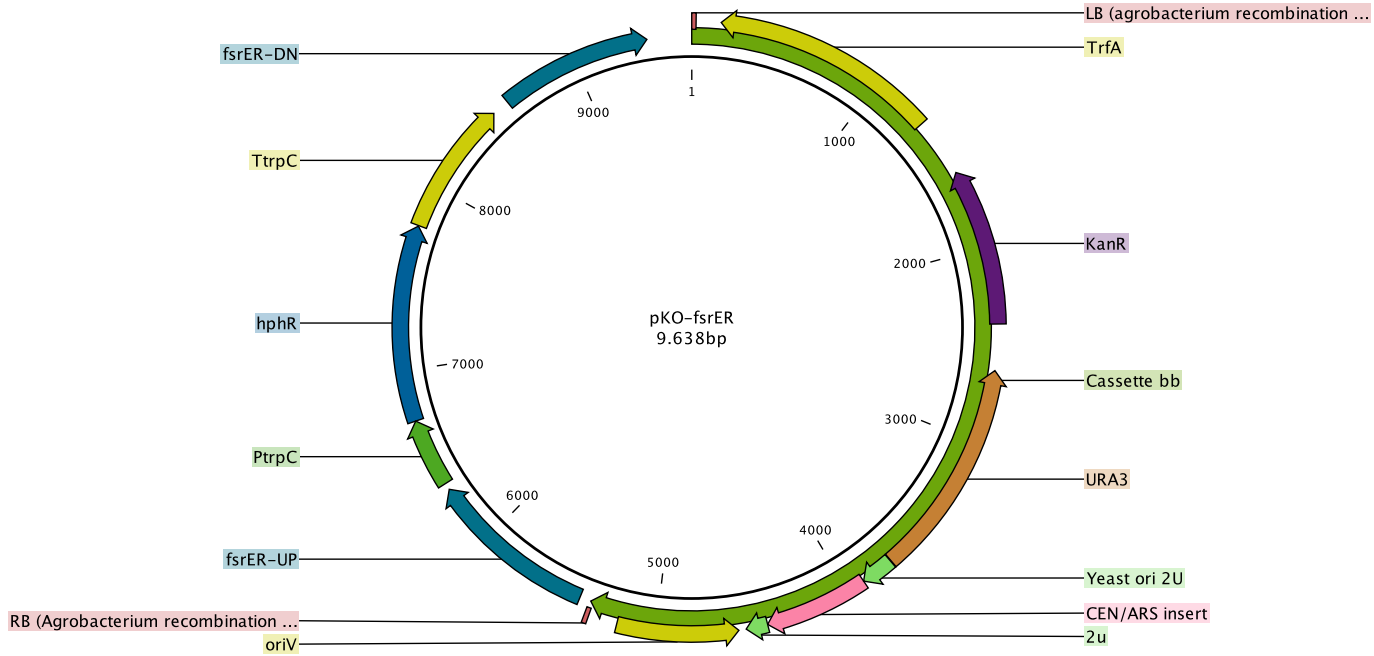

Figure 38: pKO plasmid for ER gene deletion

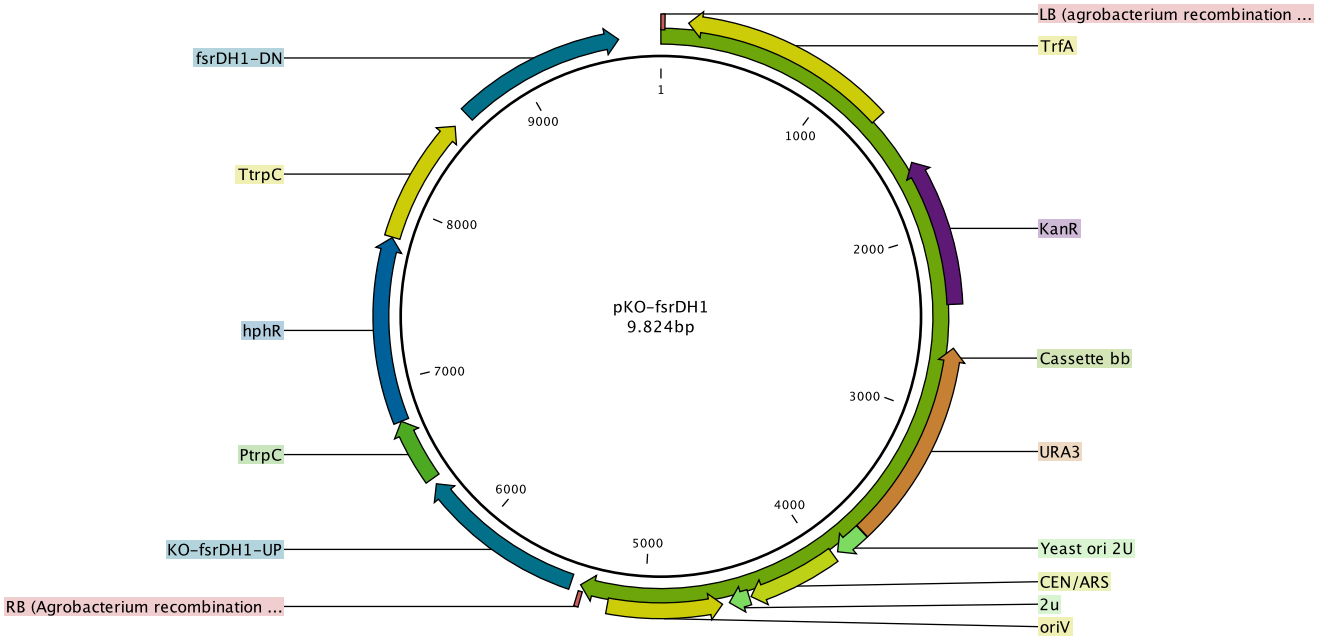

Figure 39: pKO plasmid for DH1 gene deletion

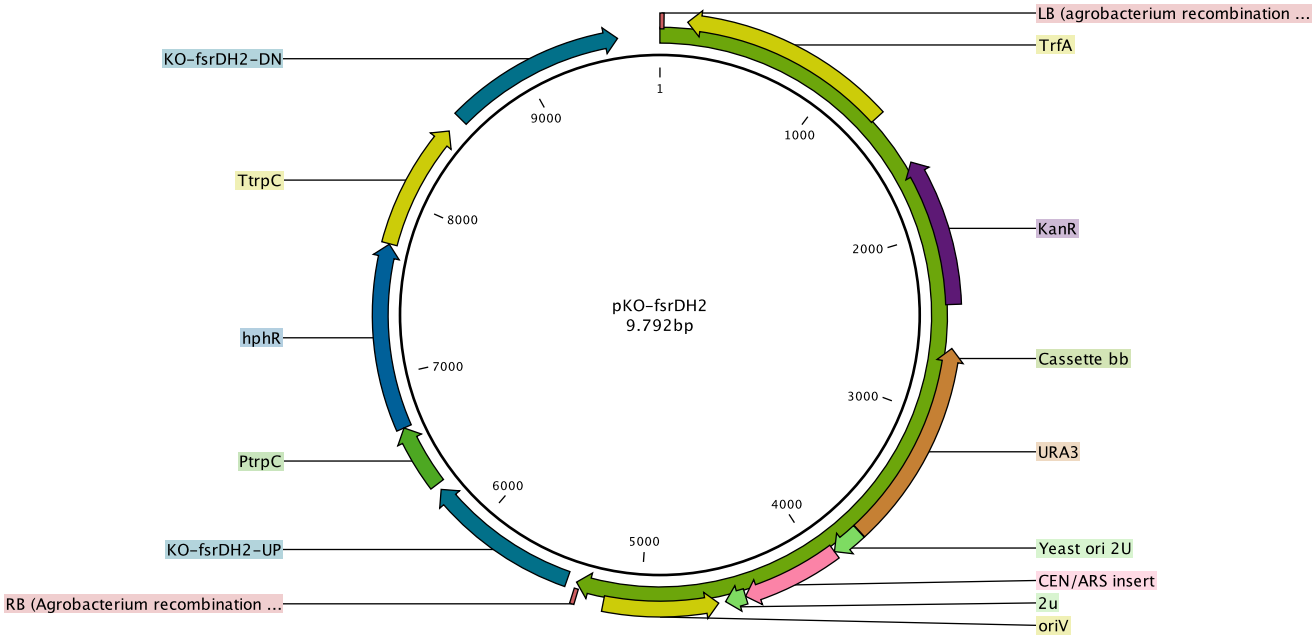

Figure 40: pKO plasmid for DH2 gene deletion

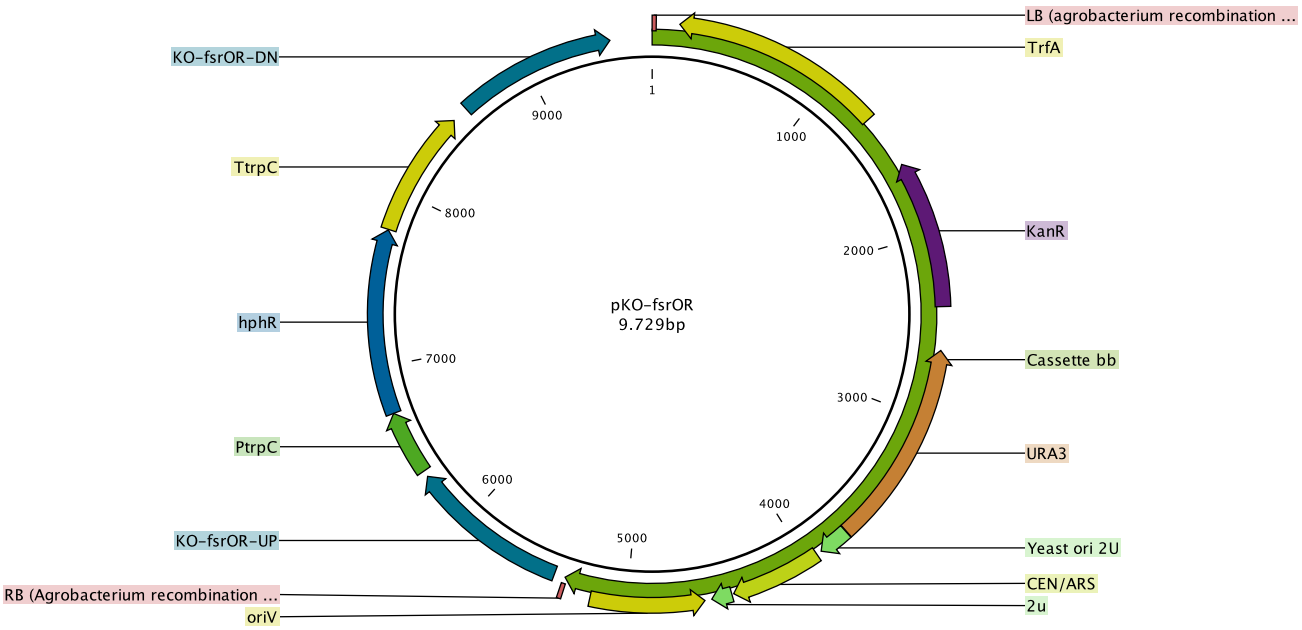

Figure 41: pKO plasmid for OR gene deletion

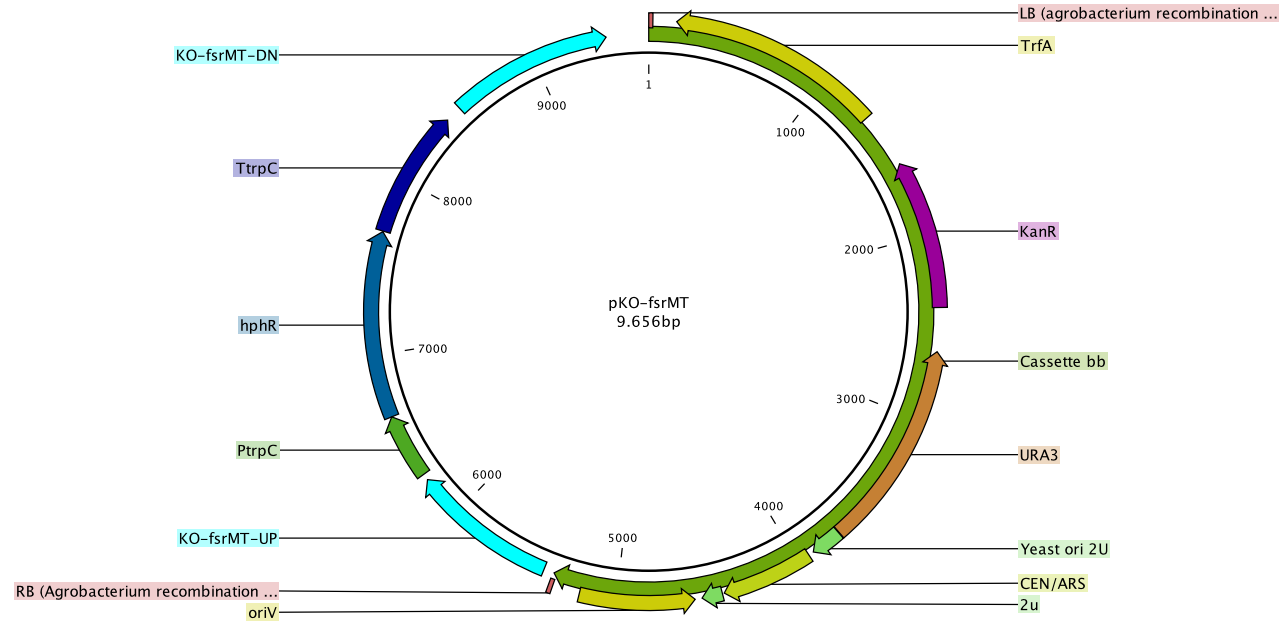

Figure 42: pKO plasmid for MT gene deletion

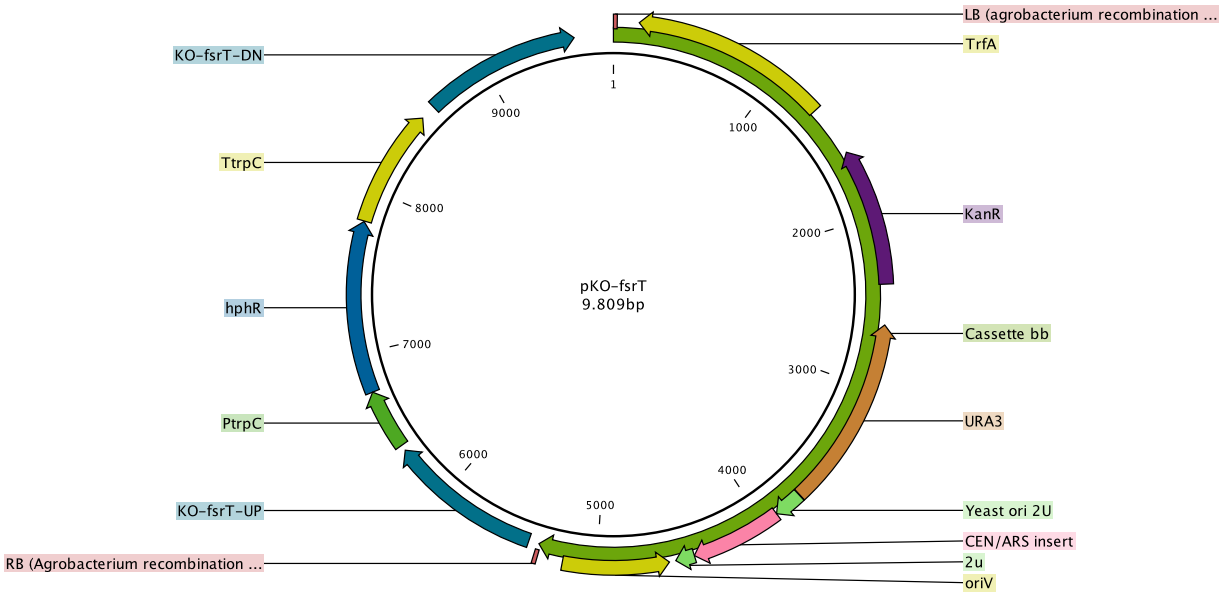

Figure 43: pKO plasmid for T gene deletion

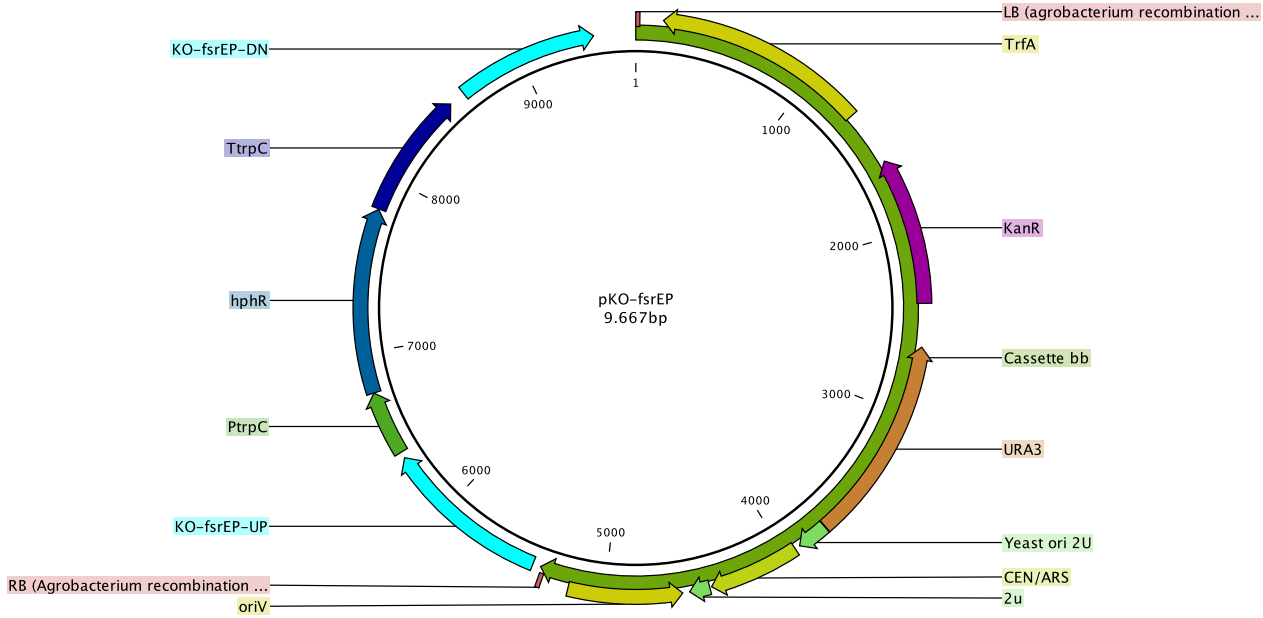

Figure 44: pKO plasmid for EP gene deletion

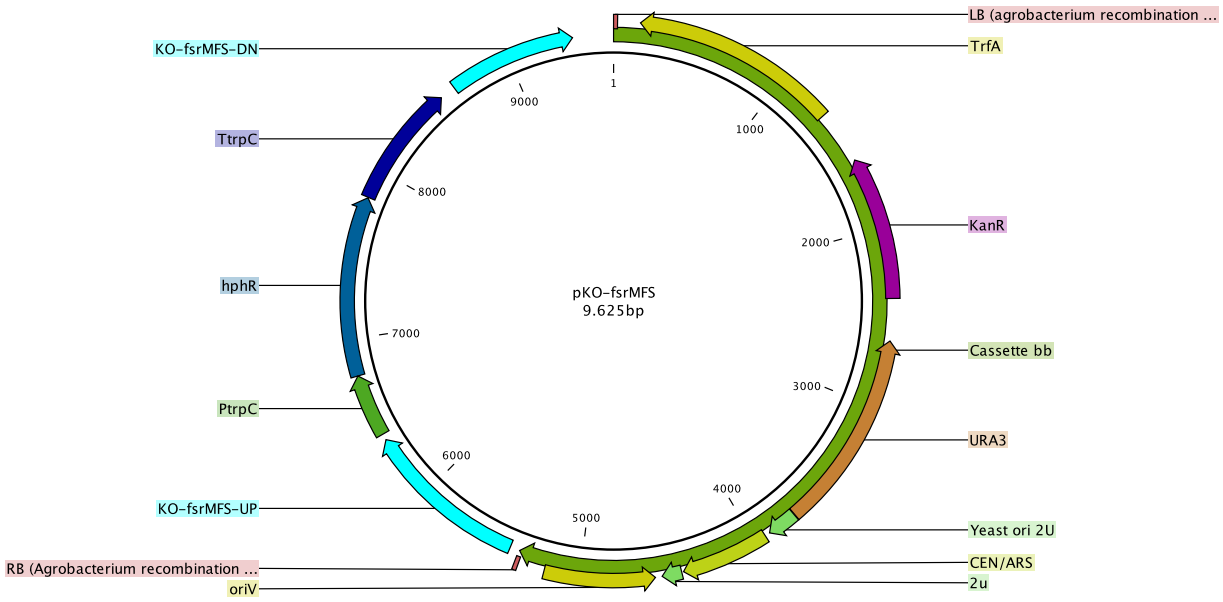

Figure 45: pKO plasmid for MFS gene deletion

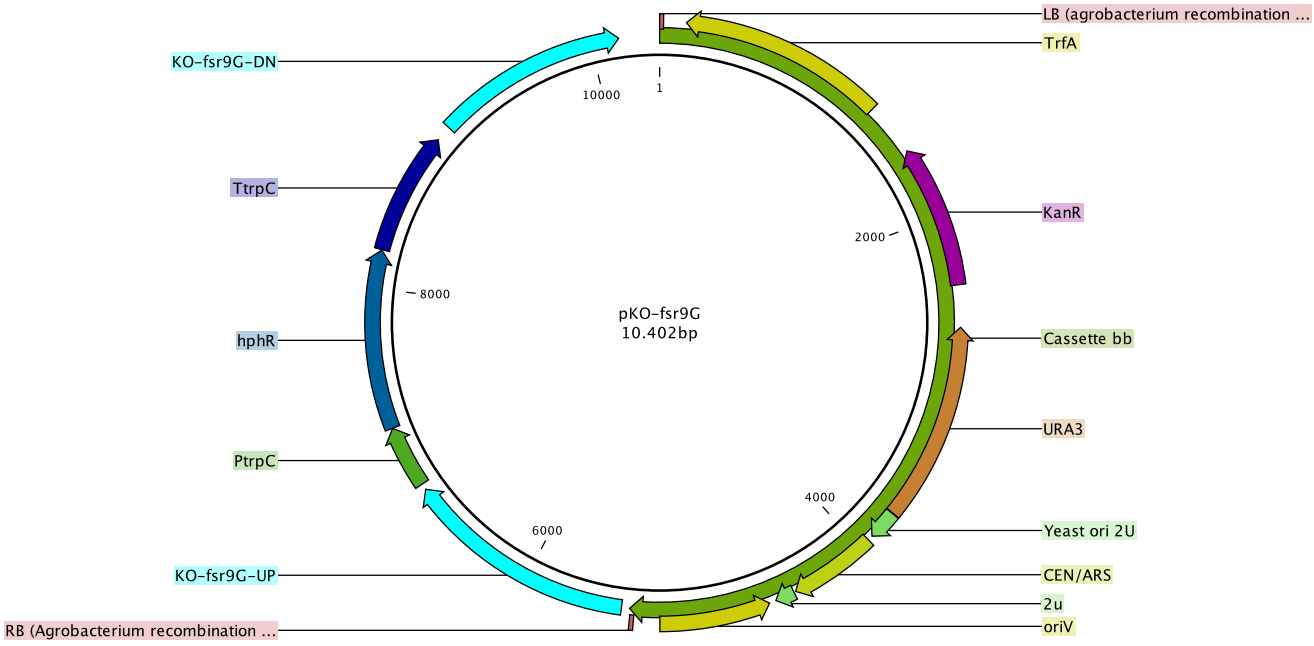

Figure 46: pKO plasmid for 9G gene deletion

11.2 Appendix II – Primer Sequences and PCR Settings

Table 7: Sequences of the primers designed for amplification of the up and down regions within the *PKS3* cluster

KO-FSR1-up-fw	CGACAATCTGATCATGAGCGAGGGAGCAAGAAACGTACGC
KO-FSR1-up-rv	GGCCCGCTGAGGACTTAATTATATGAGTCGCCGTCAGCAG
KO-FSR2-up-fw	CGACAATCTGATCATGAGCGATCCCACCTCAGCAGATCCT
KO-FSR2-up-rv	GGCCCGCTGAGGACTTAATTGGCCAAGGACTGCTGCTTAT
KO-FSR3-up-fw	CGACAATCTGATCATGAGCGTTGGTGGTCGAGGATCTTCC
KO-FSR3-up-rv	GGCCCGCTGAGGACTTAATTACGATTGATGGGTCGGATGA
KO-FSR4-up-fw	CGACAATCTGATCATGAGCGCAAGCTCTTGGGTCACCTGT
KO-FSR4-up-rv	GGCCCGCTGAGGACTTAATTCGCTATGATGGCCATGGGAT
KO-FSR5-up-fw	CGACAATCTGATCATGAGCGGGTCGCTTCCTAAAAGGCCT
KO-FSR5-up-rv	GGCCCGCTGAGGACTTAATTTGGGTGGTGATACAGGGTAGA
KO-FSR7-up-fw	CGACAATCTGATCATGAGCGAGTAGCAACGTTGACTCCCG
KO-FSR7-up-rv	GGCCCGCTGAGGACTTAATTTCGTTCATTCAGCCCTGGAC
KO-FSRER-up-fw	CGACAATCTGATCATGAGCGAGGTCCTCCCAGTACTCGAC
KO-FSRER-up-rv	GGCCCGCTGAGGACTTAATTGAACGATTGGAAGGTTCGCG
KO-FSRTF2-up-fw	CGACAATCTGATCATGAGCGCGCTCCTCGATGTTTTGCTG
KO-FSRTF2-up-rv	GGCCCGCTGAGGACTTAATTCCGGGCCGCAGCTATAATAA
KO-FSRDH1-up-fw	CGACAATCTGATCATGAGCGGGTGGGATTCATCACTGCCA
KO-FSRDH1-up-rv	GGCCCGCTGAGGACTTAATTATGGTGGCGGTTCAAGTCAA
KO-FSRDH2-up-fw	CGACAATCTGATCATGAGCGATGAACGTTTGCAGTGCACC
KO-FSRDH2-up-rv	GGCCCGCTGAGGACTTAATTTCCAGTGATGCGGTGATGTT
KO-FSROR-up-fw	CGACAATCTGATCATGAGCGAGGATCTGCGGCAAACTTCA
KO-FSROR-up-rv	GGCCCGCTGAGGACTTAATTTGACCAACCTCGGACATGTT
KO-FSRT-up-fw	CGACAATCTGATCATGAGCGGACAGCACCACCTCAGGTTT
KO-FSRT-up-rv	GGCCCGCTGAGGACTTAATTAGGAACTTTTCACCCCGTGG
KO-FSRMT-up-fw	CGACAATCTGATCATGAGCGCGTCACTGATTGCATGCGAG

KO-FSRMT-up-rv	GGCCCGCTGAGGACTTAATTATTCGGCTGGATGTTACGCT
KO-FSREP-up-fw	CGACAATCTGATCATGAGCGAACTTCGGCTGACGGAAAGT
KO-FSREP-up-rv	GGCCCGCTGAGGACTTAATTGAATATCAACCGAGGCCGCT
KO-FSR9G-up-fw	CGACAATCTGATCATGAGCGTGAGGCCCAATGAACGAGTC
KO-FSR9G-up-rv	GGCCCGCTGAGGACTTAATTCGCTATTCAACTCCAACGCG
KO-FSRMFS-up-fw	CGACAATCTGATCATGAGCGACTGCAGCAGCCATTTTGTG
KO-FSRMFS-up-rv	GGCCCGCTGAGGACTTAATTAGGCCGAGCGATGATCATTT
KO-FSR1-dw-fw	TATCGCCGACATCACCGATGTCATCCCGGCCGTTATCTTG
KO-FSR1-dw-rv	GTTTTCCCAGTCACGACGTTTTCTCAACAAACGAGGCGGA
KO-FSR2-dw-fw	TATCGCCGACATCACCGATGTCACCGAACGGATGTGACAG
KO-FSR2-dw-rv	GTTTTCCCAGTCACGACGTTCGGTGCTCATGCGATGATTG
KO-FSR3-dw-fw	TATCGCCGACATCACCGATGAACACATACCGCAGCTTGGA
KO-FSR3-dw-rv	GTTTTCCCAGTCACGACGTTCGATGATAGGGACCGTGAGC
KO-FSR4-dw-fw	TATCGCCGACATCACCGATGCGACATGGGGAAACGAGACA
KO-FSR4-dw-rv	GTTTTCCCAGTCACGACGTTGGATACTGGGACCACGTGAC
KO-FSR5-dw-fw	TATCGCCGACATCACCGATGTTGATTACGGTGTGCGACGA
KO-FSR5-dw-rv	GTTTTCCCAGTCACGACGTTCGACCCTGACAGGTTGTTCA
KO-FSR7-dw-fw	TATCGCCGACATCACCGATGTGTTCTCGTCCCCGTTACTG
KO-FSR7-dw-rv	GTTTTCCCAGTCACGACGTTAGGTGTGGTTGGAGGACATG
KO-FSRER-dw-fw	TATCGCCGACATCACCGATGGGTCCAGATCCACCACGAAG
KO-FSRER-dw-rv	GTTTTCCCAGTCACGACGTTTGGGATTCACAACTCTGCCC
KO-FSRTF2-dw-fw	TATCGCCGACATCACCGATGGGGGCTGTTGTTTGCTGATG
KO-FSRTF2-dw-rv	GTTTTCCCAGTCACGACGTTTAAAGATCTCGCCGGCGTAC
KO-FSRDH1-dw-fw	TATCGCCGACATCACCGATGCGCAGAGCAGGAATAGGGAG
KO-FSRDH1-dw-rv	GTTTTCCCAGTCACGACGTTAAGCAGATCTCGACCTCCCT
KO-FSRDH2-dw-fw	TATCGCCGACATCACCGATGTGCCAGAGCGTATCAACCTC
KO-FSRDH2-dw-rv	GTTTTCCCAGTCACGACGTTTCGGTCTCCATGCTTGTGAC

KO-FSROR-dw-fw	TATCGCCGACATCACCGATGATCCAGATCTGCGCTTGGAG
KO-FSROR-dw-rv	GTTTTCCCAGTCACGACGTTCCCATTTCCGAGGGCTTTCT
KO-FSRT-dw-fw	TATCGCCGACATCACCGATGATAAAGCGGTCAGGTCTGGC
KO-FSRT-dw-rv	GTTTTCCCAGTCACGACGTTACTTTCCGTCAGCCGAAGTT
KO-FSRMT-dw-fw	TATCGCCGACATCACCGATGGCCATGGTAAAAGGCGCAAT
KO-FSRMT-dw-rv	GTTTTCCCAGTCACGACGTTGCTGAATGACGTAGCGCATG
KO-FSREP-dw-fw	TATCGCCGACATCACCGATGCGCGTTGGAGTTGAATAGCG
KO-FSREP-dw-rv	GTTTTCCCAGTCACGACGTTTGGTCAAAGGTTGGTGCTGT
KO-FSR9G-dw-fw	TATCGCCGACATCACCGATGATCCCATGGCCATCATAGCG
KO-FSR9G-dw-rv	GTTTTCCCAGTCACGACGTTACAATCCCTAAAGCTGGGCC
KO-FSRMFS-dw-fw	TATCGCCGACATCACCGATGGAGTTCTCGCTATTCCGGCA
KO-FSRMFS-dw-rv	GTTTTCCCAGTCACGACGTTCGGTCCTGTTTGCCAACAAG
pKO-bb-fw	AACGTCGTGACTGGGAAAAC
pKO-bb-rv	CGCTCATGATCAGATTGTCG
pKO-hyg-fw	AATTAAGTCCTCAGCGGGCC
pKO-hyg-rv	CATCGGTGATGTCGGCGATA

Table 8: PCR settings for amplification of each up and down regions

PCR product	Annealing temperature (°C)	Extension time
Fsr1 up	55	45s
Fsr1 dw	55	45s
Fsr2 up	60.1, 61.9, 64.4	1 min
Fsr2 dw	52	45s
Fsr3 up	55	45s
Fsr3 dw	63, 62.3, 61.2, 59.5	1 min
Fsr4 up	55	45s
Fsr4 dw	55	45s
Fsr5 up	55	45s
Fsr5 dw	65 *	1 min
Fsr7 up	65 *	1 min
Fsr7 dw	56.5	1 min
Er up	65 *	1 min
Er dw	65 *	1 min
Tf2 up	65 *	1 min
Tf2 dw	55	1 min
Dh1 up	58	1 min
Dh1 dw	55	1 min
Dh2 up	60, 56.5	1 min
Dh2 dw	56.5	1 min
Or up	56.5	1 min
Or dw	55	1 min
T up	58	1 min
T dw	58	1 min
Mt up	58	1 min
Mt dw	56.5	1 min
Ep up	63 *	1 min
Ep dw	56.5	1 min
9g up	56.5	1 min
9g dw	56.5	1 min
Mfs up	63 *	1 min
Mfs dw	56.5	1 min
Bb	62, 61.3, 60.2, 58.5, 54.7, 53.6	5 min
Hyg	55, 55.7, 56.9, 58.8, 61.1, 63, 64.3, 65	2 min

*Touchdown technique: All TD were executed at the mentioned starting temperature and a decrease of 1 °C per cycle.

11.3 Appendix III – Nucleic Acid Concentrations

Table 9: Nucleic acid concentrations in fmol of each of the fragments used in the yeast transformation

PCR product	DNA concentration fmol/µL
Fsr1 up	67.97
Fsr1 dw	64.2
Fsr2 up	67.11
Fsr2 dw	36.62
Fsr3 up	146.92
Fsr3 dw	146.84
Fsr4 up	104.85
Fsr4 dw	122.45
Fsr5 up	132.89
Fsr5 dw	48.24
Fsr7 up	87.3
Fsr7 dw	82.75
Er up	53.8
Er dw	51.99
Tf2 up	52.35
Tf2 dw	75.46
Dh1 up	70.44
Dh1 dw	66.86
Dh2 up	27.33
Dh2 dw	53.16
Or up	44.51
Or dw	69.88
T up	58.73
T dw	80.18
Mt up	68.71
Mt dw	83.69
Ep up	65.55
Ep dw	73.02
9g up	41.13
9g dw	52.04
Mfs up	59.23
Mfs dw	57.14
Bb	49.24
Hyg	44.45

Table 10: Nucleic acid concentrations in ng/µL of each of the pKO plasmids purified from *E. coli*

PLASMID	CONCENTRATION (ng/µL)
PKO-FSR1	243
PKO-FSR2	95
PKO-FSR3	97
PKO-FSR4	390
PKO-FSR5	95
PKO-FSR7	134
PKO-ER	92
PKO-TF2	97
PKO-DH1	154
PKO-DH2	103
PKO-OR	124
PKO-MT	93
PKO-T	116
PKO-9G	150
PKO-EP	128
PKO-MFS	375

11.4 Appendix IV – List of Restriction Enzymes

Table 11: List of restriction enzymes used for digestion of each plasmid

PLASMID	RESTRICTION ENZYMES	EXPECTED SIZES OF DIGESTED FRAGMENTS (bp)
PKO-FSR1	BstXI ; PstI	3000+6500 ; 3400+6100
PKO-FSR2	BstXI ; PstI	3200+6400 ; 3400+6200
PKO-FSR3	PvuII ; PstI	5900+3200 ; 5900+3300
PKO-FSR4	BglI ; PstI	1300+100+7000 ; 3300+5900
PKO-FSR5	BglII ; PstI	3310+6200 ; 3400+6100
PKO-FSR7	XhoI ; PstI	3000+6400 ; 3400+6000
PKO-ER	BglI ; PstI	1400+1000+7000 ; 3500+6000
PKO-TF2	BstXI ; PstI	3000+6900 ; 200+3600+4100
PKO-DH1	XbaI ; PstI	2700+7000 ; 3600+6200
PKO-DH2	BstXI ; PstI	850+670+8100 ; 3400+6200
PKO-OR	XhoI ; PstI	2900+6700 ; 1500+1900+6100
PKO-MT	PvuII ; PstI	3800+5700 ; 3400+6100
PKO-T	BstXI ; PstI	2800+6800 ; 2200+3900+3500
PKO-9G	BstXI ; PstI	91+2800+3300+170+3800; 4000+6400
PKO-EP	BglI ; PstI	1400+1000+7100 ; 3500+6000
PKO-MFS	BamHI ; PstI	700+1800+7000 ; 1700+5900+1800

11.5 Appendix V – Protocol for Transformation of *F. solani* via AMT

1. MATERIALS

1.1 REAGENTS

1.1.1 Agrobacterium tumefaciens colonies

Colonies of *A. tumefaciens* strain AGL-1 must be carrying the vector of interest, streaked on LB plates and incubated at 28 °C with kanamycin and rifampicin selection.

1.1.2 F. solani spores

$1.2x10^7$ spores of *F. solani* FSSC (*N. haematococca* mpVI 77-13-4) per transformation experiment and control experiment, kept on ice during the transformation proceedings.

1.1.3 2-[N-morholino]ethnasulfonic acid (MES)

Dissolve 19.52 g MES in 100 mL of Milli-Q water. The solution must be stirred with a small magnet several minutes before complete dissolution of MES. Adjust the pH to 5.3 with 5 M KOH. Filter-sterilize into a clean centrifuge tube.

> Note: Approximately 1 mL of 5M KOH is required to reach pH of 5.3. Add KOH progressively. MES can be stored in centrifuge tubes at -20 °C. However, MES precipitates quickly and would require 15 min of vortexing to redissolve again.

1.1.4 Acetosyringone (AS)

In a tinfoil-covered beaker, carefully dissolve 98.1 mg of AS in 50 mL of Milli-Q water by stirring with a small magnet. Adjust the pH to 8.0 with 5M KOH to facilitate the dissolution of AS. Cover the glass with parafilm while stirring to avoid evaporation. Once dissolved, the solution should turn light yellow. Filter-sterilize into a clean centrifuge tube and keep cold in fridge or on ice until needed.

> Note: If the powder adheres to the side of container, use a Pipetteman to mix. AS is difficult to dissolve in water so the dissolution could take up to 1.5 h. Add KOH progressively, approximately 50 µL is required to reach pH of 8.0. After use, fill the container with inert gas to avoid contact with air. Must always be made fresh. If the solution does not turn to yellow, the AS is old and cannot be used.

1.1.5 5M KOH

Dissolve 7.013 g of KOH pellets in 25 mL Milli-Q water.

1.1.6 20 % w/vol Glucose stock

Dissolve 20 g D-(+)-glucose with 70 mL Milli-Q water in a 100 mL volumetric flask. After the sugar is dissolved, fill Milli-Q water up to the 100 mL. Filter-sterilize into a clean centrifuge tube.

1.1.7 20 % w/vol Glycerol stock

Mix 17.4 mL 87 % glycerol with 82.6 mL Milli-Q water in a 100 mL bluecap flask. Autoclave at 121 °C for 15 min.

1.1.8 2.5X Salt solution for IMAS

Add the following salts in 1 L of Milli-Q water at low heat and constant stirring: 3.625 g KH_2PO_4, 5.125 g K_2HPO_4, 0.375 g NaCl, 1.250 g $MgSO_4*7H_2O$, 1.250 g $(NH_4)_2SO_4$, 0.0062 g $FeSO_4*7H_2O$ Filter-sterilize the dissolved salts into a sterile flask with the help of a large sterile 0.45 µm mounted filter with pressure-suction.

Note: Never autoclave the dissolved salts to avoid scaling.

1.2 ANTIBIOTICS

1.2.1 Kanamycin (50 µg/mL)

Place 500 mg of kanamycin powder in a sterile 50 mL centrifuge tube and add 10 mL Milli-Q water. Vortex until completely dissolved. Filter-sterilize the antibiotic into 10 sterile Eppendorf tubes. Use 1 µL stock per mL of medium to result in a final antibiotic concentration of 50 µg/mL. Store at -20 °C.

1.2.2 Rifampicin (10 µg/mL)

While wearing protective gloves, dissolve 30 mg of rifampicin powder in 3 mL of methanol and in sterile container and vortex vigorously. Store at -20 °C freezer until use. Completely thaw the sample and vortex again to dissolve any particles right before application in medium. Use 1 µL per mL of medium to achieve a final concentration of 10 µg/mL.

Note: If used for agar plates, use 2 µL of rifampicin per mL of molten agar.

1.2.3 Hygromycin B (120 µg/mL)

Dissolve 1.2 g of hygromycin B powder in 10 mL Milli-Q water in sterile container, and vortex until completely dissolved. Filter-sterilize the antibiotic into 10 sterile Eppendorf tubes. Use 1 mL per L of molten V8 agar, resulting in a final concentration of 120 µg/mL. Store at -20 °C.

1.2.4 Cefoxitin sodium salt (300 µg /mL)

Weigh off 300 mg of cefoxitin sodium salt in a 50 mL centrifuge tube. Add 20 mL of Milli-Q water and vortex until completely dissolved. Filter-sterilize the antibiotic into a clean test tube or directly into 1 L of molten V8 agar, while stirring, resulting in a final concentration of 300 µg /mL. Store at -20 °C.

1.2.5 Geneticin G418 (150 µg/mL or 200 µg/mL)

Weigh off 1.0 g of geneticin powder in a sterile 50 mL centrifuge tube. Add 10 mL of Milli-Q water, and vortex until completely dissolved. Filter-sterilize the antibiotic into a clean tube and divide the sterile antibiotic solution into 10 Eppendorf tubes.
In V8 agar plates, use 1.5 µL stock per mL of medium to result in a final concentration of 150 µg/mL.
In YPD agar plates, use 2 µL stock per mL of medium to in a final concentration of 200 µg/mL.

1.3 MEDIA

1.3.1 ½ LB liquid broth

For 1 L medium: 5 g peptone (Sigma-Aldrich), 2.5 g bacto yeast extract, 5 g NaCl. Adjust pH to 7.7 using 1 M NaOH before autoclaving. Autoclave for 15 min at 121 °C. Once cooled down, add 50 µg/mL kanamycin (1 µL stock/mL) and 10 µg/mL rifampicin (1 µL stock/mL).

> Note: Prepare about 20 mL of LB broth per each transformation experiment and control experiment.

1.3.2 IMAS liquid medium

For 250 mL medium: 100 mL 2.5x salts solution, 2.5 mL 20% w/v glucose, 6.25 mL 20% w/v glycerol, 10 mL 1 M MES, 5 mL 10 mM AS, 126.25 mL sterile Milli-Q water. All reagents are sterilised beforehand and must be poured in a complete sterile blue cap flask.

> Note: Prepare 35 mL per experiment, including control experiments. Mix right before inoculation of *Agrobacterium* on day 2.

1.3.3 IMAS agar

For 500 mL medium: Dissolve 10 g agar with 252.5 mL of Milli-Q water, add stirring magnet and autoclave for 20 min at 121 °C. Carefully pour 200 mL of 2.5x salts, 5 mL 20% w/v glucose, 12.5 mL 20 % w/v glycerol into the molten agar. Move quickly as the agar will solidify, stir the agar at room temperature.
Add 20 mL 1 M MES and 10 mL 10 mM AS before pouring into inoculation plates. Pour approximately 20 plates per 500 mL flasks.

1.3.4 V8 agar plates

For 500 mL medium: 87.5 mL V8 tomato juice, 1.5 g CaCO3, 10 g agar. Adjust pH to 6.4 with 5M NaOH. Autoclave at 121 °C for 20 min. Once cooled down to approximately 50 °C, add the necessary antibiotics and pour into plates. For the first selection round, add 300 µg/mL (0.3 g/L) cefoxitin and 120 µg/mL hygromycin or 150 µg/mL geneticin. For the second selection round, add 120 µg/mL hygromycin or 150 µg/mL geneticin.

1.3.5 PDA

For 500 mL medium: 10 g dextrose, 2 g potato extract, 10 g agar, 1 mL tracer metals solution. Autoclave at 121 °C for 20 min. Once cooled down, add the necessary antibiotics and pour into plates.

1.4 EQUIPMENT

1.4.1 Sterilised tools

Before transformation, autoclave 100 mL Erlenmeyer flasks capped with wool and tinfoil. Prepare 4 flasks per transformation experiment. Autoclave 10 black filter papers (Frisenette 140.185) of 80 mm diameter per experiment in a glass bowl covered with tinfoil, a few pairs of tweezers and drigalski spatulas. Rinse all glass flasks and equipment with Milli-Q water before sterilisation.

2. METHODS

All steps must be carried in sterile conditions at room temperature unless otherwise specified.

Day 1

2.1 Start a pre-culture of *Agrobacterium* AGL-1 by inoculating a colony in 20 mL of ½LB medium with rifampicin and kanamycin in a 100 mL Erlenmeyer flask. Incubate at 28 °C and 100 rpm for 1 or 2 days.

Note: The pre-culture will look cloudy when it is ready. Pipetting up and down through the incubation time will help homogenisation.

Day 2

2.2 Prepare IMAS liquid medium (33 mL per experiment) and keep in fridge.

2.3 Prepare the IMAS agar and pour 10 plates per transformation experiment and controls (1 per fungal strain, 1 per plasmid).

2.4 Pour 10 mL of IMAS medium in the 3 Erlenmeyer flasks and add 100 µL, 200 µL, 500 µL of Agrobacterium pre-culture respectively. Add 50 µg/mL kanamycin in IMAS culture and incubate at 28 °C, 100 rpm until the OD_{600} reaches 0.4-0.6.

Note: This step usually takes 16-18 hours before the cells reach optimal OD.

2.5 With the help of sterilized tweezers, place black filter papers every IMAS agar plate. Eliminate air bubbles by flattening the filters with a sterile drigalski spatula. Keep plates in the fridge overnight.

Note: Soak all black filter papers in 100 µL of liquid IMAS to help the filters stick. Make sure to have 10 plates with black filter papers per experiment and extra for controls.

Day 3

2.6 Thaw the frozen spores of *F.solani* and add $6*10^6$ sp/mL in 2.2 mL of cold liquid IMAS and keep on ice. When the *Agrobacterium* cultures has reached the correct OD, mix fungal spores and with 2.2 mL of *Agrobacterium culture* in a total volume of 4.4 mL in a sterile 50 mL centrifuge tube. Inoculate the co-cultivation for 1 h at 28 °C and 100 rpm.

2.7 Spread 400 µL of the co-culture onto each 10 IMAS plates fitted with a black filter on top. For controls: spread 100 µL diluted spores or 100µL *Agrobacterium* IMAS culture onto plates without filters. In addition, spread 100 µL of diluted spores to an IMAS plate holding a black filter paper. Incubate the plates at 21-22 °C for 2-3 days in complete darkness.

Note: A light white aerial mycelium will appear on top of the black filters after 2 days. The aerial mycelium should not become too dense before continuing to the next step.

Day 6

2.8 Autoclave and pour 10 V8 agar plates containing the appropriate antibiotics for the first selection. Using sterile tweezers, carefully transfer the black filter from the IMAS plates to V8 agar plates. Avoid air bubbles by placing the filter smoothly.

2.9 Incubate the plates at 21-22 °C in darkness again.

Note: The following days, most of the areal mycelium will disappear due to the antibiotic selection, and the filters may appear completely blank until colonies arise.

Day 10-14

2.10 Autoclave and pour 10 V8 agar plates containing the appropriate antibiotics for the second selection. Using sterile tweezers, carefully transfer the black filter from the first V8 plates to the second V8 agar plates. Avoid air bubbles by placing the filter smoothly.

2.11 Incubate the plates at 21-22 °C in darkness again until colonies are observed.

Day 13-20

2.12 Pour small PDA plates (Ø = 50 mm) containing the appropriate antibiotics. Streak the newly emerged mutants individually and incubate at 28 °C until validation such as diagnostic colony PCR.

11.6 Appendix VI – Annotated Restriction Digest Results

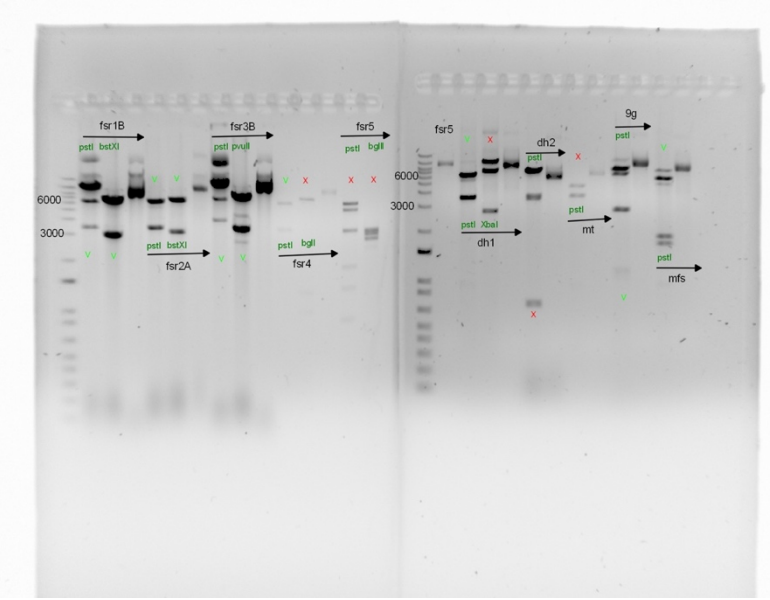

Figure 47: Results from the correct digestion of pKO plasmids fsr1, fsr2, fsr3, 9G and MFS

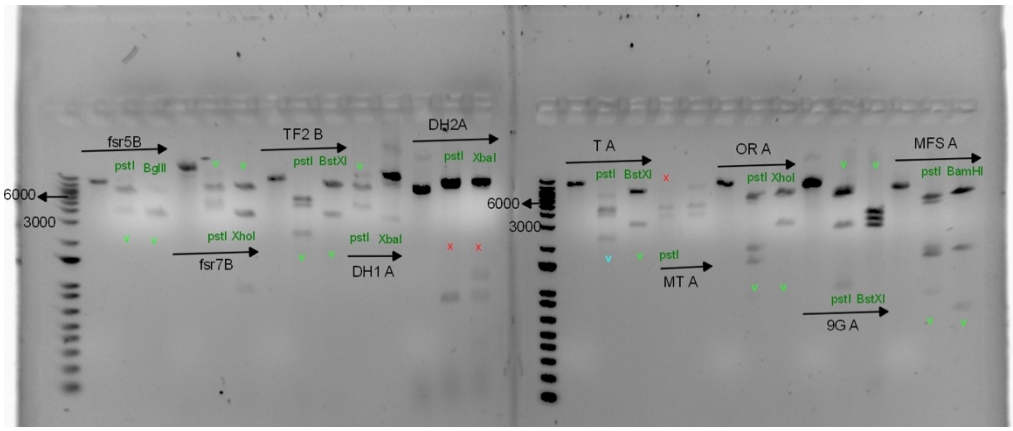

Figure 49: Results from the correct digestion of pKO plasmids fsr5, fsr7, TF2, T, OR, 9G and MFS

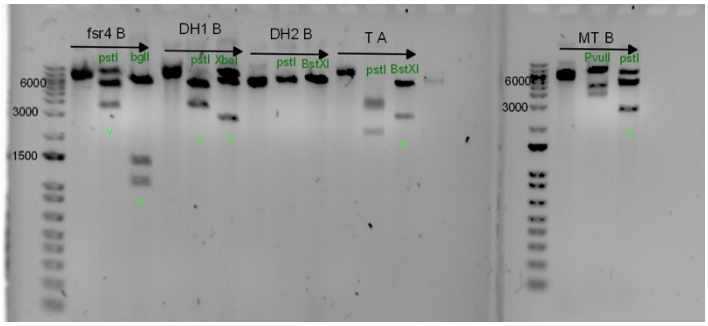

Figure 48: Results from the correct digestion of pKO plasmids fsr4 and DH1

11.7 Appendix VII – Sequencing Results of pKO Plasmids

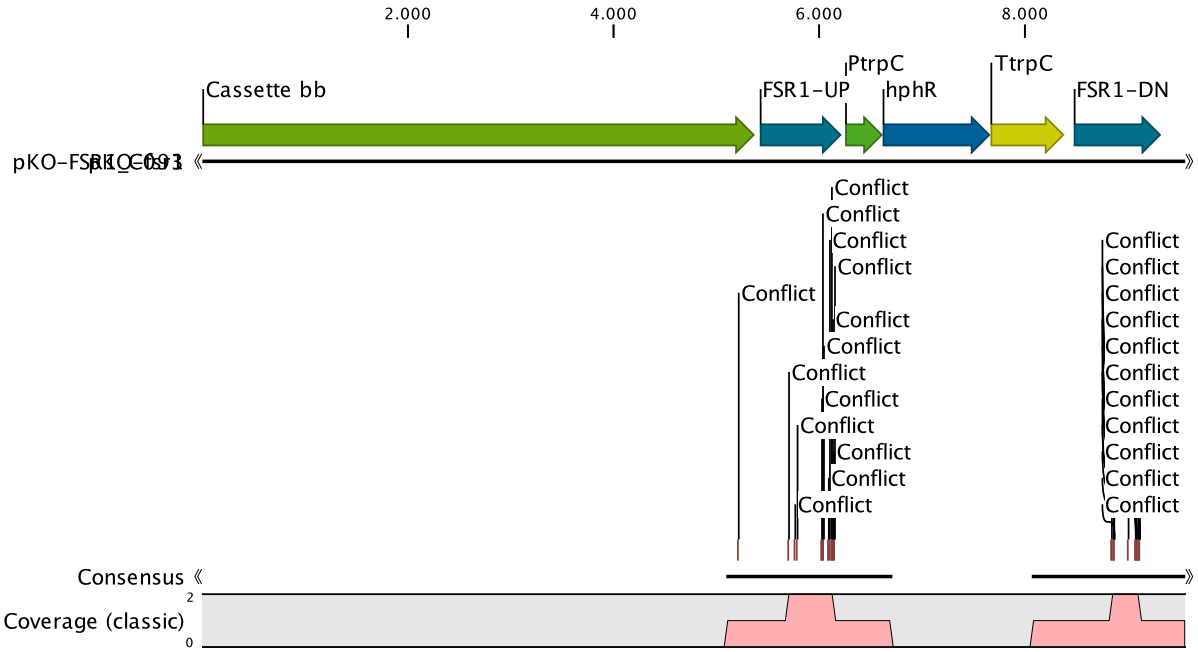

Figure 50: Results from sequence assembly of up and down regions of FSR1 and sequenced results from Eurofins Genomics

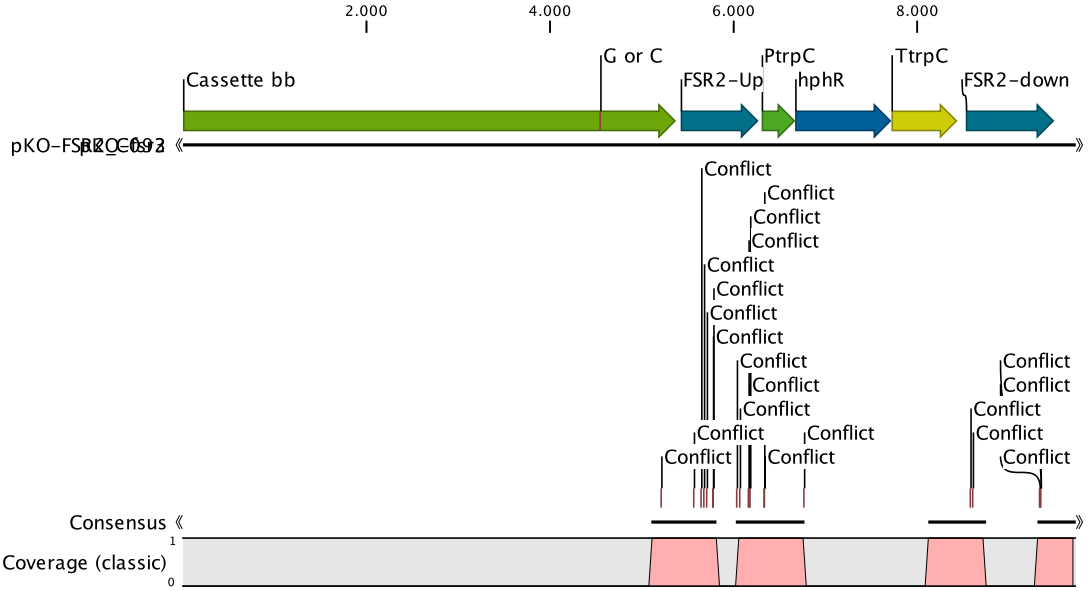

Figure 51: Results from sequence assembly of up and down regions of FSR2 and sequenced results from Eurofins Genomics

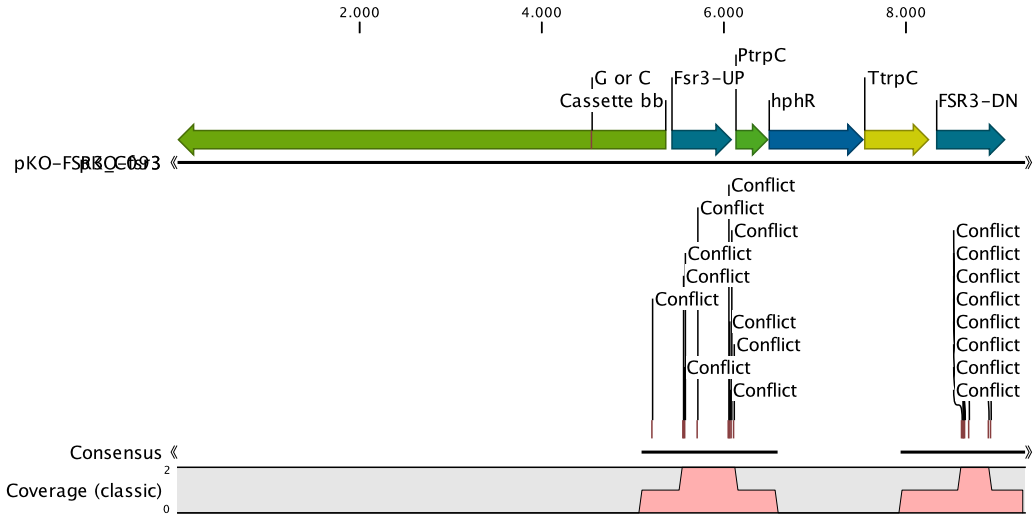

Figure 52: Results from sequence assembly of up and down regions of FSR3 and sequenced results from Eurofins Genomics

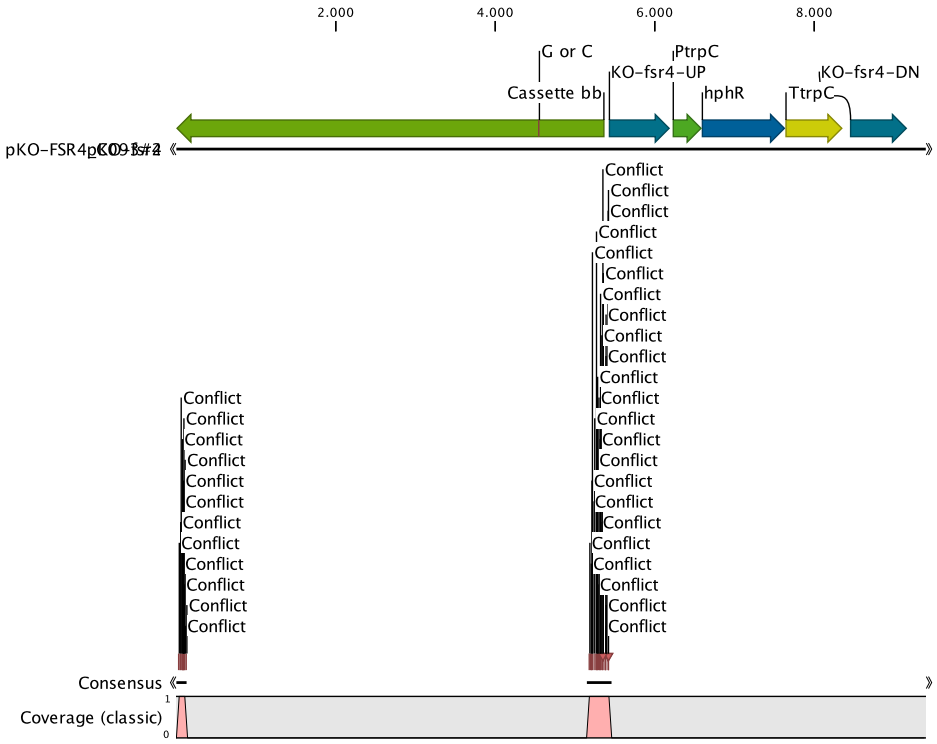

Figure 53: Results from sequence assembly of up and down regions of FSR4 and sequenced results from Eurofins Genomics

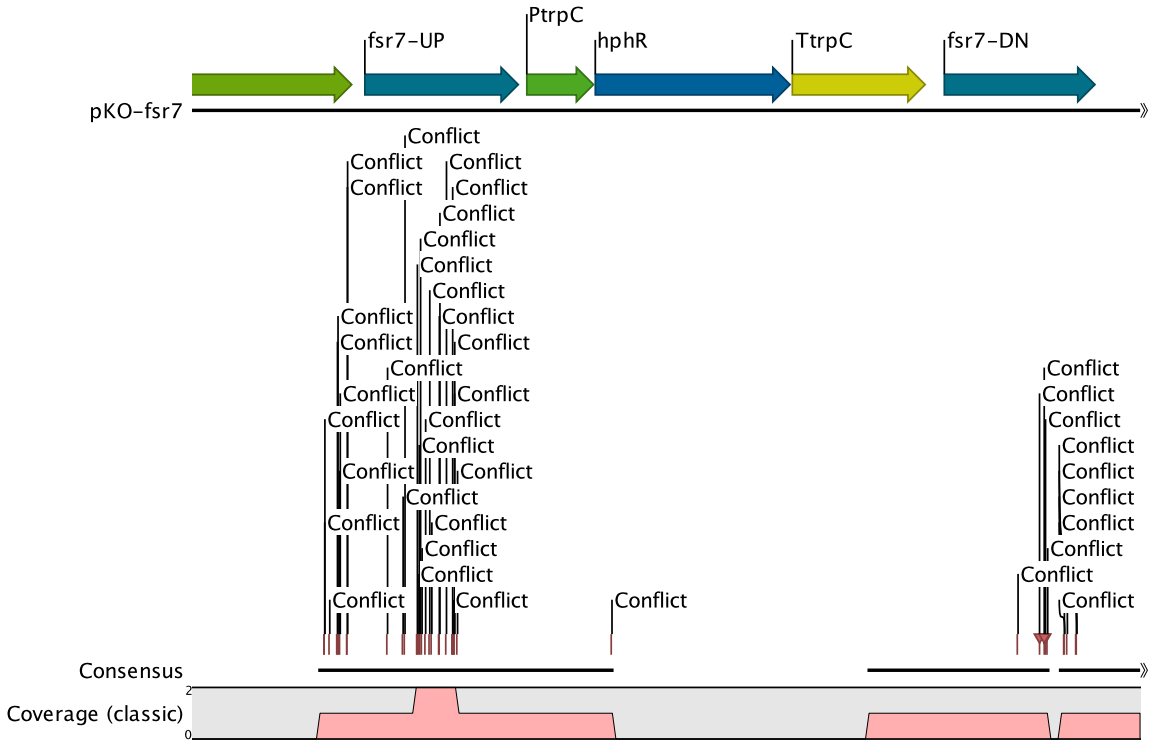

Figure 54: Results from sequence assembly of up and down regions of FSR7 and sequenced results from Eurofins Genomics

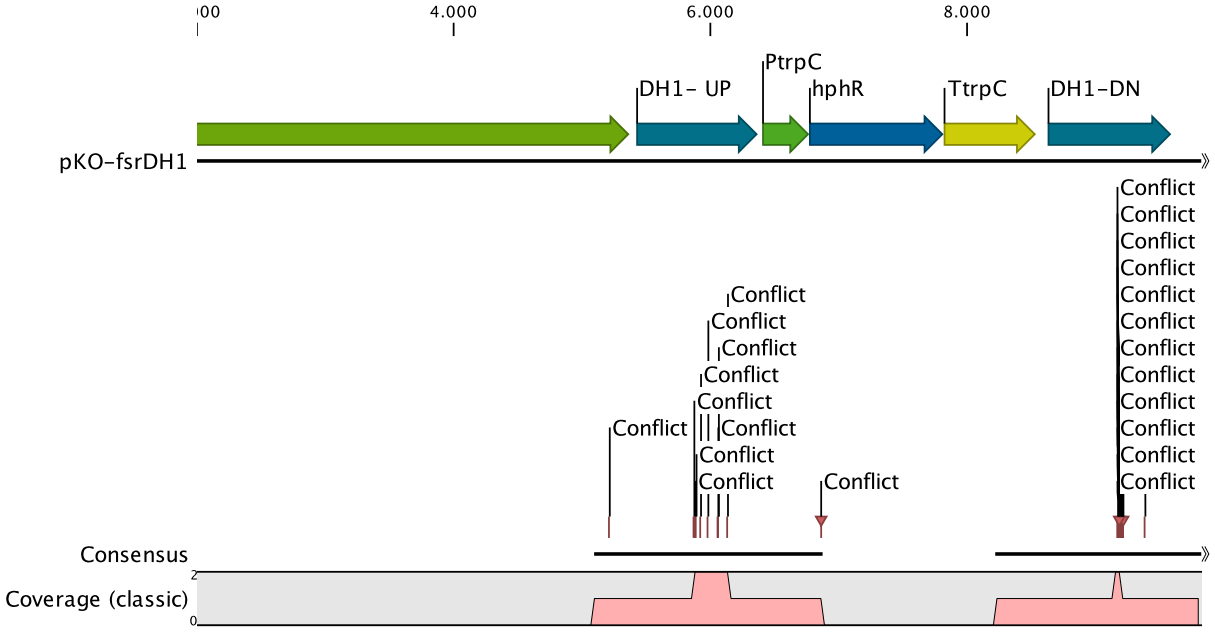

Figure 55: Results from sequence assembly of up and down regions of DH1 and sequenced results from Eurofins Genomics

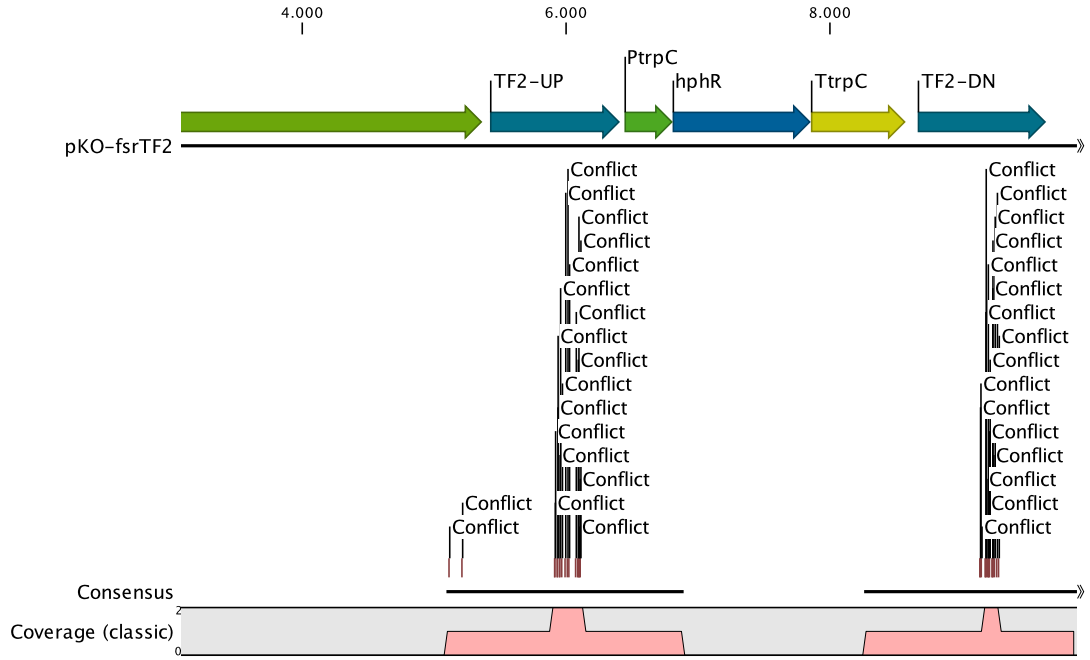

Figure 56: Results from sequence assembly of up and down regions of TF2 and sequenced results from Eurofins Genomics

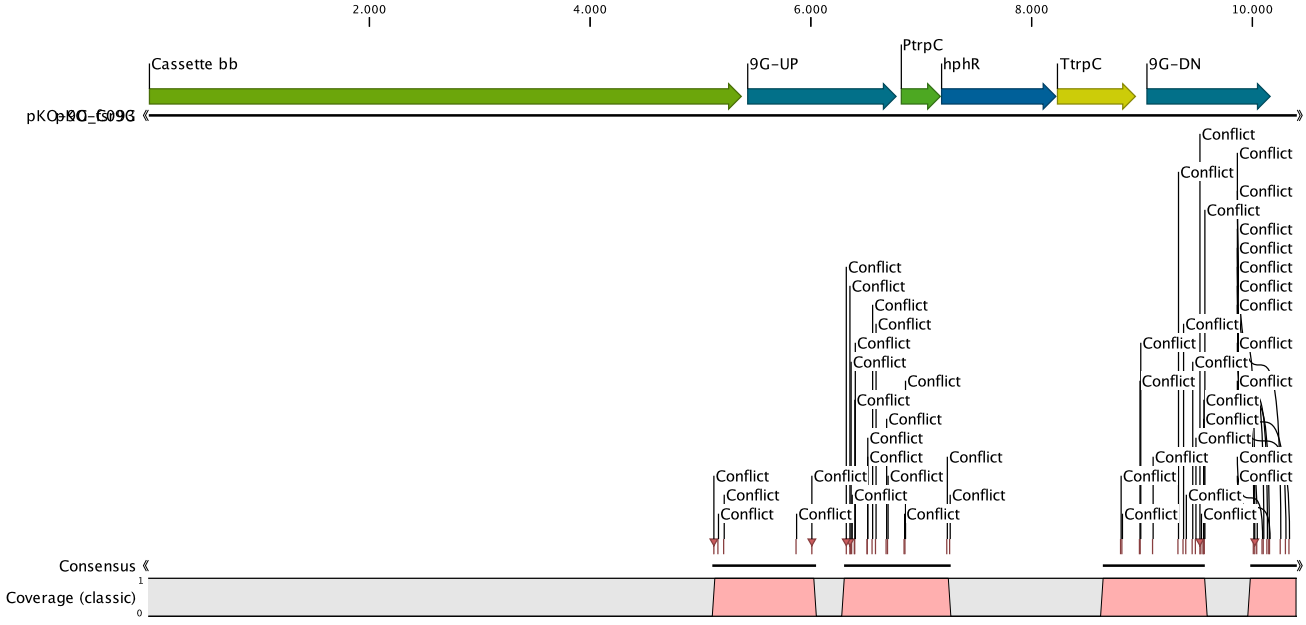

Figure 57: Results from sequence assembly of up and down regions of 9G and sequenced results from Eurofins Genomics

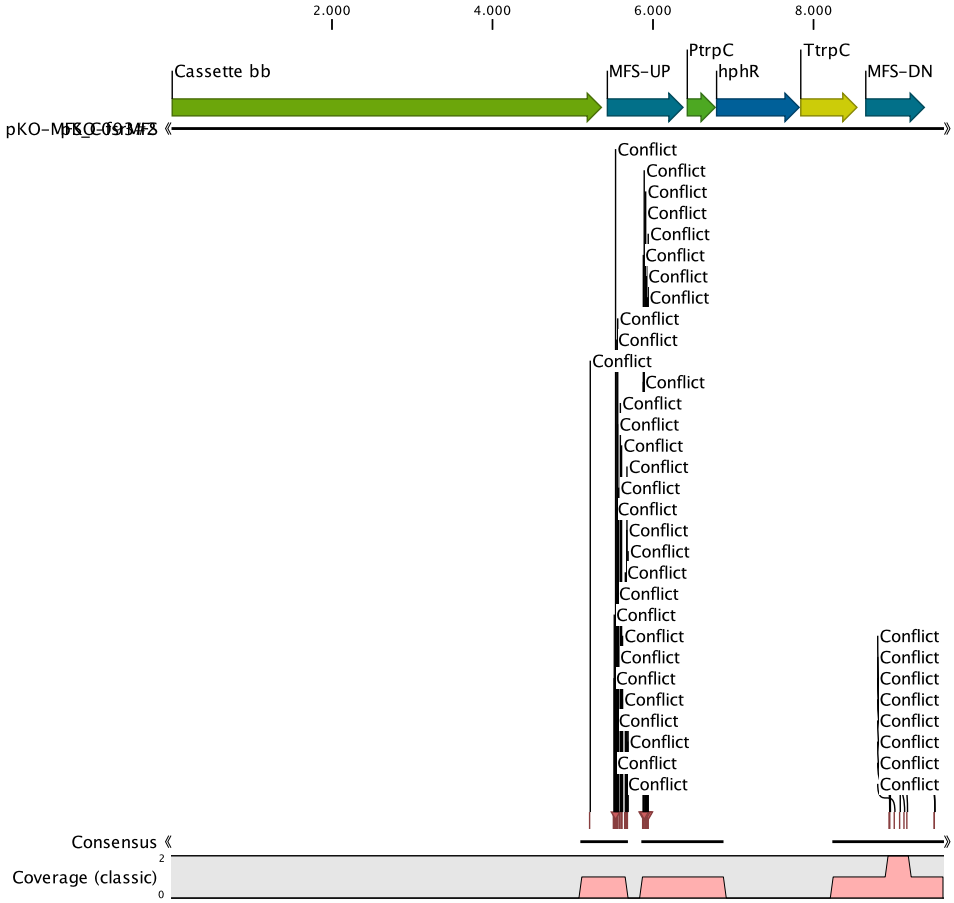

Figure 58: Results from sequence assembly of up and down regions of MFS and sequenced results from Eurofins Genomics

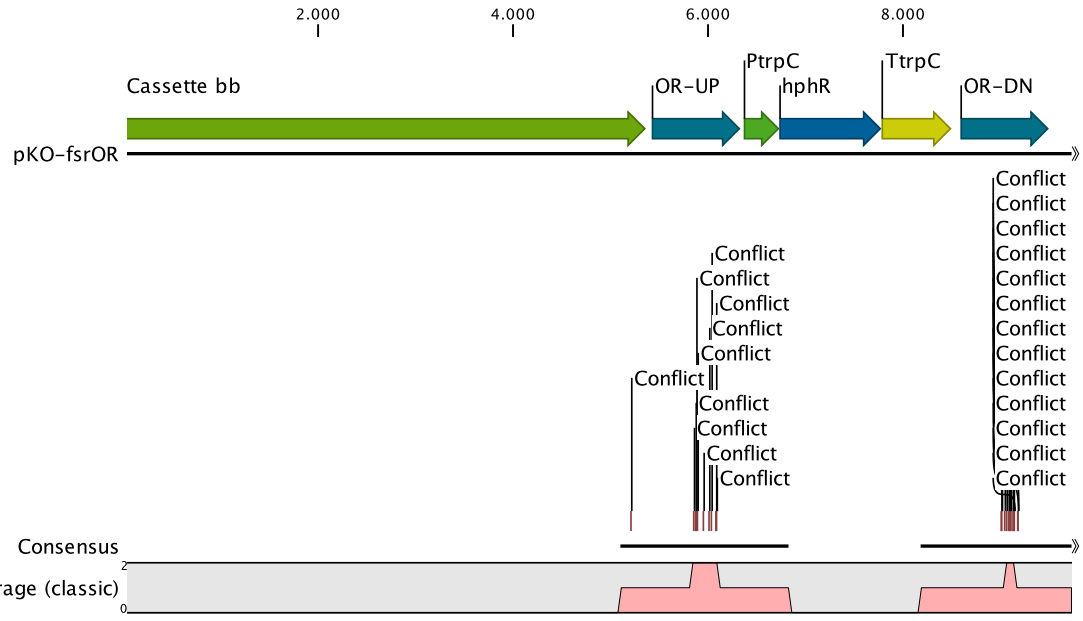

Figure 59: Results from sequence assembly of up and down regions of OR and sequenced results from Eurofins Genomics

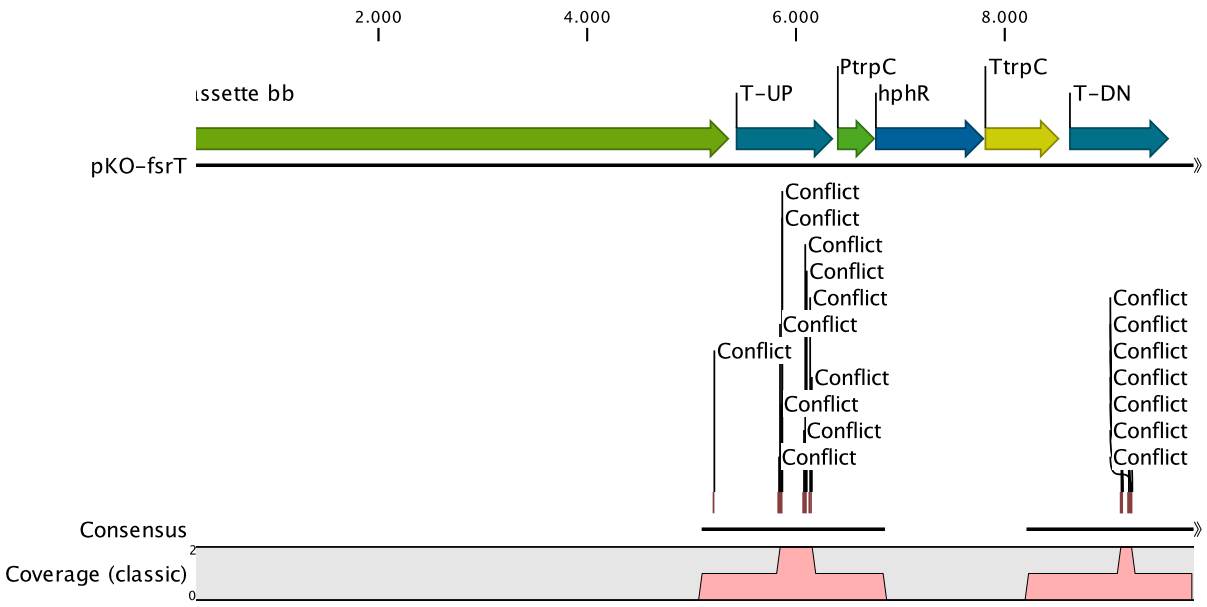

Figure 60: Results from sequence assembly of up and down regions of T and sequenced results from Eurofins Genomics